Small Carbon Clusters: Spectroscopy, Structure, and Energetics

Alan Van Orden† and Richard J. Saykally*

Department of Chemistry, University of California, Berkeley, California 94720

Received January 14, 1998 (Revised Manuscript Received July 10, 1998)

Contents

* To whom correspondence should be addressed.
† Present address: Chemical Science and Technology Division, Mail Stop M888, Los Alamos National Laboratory, Los Alamos, NM 87545.

S0009-2665(97)00086-1 CCC: $30.00
Published on Web 09/01/1998

Alan Van Orden was born January 2, 1966, in Champaign, IL, and raised in Pocatello, ID. He earned a B.S. degree in Chemistry from Brigham Young University (Provo, UT) in 1990 and a Ph.D. in Physical Chemistry from the University of California at Berkeley in 1996. His graduate research was conducted under the supervision of Professor Saykally and focused on elucidating the structural and spectroscopic properties of carbon and silicon–carbon clusters using high-resolution laser spectroscopy techniques. At present, he is a postdoctoral research associate in the Chemical Science and Technology Division at the Los Alamos National Laboratory (Los Alamos, NM), under the direction of Richard A. Keller. He thanks his wife, Jill, and daughters, Amanda and Emma, for their patience and support during the preparation of this review.

Richard Saykally was born in Rhinelander, WI. He received a B.S. degree from the University of Wisconsin—Eau Claire in 1970, and a Ph.D. from UW—Madison in 1977 under the direction of R. C. Woods. After spending two years at NIST in Boulder as a NRC postdoctoral fellow with K. M. Evenson, he joined the UC—Berkeley Chemistry faculty in 1979. He has received numerous honors and awards, including the Harrison–Howe Award, the Lippincott Prize for Vibrational Spectroscopy, the Bomem Michelson Award in Spectroscopy, the E. K. Plyler Prize for Molecular Spectroscopy, the Bourke Lectureship of the Royal Society of Chemistry, and a Humboldt Senior Scientist Award. He has been a Presidential Young Investigator and a Dreyfus Scholar, and is a Fellow of the American Physical Society, the Optical Society of America, the Royal Society of Chemistry, and the American Academy of Arts and Sciences. He serves on the editorial boards of *The Journal of Chemical Physics*, *Molecular Physics*, *Chemical Physics Letters*, *The Review of Scientific Instruments*, *The Journal of Molecular Spectroscopy*, and *Spectroscopy*. Also recognized as an outstanding teacher, Professor Saykally has received the Berkeley Distinguished Teaching Award, and was the co-director of Science for Science Teachers, a national program for secondary school teacher enhancement. He has published over 200 papers on subjects ranging from intermolecular forces and molecular ions to astrophysics.

I. Introduction

The study of pure carbon molecules has engaged great interest for many decades.[1] Molecules of this kind were first detected in astrophysical sources over a century ago and continue to be intensely studied in connection with the chemistry of carbon stars,[2,3] comets,[4] and interstellar molecular clouds.[5−9] In particular, long carbon chains have recently been proposed as possible carriers of the diffuse interstellar bands.[10,11] Carbon clusters are known to be present in hydrocarbon flames and other soot-forming systems,[12−14] and the study of these species is necessary for acquiring a thorough understanding of these complex chemical environments. Carbon clusters are also thought to be intermediates in the gas-phase chemistry taking place in chemical vapor deposition systems for production of thin diamond and silicon carbide films.[15,16] Clearly, a detailed knowledge of the physical and chemical properties of carbon clusters is important for understanding a large variety of chemical systems.

In addition to such practical considerations, carbon clusters are fascinating examples of the richness and variety of carbon chemistry in itself. Due to the enormous bonding flexibility of carbon, viz. its unique ability to form stable single, double, or triple bonds, carbon clusters appear in a wide range of structural forms that are synthesized spontaneously in hot carbon plasmas. For example, researchers have been puzzling for more than a decade over the ability of a molecule as symmetric as the icosohedral C_{60} cluster to form in such a spontaneous way.[17] Elucidating the evolution of carbon cluster structure, from linear chains to rings to closed spheroidal cages to nanotubes, that takes place as the cluster size increases constitutes a major scientific challenge and requires an intimate interplay of state of the art experimental and theoretical techniques. While great progress has been made in recent years, many unanswered questions still remain.

The enormous volume of carbon cluster research that occurred prior to 1989 was the subject of a comprehensive review article by Weltner and Van Zee.[1] In the years since the publication of that review, an explosion in carbon cluster research has occurred. The ability to efficiently synthesize C_{60}, C_{70}, and other fullerene species in bulk quantities[18] has spawned a new branch of chemistry, which was recently recognized with the Nobel Prize. Many researchers from around the world have contributed to a vast and expanding literature on the physical and chemical properties of this third stable allotrope of carbon. New nanoscale materials have also been discovered as an outgrowth of this research, e.g. the so-called "buckytubes",[19−22] and much effort has been expended in developing technological applications for these species. Recent research on fullerenes and nanotubes is the subject of numerous books and review articles. See for example, refs 23−27.

Prior to the 1985 discovery of fullerenes, the existence of a stable sp allotrope of carbon, composed of long acetylenic chains of sp-hybridized carbon atoms (polyynes) was proposed. Carbon chains, such as HC_nN, possessing as many as 11 carbon atoms, had been observed in the interstellar medium,[28−30] and evidence for the existence of even larger species of this kind was obtained from laboratory measurements.[31−33] In more recent years, Lagow et al.

succeeded in synthesizing bulk quantities of such carbon chains containing as many as 28 carbon atoms by stabilizing the terminal carbons with bulky organic end-capping groups.[34] These authors also reported evidence for gas-phase carbon chains produced with as many as 300 atoms. On the basis of these observations, they suggested that long chains of sp-hybridized carbon atoms may constitute a "fourth stable allotrope of carbon".

sp carbon molecules in their pure form are known to exist in a rich variety of structures, including chains and monocyclic and polycyclic rings. These molecules are highly reactive, transient species and are extremely difficult to produce and study in the laboratory. Nevertheless, great progress has been made in the study of these systems since the publication of Weltner and Van Zee's review, especially for clusters in the C_3 to C_{20} size range. In particular, very little detailed experimental information that could directly elucidate the structural properties of polyatomic carbon clusters larger than C_3 existed prior to 1989. This situation has largely been rectified in more recent years, especially for the linear isomers of C_4-C_7, C_9, and C_{13},[35−38] for which extremely precise high-resolution infrared laser spectroscopy experiments have been performed. Many other spectroscopic techniques have also been developed to study carbon molecules in the gas phase and trapped in cryogenic matrices. For example, new experimental and theoretical studies of the optical spectra of C_3 have led to a much more detailed understanding of the unusual bending dynamics of this molecule.[39,40] In addition, vibrationally resolved photoelectron spectroscopy has been used to characterize numerous vibrational and electronic states of gas-phase clusters up to C_{11}.[41,42] The study of carbon clusters trapped in cryogenic matrices is a continuing area of active research. In recent years, numerous infrared absorption bands observed in matrices have been assigned, through the interplay of isotopic substitution measurements, ab initio calculations, and subsequent gas-phase measurements. Very recently, two infrared absorption transitions observed in an Ar matrix have been assigned to vibrational modes of the elusive cyclic isomers of C_6 and C_8.[43−45]

Much of this recent experimental progress has been devoted to characterizing carbon clusters in their ground electronic states, and traditionally, much less has been known about the excited electronic states of clusters larger than C_3. However, beginning in 1995, there has been a recent flurry of activity in this area. A significant new development in the field of matrix spectroscopy is the ability to trap mass-selected carbon cluster anions in solid matrices.[46] Optical emission and absorption spectroscopy measurements have been performed for both the anionic and neutral forms of mass-selected linear carbon chains ranging in size from C_4 to C_{20}, leading to unambiguous assignments of numerous electronic transitions. Many of these transitions have also been observed recently for the anionic carbon clusters in the gas phase, using multiphoton electron detachment techniques.[47−50]

Another area of carbon cluster research that has been notoriously difficult to address has been to obtain structural information about carbon clusters in the intermediate size range between small chains and rings and large closed-cage fullerene species. It was recently discovered that much could be learned about carbon cluster ions in this size range by measuring their ion mobilities using gas-phase ion chromatography.[51−53] Structural properties, isomer distributions, and relative energies have been elucidated in detail for cluster ions as small as $C_7^{+/-}$ and as large as C_{84}^+ in this way. Finally, much more accurate measurements of electron affinities, ionization potentials, and dissociation energies for carbon clusters as large as C_{24} are now available.[41,54,55]

Many of the issues discussed above are being addressed by applying new theoretical methods to increasingly larger carbon clusters, including fullerenes.[56] For example, powerful coupled cluster techniques, which have become widely available only in the past few years, have now been used to calculate the properties of carbon clusters as large as C_{10} with unprecedented accuracy.[57,58] Recent improvements in density functional theory methods have also permitted accurate ab initio calculations to be carried out for clusters as large as C_{28}.[59−65] Clearly, much new insight now exists, and the purpose of the present article will be to review this recent progress. Weltner and Van Zee's review covered a time period that extended back to the earliest days of carbon cluster research in the 1940s and 1950s, up until the time of publication in 1989.[1] This paper will concentrate on recent developments that have taken place since that time. The main focus will be on the structural, spectroscopic, and energetic properties of pure sp carbon clusters and their ions in the C_2 to $\sim C_{30}$ size range.

II. Structure, Bonding, and Vibrational Dynamics

A. Geometric Structures

Ever since the pioneering molecular orbital calculations of Pitzer and Clementi,[66] it has been recognized that carbon clusters smaller than C_{10} possess low-energy linear structures. Cumulenic bonding (:C═C···C═C:), with nearly equivalent bond lengths, as opposed to acetylenic bonding, (·C≡C−C···C≡C·) with alternating bond lengths, was predicted to be the preferred bonding configuration. Odd-numbered linear chains were thought to possess $^1\Sigma_g^+$ ground electronic states, whereas the ground states were $^3\Sigma_g^-$ for the even-numbered chains. Clusters larger than C_{10} were believed to occur as monocyclic rings, due to the reduction in angle strain of the larger rings and the added stability arising from an additional C−C bond. For the most part, these early predictions have been vindicated by sophisticated ab initio calculations, at least in a qualitative sense.[58,67,68] Linear chains are indeed low-energy isomeric forms for the smaller clusters, and a transition to rings is still thought to occur at C_{10}. In addition, the acetylenic configurations of the even-numbered linear chains are found to be higher in energy than the cumulenic forms,[68−70] although there is evidence that

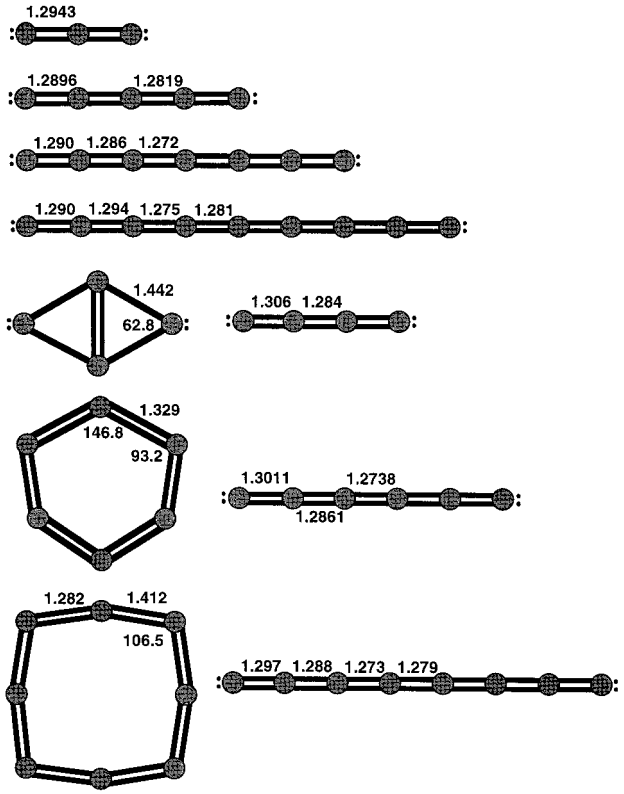

Figure 1. Equilibrium geometries of the low-energy structural isomers of small carbon clusters. Bond lengths (Å) and bond angles (degrees) were calculated for each cluster as follows: C_3, CCSD(T)/cc-pVQZ;[40] linear and cyclic C_4, CCSD(T)/PVTZ;[71] C_5, CCSD(T)/275cGTOs;[74] linear C_6, RCCSD(T)/204cGTOs;[75] cyclic C_6, CCSD(T)/TZ2P;[72] C_7, MCCSD(T)/238cGTOs;[57] linear C_8, RCCSD(T)/cc-pVTZ;[76] cyclic C_8, CCSD(T)/cc-pVDZ;[58] and C_9, CCSD(T)/cc-pVDZ.[58]

the energy separation between the two forms reduces as the length of the chain increases. At the CISD/DZP level of theory, for example, the cumulenic form of C_4 was 33 kcal/mol more stable than the acetylenic structure,[70] while for linear C_{10} the energy difference was only 4.9 kcal/mol at this level.[68] Recent evidence from density functional theory has shown that the ground-state planar monocyclic ring isomers of C_8, C_{12}, and C_{16} may actually be polyacetylenic structures.[62]

In more recent years, a major caveat to the early molecular orbital calculations was discovered. For the even-numbered clusters, C_4, C_6, and C_8, cyclic isomers were also found to be low-energy structures and are now thought to be isoenergetic to or lower in energy than their linear counterparts.[58,67,71−73] Despite this, the cyclic isomers of the neutral clusters have been notoriously difficult to detect and characterize spectroscopically, and it is the linear isomers that are observed in the vast majority of experimental studies. This is the case even for clusters as large as C_{15}. The first spectroscopic information for small cyclic carbon clusters was obtained only very recently from infrared absorption spectra of cyclic C_6 and C_8 trapped in Ar matrices.[43−45] Figure 1 displays the low-energy structural isomers, along with bond lengths and bond angles, determined from the latest ab initio calculations for C_2 through C_9.[40,57,58,71,72,74−76]

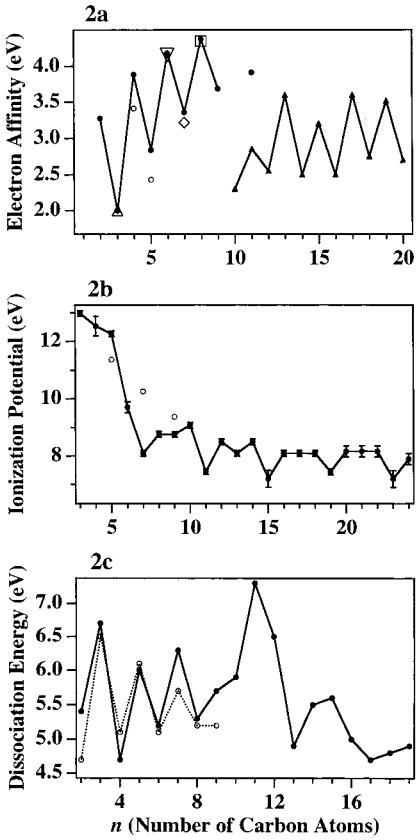

Figure 2. (a) Experimental and theoretical electron affinities for C_2-C_{20}: (-●-) adiabatic electron affinities for linear C_2-C_{11}, obtained by vibrationally resolved anion photoelectron spectroscopy;[41] the uncertainties in these measurements are between about 0.2 and 1%; (-▲-) vertical electron affinities for $C_{10}-C_{20}$ obtained from UV photoelectron spectroscopy;[78] the uncertainties are 2−5%; (theoretical calculations) (△) ref 57; (○) coupled cluster and first-order correlation orbital method[84] (a better prediction for the EA of C_5 is published in ref 83); (▽) RCCSD(T)/288 cGTO;[75] (◇) RCCSD(T)/301 cGTO;[57] (□) adiabatic electron affinity from RCCSD(T).[57] (b) (-●-) Adiabatic ionization potentials of C_3-C_{24} obtained using the charge-transfer bracketing technique;[54,79] (○) calculated IPs of C_3, C_5, C_7, and C_9 using the OVGF method;[88] (c) (-●-) dissociation energies for the lowest energy dissociation channels of $C_2^+-C_{19}^+$ from collision-induced dissociation measurements;[55,81] and (••○••) theoretical dissociation energies of $C_2^+-C_9^+$.[67]

B. Ground-State Electronic Structures: Electron Affinities, Ionization Potentials, and Dissociation Energies.

As stated above, the ground states are of $^1\Sigma_g^+$ and $^3\Sigma_g^-$ character for the odd- and even-numbered clusters, respectively. Among the physical properties that are most sensitive to the nature of the electronic states are the electron affinities (EA's), the ionization potentials (IP's), and the dissociation energies (DE's). Measurements of these properties provide, for example, experimental support for the alternation between singlet and triplet electronic states for odd- and even-numbered linear chains. The latest experimental and theoretical values for EA's and IP's are plotted in Figure 2a,b. DE's for the most favorable dissociation channels of carbon cluster cations are plotted in Figure 2c. A similar even−odd alteration

of DE's for C_3-C_9 is expected to occur for the neutral species as well.

UV photoelectron spectroscopy measurements of mass selected C_n^- ions ($3 \le n \le 84$) were first used to determine EA's.[77,78] The EA's of C_2-C_9 alternated between larger values for *n*-even and smaller values for *n*-odd, consistent with the predicted spin multiplicity of the linear chains. An abrupt decrease in the electron affinity was observed for C_{10}, which was taken as support for a transition to monocyclic rings. More precise values for the EA's of C_2-C_{11} were later obtained by Arnold et al. using vibrationally resolved photoelectron spectroscopy techniques.[41]

Estimates for the IP's of carbon clusters were first provided by Rohlfing et al. on the basis of laser photoionization measurements of the neutrals.[31] More recent measurements have been made using the charge-transfer bracketing technique,[54,79] wherein carbon cluster cations are reacted with compounds of known IP, to determine whether a charge-transfer reaction occurs. Much more precise values for the IP's of C_3-C_{24} have been obtained in this way. Figure 2b reveals minima in the cluster size distribution of IP's corresponding to C_7, C_{11}, C_{15}, C_{19}, and C_{23}. These clusters are often observed as "magic number" peaks in photoionization mass spectra. The unusual abundance of these clusters may thus be due to their low IP's rather than to a special degree of stability.

Finally, Radi et al.[80] and Sowa-Resat et al.[55,81] performed collision-induced dissociation measurements to determine the dissociation behavior of C_n^+ ($2 \le n \le 19$). For $C_2^+-C_4^+$, the lowest energy dissociation channel was the loss of C^+. Loss of C_3^+ was the lowest energy channel for $C_5^+-C_9^+$. A striking even−odd alteration in these dissociation energies was observed, revealing the *n*-odd species to be more stable than the *n*-even chains for $n = 2-9$. These authors predicted that the same trend would also be observed for the neutral species. Bouyer et al. deduced dissociation energies of larger carbon cluster cations ($16 \le n \le 36$) from photodissociation studies.[82] These authors found that the stability of the clusters gradually decreased with cluster size up to C_{29}^+, and then abruptly increased at C_{30}^+, which they attributed to the onset of fullerene formation. Several theoretical studies have been performed to calculate EA's,[57,75,76,83−88] IP's,[88] and DE's[67] of small carbon clusters. In general, these calculations are in reasonable agreement with the experimental results for clusters smaller than C_{10}.

C. Bending Vibrational Dynamics of Linear Chains

The bending dynamics of linear polyatomic carbon clusters are characterized by unusually large amplitude motion, resulting in low ($\le$100 cm^{-1}) bending frequencies, as will be shown dramatically for C_3.[89] The high density of states that results from this type of motion has important consequences for the formation of carbon clusters. For example, since large amplitude motion probably does not occur for the cyclic isomers, the formation of linear structures is entropically favored under most experimental conditions, even when the cyclic species are enthalpically more stable. In addition, the condensation of linear chains becomes a facile process due to the added stability imparted to linear collision complexes. Some insight into the reason for this unusual bending motion can be gained from the diagrams of the highest occupied molecular orbitals (HOMO) in Figure 3.[90] Clusters possessing orbitals of π_u symmetry exhibit constructive overlap of the valence orbitals when the molecule is bent about the center of symmetry, perhaps enhancing bending vibrational motion. Destructive overlap occurs for clusters possessing HOMO's of π_g symmetry, which destabilizes the bent configuration. Thus, C_3, C_6, C_7, and C_{10} are expected to be more floppy than C_4, C_5, C_8, and C_9, although all of these clusters are believed to possess relatively low bending frequencies. Experimental evidence to support this picture will be presented below.

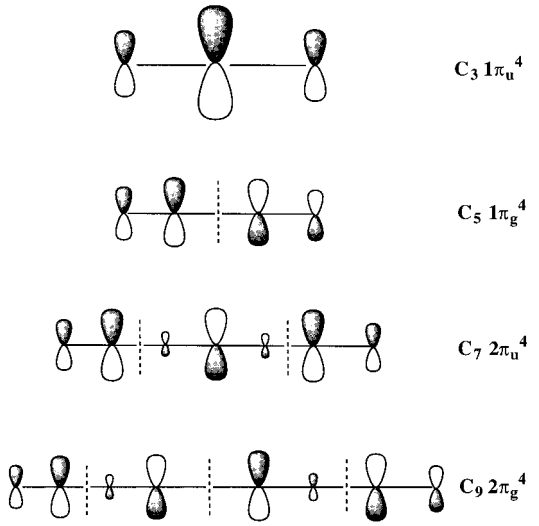

Figure 3. Diagrams of the highest occupied molecular orbitals of odd-numbered C_3 through C_9. (Produced from data in ref 90.)

III. Formation of Carbon Clusters

Carbon clusters form spontaneously in plasmas that are produced during the energetic processing of carbon-rich materials. Such natural environments include the atmospheres surrounding carbon stars, interstellar dust clouds irradiated by intense UV light, and terrestrial sooting flames. The most widely used laboratory technique for producing carbon clusters has been laser vaporization of graphite followed by supersonic expansion into an inert carrier gas, usually He or Ar. Smalley and co-workers first developed this technique, which was employed by Kroto et al. in the discovery of fullerenes.[17] Neutral, anionic, and cationic carbon clusters form directly from the laser initiated plasma in sizes ranging from one to hundreds of atoms. The size distribution and the isomeric forms produced in this way can be controlled by varying such experimental parameters as laser power, gas pressure, and the geometry of the supersonic nozzle. Magic number peaks sometimes are observed in the mass spectra of smaller C_n^+ ions for odd-numbered clusters, especially $n = 3$, 11, 15, and 19.[31,91] In contrast, for small C_n^- ions, magic

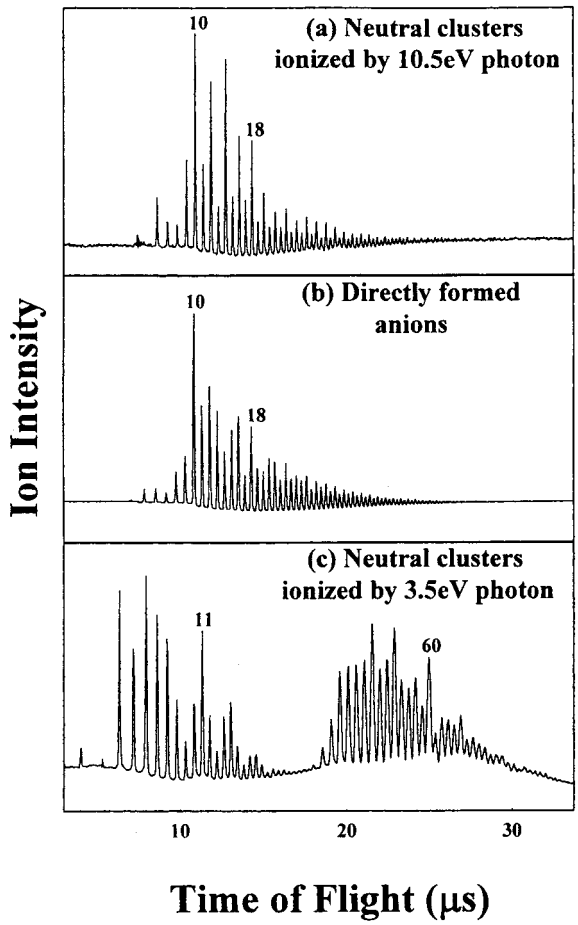

Figure 4. (a) Photoionization TOF mass spectrum of carbon clusters using a photon energy of 10.5 eV. (b) TOF mass spectrum of carbon cluster anions produced directly from the cluster source. (c) Photoionization TOF mass spectrum using a photon energy of 3.5 eV. In all three cases, the clusters were formed by laser desorption from graphite. (Reprinted with permission from ref 94. Copyright 1997 American Institute of Physics.)

number peaks have been observed to occur for even-numbered clusters.[92,93]

Measurement of the neutral carbon cluster distribution produced by laser vaporization of graphite has been hindered by the lack of a "soft" ionization technique, wherein the neutrals are ionized without fragmentation. Recently, Kaizu et al. used single photon (10.5 eV) ionization of the neutrals, as opposed to previously reported multiphoton ionization, to obtain a reliable measurement of the neutral cluster size distribution (see Figure 4).[94] These authors found that, under moderate vaporization laser fluences (0.1−1.0 J/cm^2), magic number peaks occurred at n = 10, 12, 14, 16, and 18, analogous to the anion distribution. In contrast, the size distribution observed after multiphoton ionization at 3.5 eV revealed the familiar bimodal distribution[31] dominated by odd-numbered peaks in the lower mass range and even-numbered fullerenes in the higher mass range. The authors concluded that under these conditions, the neutrals were produced predominantly as even numbered monocyclic rings, and that formation of the anions proceeded by electron capture of the neutrals.

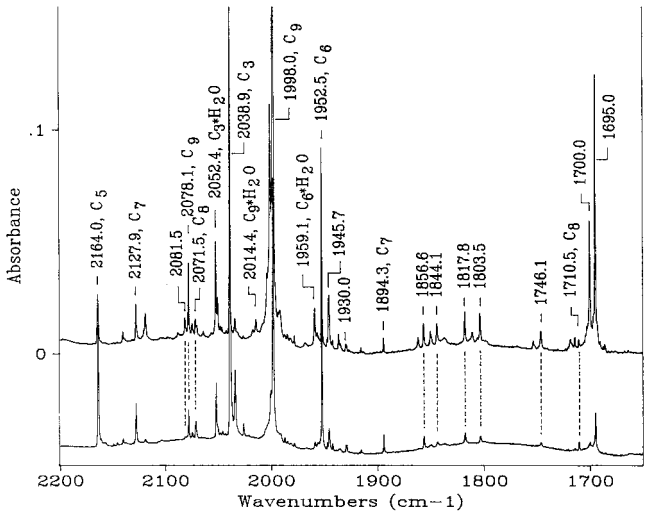

Figure 5. Infrared spectra of carbon clusters trapped in an Ar matrix. The temperature at which the lower spectrum was recorded was 20 K and that of the upper spectrum was 36 K. (Reprinted with permission from ref 113. Copyright 1996 Elsevier Science B.V.)

The use of laser vaporization−supersonic expansion sources continues to be an important means of producing carbon clusters for their study in the gas phase. Laser vaporization of thin diamond films and organic polymers has also been used to produce carbon clusters,[95−97] as has laser vaporization of a metal target in the presence of small hydrocarbons seeded into the carrier gas.[98] Other methods of producing carbon clusters that do not involve laser vaporization include the carbon arc synthesis of macroscopic quantities of fullerenes and nanotubes,[22] electric discharge, photolysis, or pyrolysis of small hydrocarbon precursors,[89,99−102] CO_2 laser vibrational activation of SF_6 in the presence of acetylene,[103] and Cs ion sputtering of graphite.[104] Diederich and co-workers[105−109] and others[110] have been developing techniques to systematically synthesize specific sized carbon clusters from organic precursors. They have shown, for example, that C_{18} can be produced by photolyzing an 18-membered cyclic carbon ring stabilized by organic leaving groups.[106]

Although most of the techniques mentioned above involve synthesis and characterization of carbon clusters in the gas phase, major contributions to carbon cluster research have been made by trapping the clusters in cryogenic matrices and measuring UV/vis, infrared, and ESR spectra.[1,46,111] Larger carbon clusters are built up from smaller precursors by annealing the solid matrix. Early matrix studies by Weltner and co-workers date back to the 1960s, but advances continue to be made, due to the availability of more sophisticated theoretical methods for predicting vibrational frequencies and isotope substitution patterns for assigning infrared spectra. Rare gas matrices are typically used, although solid para-hydrogen has recently been shown to give higher resolution IR spectra.[112] Figure 5 displays a recent IR absorption spectrum of carbon clusters trapped in an Ar matrix.[113] While many of the peaks have been assigned to fundamental vibrational transitions of different sized carbon clusters, numerous unas-

signed transitions still remain. Analysis of these data is complicated by the fact that a broad distribution of cluster sizes is present in the matrix, and several regions of the spectrum are too congested to perform reliable isotopic substitution measurements. This weakness is currently being overcome by depositing mass-selected carbon cluster anions into the matrix, followed by electron photodetachment to form the neutral.[46] Another difficulty is that the matrix environment may perturb the structure and spectral properties of the molecules being studied, as will be shown in several cases below. As will soon become clear, most of the assignments that have been made have been accomplished in recent years, through a combination of isotopic substitution measurements, ab initio calculations, and gas-phase infrared laser spectroscopy.

IV. Thermodynamic Properties

A long-standing problem in studying the physical properties of graphite has been to determine an accurate value for the heat of vaporization. Complexity arises due to the large distribution of clusters present in the equilibrium vapor, and it becomes necessary to determine accurate heats of formation for each individual carbon cluster. This problem has been investigated in recent years on both experimental[114−116] and theoretical[117,118] grounds.

Gingerich et al. used Knudsen effusion mass spectrometry to measure the equilibrium partial pressures of the C_2-C_7 carbon clusters in graphite vapor at temperatures ranging from 2660 to 2850 K.[114−116] Of the pure carbon species present in the vapor, C_1, C_2, and C_3 accounted for nearly all of the total vapor pressure. C_3 was the major component, accounting for about 80% of the vapor pressure at 2700 K, while C_1 and C_2 were present at about 14% and 6%, respectively. The larger clusters (C_4-C_7) existed only in trace quantities at these temperatures, accounting for less than 0.1% of the pure carbon species. Molecular partition functions were calculated within the rigid rotor−harmonic oscillator approximation using experimental and theoretical spectroscopic data. From the partial pressure data and the calculated partition functions, the authors deduced thermodynamic properties, including third law heats of formation, $\Delta H_f°$, and total atomization energies, ΣD_0, for linear C_2-C_7. Martin and Taylor recently calculated ΣD_0 values for C_2-C_{10} using coupled cluster methods.[118] Table 1 compares their results to the experimental values.

Two weaknesses exist in deducing ΔH_f^0 and ΣD_0 values from the vapor pressure measurements. The first, and most serious, is the assumption of a rigid rotor−harmonic oscillator model in the third law extrapolations, since large anharmonicities are present in the bending modes of the linear systems, especially for C_3 and C_7. A second weakness is that the authors assumed only the linear isomers to be present for the even-numbered C_4 and C_6 clusters, even though cyclic isomers are predicted to be present as well. However, it has been shown that due to the higher density of states of the linear isomers, resulting from their low bending frequencies, these species possess higher entropies of formation.[119,120] Thus, the linear isomers may be formed more readily at temperatures attained in the partial pressure measurements, as well as for laser vaporization conditions, even when the cyclic species are lower in energy. For example, Slanina estimated that the rhombic isomer of C_4 would account for no more than 10% of the C_4 clusters present in the vapor at equilibrium, based on theoretical calculations.[120] In a similar study, the percentage of cyclic C_6 was found to be only 3% at 2500 K.[119] Therefore, the assumption that only linear isomers are present under these conditions is probably a reasonable one to make.

Table 1. Third Law Heats of Formation and Total Atomization Energies for C_2-C_7 from Experiment and Theory[a]

		experiment[b] (kcal/mol)	theory[c] (kcal/mol)
C_2	$\Delta H_f°$	195(2)	
	ΣD_0	144(2)	
C_3	$\Delta H_f°$	199(3)	
	ΣD_0	311(3)	314.3
C_4	$\Delta H_f°$	251(4)	
	ΣD_0	429(4)	426.1
C_5	$\Delta H_f°$	258(4)	251.7
	ΣD_0	592(4)	594.0
C_6	$\Delta H_f°$	314(4)	
	ΣD_0	706(5)	708
C_7	$\Delta H_f°$	317(4)	
	ΣD_0	873(5)	870.9

[a] Numbers in parentheses are uncertainties in the last digits. [b] References 114−116. [c] References 117 and 118.

V. C_2

A. Structure and Spectroscopy

As discussed above, C, C_2, and C_3 are the primary components of equilibrium carbon vapor at temperatures in the range of 2000−5000 K. These species are reaction intermediates in a wide variety of chemical systems involving hydrocarbons, including photolysis, electric discharges, and combustion systems. The largest fraction of the carbon present in the universe is in the form of C or one of its ions, while the molecular form of CO accounts for the second largest fraction. C_2 and C_3 are also present in astrophysical sources and are thought to be important reactants in the chemistry of the interstellar medium. The spectroscopy of these species has been studied for decades, making C_2 and C_3 by far the most well-characterized of all the carbon clusters. In fact, one author recently described C_3 as "one of the most well-characterized nonrigid triatomics in existence".[121]

The C_2 molecule exists in a $X^1\Sigma_g^+$ ground electronic state. There are three low lying electronic states that have also been characterized, the $a^3\Pi_u$ state, lying 716 cm^{-1} above the ground state, the $b^3\Sigma_g^-$ state at 6434 cm^{-1}, and the $A^1\Pi_u$ state at 8391 cm^{-1}. In addition to these low-lying states, about 14 other electronic states have been observed giving rise to a rich spectroscopy. Since C_2 is most often produced in an emissive state, many well-known band systems have been characterized. The most prominent of

these is the Swan system ($d^3\Pi_g - a^3\Pi_u$) at ~19 400 cm^{-1}. Others include the Phillips bands ($A^1\Pi_u - X^1\Sigma_g^+$) and the Mulliken bands ($D^1\Sigma_u^+ - X^1\Sigma_g^+$) at 43 227 cm^{-1}. The most recent states to be characterized were the $B^1\Delta_g$ and $B'^1\Sigma_g^+$ states, which were detected by Douay et al. via the $B^1\Delta_g - A^1\Pi_u$ and the $B'^1\Sigma_g^+ - A^1\Pi_u$ infrared emission spectra of a hydrocarbon discharge,[122] and the $1^1\Delta_u$ state, observed by Goodwin and Cool via the $1^1\Delta_u - A^1\Pi_u$ transition.[123] Gong et al. have recently measured radiative lifetimes of several vibronic states of $C_2(B'^1\Sigma_g^+)$.[124] The structural and spectroscopic properties of C_2 known prior to 1977 were tabulated by Huber and Herzberg.[125] Experimental and theoretical studies up to 1989 were summarized in Weltner and Van Zee's review article.[1] Finally, Martin reviewed the spectroscopy and kinetics of all the C_2 electronic states studied up to 1992.[126] Calculated and experimental molecular constants, vibronic frequencies, excited-state lifetimes, oscillator strengths, and electronic transition moments for most of the observed electronic states are reported in these references.

Experimental and theoretical work on C_2 since 1992 has mostly aimed at refining and improving the accuracy of the calculated properties and the measured molecular parameters and resolving a few discrepancies that existed in the earlier work. Watts and Bartlett calculated equilibrium bond lengths, harmonic vibrational frequencies, dissociation energies, and the electronic term energies for C_2 in its $X^1\Sigma_g^+$, $a^3\Pi_u$, and $b^3\Sigma_g^-$ states.[127] One of the purposes of this study was to provide a benchmark for extending coupled cluster techniques to larger carbon clusters. Various coupled cluster techniques using different methods for treating triple excitations were compared. Although the most accurate of these was the full CCSDT approach, the CCSD(T) method was found to be the best compromise between accuracy and cost. The most accurate calculations were performed using the cc-pVQZ basis set. Pradhan et al. used multireference configuration interaction methods to obtain the ground-state spectroscopic constants of C_2.[128] Various basis sets were compared, the largest one being the cc-pV6Z basis set.

The Swan system of C_2 was recently studied by Prasad and Bernath using Fourier transform spectroscopy of C_2 molecules cooled in a supersonic jet.[129] These authors reported refined values for the molecular constants of $v'' = 0-4$ and $v' = 0-3$. The "high-pressure band system" is observed as an enhancement of the $v' = 6$ level population within the Swan system that takes place in CO discharges as well as a variety of other experimental conditions. Thareja and Abilasha observed high-pressure bands in a laser produced carbon plasma and concluded that the bands resulted from the recombination of ground-state carbon atoms.[130] Caubet and Dorthe attempted to elucidate the origin of the high-pressure bands produced in a microwave discharge of CO.[131] Previously, it was suggested that the enhancement results from collisional transfer between the metastable $^5\Pi_g$ state and $d^3\Pi_g$, $v = 6$. These authors found that population of the $^5\Pi_g$ resulted from the reactions $C + C + M \rightarrow C_2 + M$ and $C + C_2O \rightarrow C_2 + CO$.

Table 2. Molecular Parameters of the $D^1\Sigma_u^+$ ($v'' = 0$) State of C_2[a,b]

band	ν_0 (cm^{-1})	B_v (cm^{-1})	D_v ($\times 10^6$ cm^{-1})
0−0	43227.33(40)	1.82322(15)	7.39(29)
1−1	43209.31(33)	1.80370(39)	7.29(20)
2−2	43175.77(23)	1.78390(06)	7.19(30)
3−3	43151.14(25)	1.76470(50)	7.09(35)
4−4	43121.92(15)	1.74724(20)	7.6(20)

[a] Adapted from ref 135. [b] Numbers in parentheses are uncertainties in the last digits.

One of the discrepancies that had existed between experiment and theory was the value of the oscillator strength of the Phillips System. Experimental measurements were consistently lower than the theoretical calculations. A new value for $f_{2,0}^{A-X}$ was recently deduced by Lambert et al., on the basis of astrophysical observations using the Hubble Space Telescope, that was in better agreement with theory.[132] Erman and Iwamae remeasured radiative lifetimes of the Phillips system and determined a value for $f_{2,0}^{A-X}$ of $(1.36 \pm 0.15) \times 10^{-3}$, which is compared to the astrophysical estimate of $(1.23 \pm 0.16) \times 10^{-3}$ and the theoretical value of 1.45×10^{-3}.[133] Lask et al. studied the Phillips bands of $^{12}C_2$ and $^{13}C_2$ trapped in Ne and Ar matrices by laser induced fluorescence.[134] They found that radiationless intersystem crossing efficiently populates the $a^3\Pi_u$ and $b^3\Pi_g$ states upon excitation of the Phillips bands, while the $d^3\Pi_g$ state was populated by two-photon absorption, permitting the observation of the Swan bands.

The Mulliken bands were first observed in 1930, and the molecular constants determined in 1939.[126] No other measurement of the molecular constants were reported until the laser induced fluorescence study of Blunt et al., who determined revised values for the $D^1\Sigma_u^+$ state.[135] Table 2 displays selected molecular constants for the Mulliken band recently obtained by these authors.

B. C_2^-

Production of neutral carbon clusters is often accompanied by the formation of carbon cluster ions. Although the relative abundances of these ions is usually much lower than those of the neutrals, their high chemical reactivity makes them important components in the growth and annealing of carbon clusters. C_2^- is the most well-characterized of all the carbon cluster ions. This molecule is particularly interesting because it possesses valence electronic states that are bound with respect to electron autodetachment. The most sophisticated theoretical study to be performed on C_2^- to date are the coupled cluster (CCSDT) calculations of Watts and Bartlett.[127] These authors calculated the equilibrium bond length, the vibrational frequency, the dissociation energy, and molecular constants for the $X^2\Sigma_g^+$ ground state and the $B^2\Sigma_u^+$ and $A^2\Pi_u$ excited states. High-resolution gas-phase spectroscopy has been used to characterize the $B^2\Sigma_u^+ - X^2\Sigma_g^{+1}$ and the $A^2\Pi_u - X^2\Sigma_g^+$,[136] providing molecular constants, oscillator strengths, and excited-state lifetimes. More recently, de Beer et al. used stimulated Raman pumping to characterize C_2^-.[137]

Table 3. Molecular Parameters of the $X^4\Sigma_g^-$ ($v'' = 0$) and the $B^4\Sigma_u^-$ ($v' = 1$) State of C_2^+[a-c]

parameter	$X^4\Sigma_g^-$	$B^4\Sigma_u^-$
T_v (cm^{-1})	0.0	21213.1958(90)
B_v (cm^{-1})	1.41786(7)	1.52234(9)
D_v (10^{-6} cm^{-1})	6.32(10)	6.46(13)
γ_v (10^{-4} cm^{-1})[d]	–	−4.00(20)
ϵ_v (10^{-2} cm^{-1})[e]	4.2(11)	5.4(5)

[a] Adapted from ref 141. [b] Numbers in parentheses are uncertainties in the last digits. [c] The parameters of the B state were obtained from analysis of the spin−orbit interaction between the B state and the close-lying $(2)^2\Pi_u$ state. [d] Spin−rotation coupling constant. [e] Spin−spin coupling constant.

Resonant two-photon photodetachment (R2PD), via transitions to the $B^2\Sigma_u^+$ state, followed by detection of the zero kinetic energy (ZEKE) electrons, was used to monitor the ground-state population as a function of Stokes frequency.

C. C_2^+

The C_2^+ ion was considerably more difficult to characterize using high-resolution spectroscopy techniques than C_2^-, and a complete picture of its spectroscopic properties has emerged only recently. C_2^+ was first observed in the gas-phase with rotational resolution by Maier and Rösslein, who analyzed vibronic bands in the $B^4\Sigma_u^+-X^4\Sigma_g^+$ system.[138] Later, Celii and Maier used stimulated emission pumping (SEP) spectroscopy to access higher excited vibrational states ($v = 4-6$) in the $X^4\Sigma_g^+$ ground state.[139] The resolution of the rotational lines was about 0.3 cm^{-1}. Carré et al. studied the (1,0) transition of the $B^4\Sigma_u^+-X^4\Sigma_g^+$ spectrum using fast-ion beam laser spectroscopy.[140] Rather than tuning the laser over the transition, laser induced fluorescence signals were observed by Doppler scanning the transition into resonance with a fixed-frequency laser. Using this technique, the authors observed the rovibronic transitions with line widths of 0.004 cm^{-1}. With this large improvement in the resolution, spin−spin and spin−rotation splittings were resolved and analyzed for both electronic states. More recently, Boudjarane et al. used this same technique to analyze the spin splitting parameters in the (1,1) transition of the $B^4\Sigma_u^+-X^4\Sigma_g^+$ spectrum.[141] Improved constants for the (1,0) band were also obtained. Table 3 displays selected molecular constants obtained by these authors. Finally, Zackrisson et al. used velocity modulation spectroscopy to observe the (0,1) transition of $B^4\Sigma_u^+-X^4\Sigma_g^+$.[142] These authors analyzed a spin−orbit interaction between the $B^4\Sigma_u^+$ state and the nearby $2^2\Pi_u$ state.

Recent theoretical studies of C_2^+ include the MRD-CI calculations of Bruna et al.[143] and the large-scale coupled cluster calculations of Watts and Bartlett.[127] These latter authors calculated the equilibrium bond lengths, the vibrational frequency, the dissociation energy, and the electronic term energies for the ground $X^4\Sigma_g^+$ state and three excited electronic states. The C_2^{2+} dication has also been studied theoretically.[144]

VI. C_3

A. Early Experimental Work

The spectroscopy of C_3 has a long and rich history, and only a brief outline will be given here. Weltner and Van Zee provided an excellent discussion of the early developments in their review article.[1] The $A^1\Pi_u-X^1\Sigma_g^+$ emission spectrum of C_3, near 4050 Å, was first observed from the tail of a comet by Huggins in 1882.[145] These same bands were later observed in the laboratory by Herzberg in 1942,[146] and were finally identified by Douglas in 1951.[4] Rotational analysis of the $A^1\Pi_u-X^1\Sigma_g^+$ bands was consistent with a linear structure for C_3 in both the ground and upper electronic states. However, very early on it was recognized that the ground-state ν_2 bending frequency was extraordinarily low, about 63.3 cm^{-1}, indicating extremely anharmonic, large amplitude bending motion.[147] The spectroscopic characterization of gas-phase and matrix-isolated C_3 continued through the 1980s, resulting in the assignment of most of the ground and upper state vibrational frequencies in the $A^1\Pi_u-X^1\Sigma_g^+$ band (except ν_3' in the upper state), the characterization of the unusually large Renner−Teller effect in the $A^1\Pi_u$ state, and the discovery and characterization of a low-lying triplet electronic state manifold.[148-152] In 1988, several rotational absorption transitions arising from the ν_3'' fundamental vibration of C_3 were discovered in the circumstellar shell of a carbon star by Hinkle et al. (see Figure 6).[2] This same year a detailed characterization of the ground-state antisymmetric stretch vibration was accomplished by Hirota and coworkers using rotationally resolved infrared diode laser spectroscopy of C_3 clusters produced in a laser photolysis cell.[100,153] Many of the transitions observed were hot bands arising from excited bending levels. Analysis of these bands revealed unusual behavior of the C_3 bending mode, leading these authors to speculate on the possibility of a quasilinear bending potential. Below, we recount the new developments that have taken place since 1989.

B. Mid-IR and Far-IR Spectroscopy

Schmuttenmaer et al. performed a direct measurement of the low-frequency ν_2 bending vibration of C_3 using a tunable far-infrared laser spectrometer.[154] Rotationally cold clusters ($T_{rot} \approx 10$ K) were produced by laser vaporization of graphite in a supersonic molecular beam source. Six P-, Q-, and R-branch rovibrational transitions were measured with uncertainties in the line positions of about 0.000 02 cm^{-1}. Figure 7 displays the experimentally observed Q(6) rovibrational transition. This high precision measurement permitted an extremely accurate determination of the ground- and excited-state molecular parameters for the ν_2 bending state to be performed. Table 4 presents the ground- and excited-state molecular parameters. Due to the nuclear spin statistical weight of $^{12}C_3$ ($I = 0$), only rotational levels of positive parity are present. Therefore, the selection rules s ↔ s and + ↔ − prevent the ν_2 frequency from being measured by combination differences of infra-

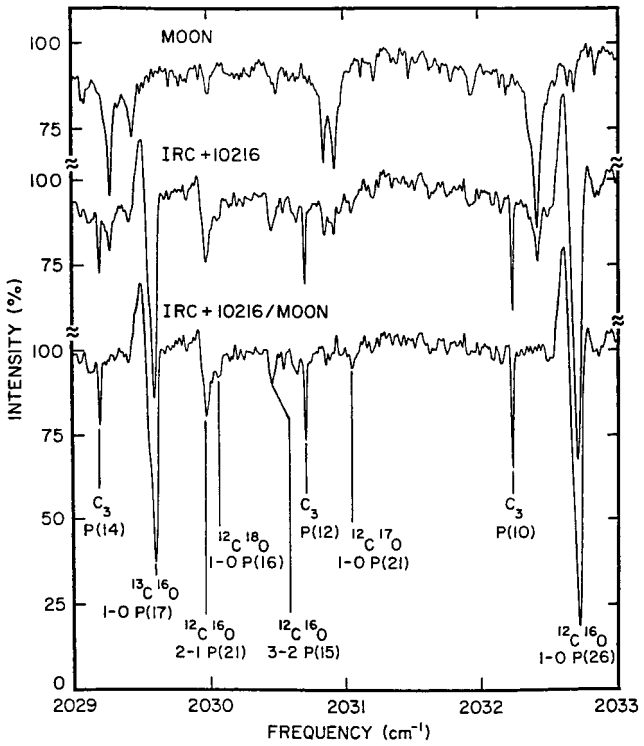

Figure 6. Part of the infrared absorption spectrum of the moon, the carbon star IRC+10216, and the ratio IRC+10216/moon observed using the 4-m telescope and the Fourier transform spectrometer located at the Kitt Peak National Observatory. Three rovibrational transitions of the ν_3 antisymmetric stretch of C_3 are displayed in the lower spectrum. The frequency scale was not corrected for the earth's velocity. (Reprinted with permission from ref 2. Copyright 1988 American Association for the Advancement of Science.)

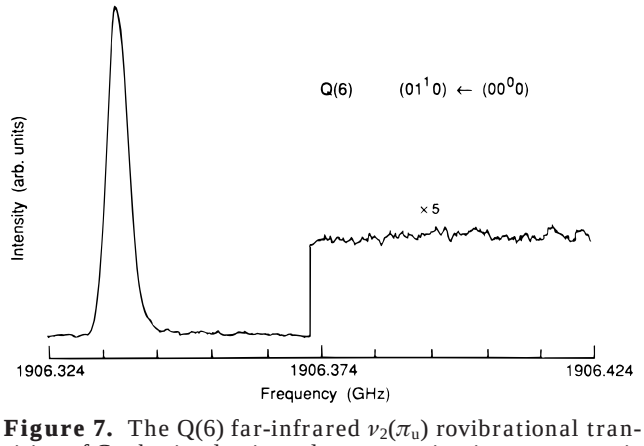

Figure 7. The Q(6) far-infrared $\nu_2(\pi_u)$ rovibrational transition of C_3 obtained using a laser vaporization−supersonic expansion source to produce the clusters and a tunable far-infrared laser spectrometer to record the spectrum. (Reprinted from ref 154. Copyright 1990 American Association for the Advancement of Science.)

red or optical transitions. Only a far-infrared absorption measurement can provide a direct observation of the ν_2 vibration. As a consequence of the large amplitude bending motion of C_3, the relative intensity of ν_2 was found to be of the same order as the ν_3 antisymmetric stretch, in contrast to earlier theoretical calculations that found the intensity of ν_3 to be 20−30 times larger than ν_2.[155] A more recent calculation of the CASSCF dipole moment surface for C_3 found the ν_2 band to be less intense than ν_3 by only a factor of 2, in much better accord with the experimental observation.[156]

Table 4. Molecular Parameters of the Fundamental Vibrations in the $X^1\Sigma_g^+$ Ground State of C_3[a]

	parameter	experiment	theory[b]
		$^{12}C_3$	
(00^00)	B_0 (cm^{-1})	0.4305723(56)[c]	0.42767
	D_0 (10^{-5} cm^{-1})	0.1472(13)[c]	0.15
	r_0 (Å)	1.277247(1)[c]	1.29452
(01^10)	ν_0 (cm^{-1})	63.416529(40)[c]	64.301
	B (cm^{-1})	0.4424068(52)[c]	0.43949
	D (10^{-5} cm^{-1})	0.2361(16)[c]	0.24
	q (cm^{-1})	0.005694(2)[c]	0.0056
(10^00)	ν_0 (cm^{-1})	1226.6[d]	1218.950
	B (cm^{-1})	0.41985(89)[d]	0.42212
	D (10^{-5} cm^{-1})	1.52(23)[d]	0.07
(00^01)	ν_0 (cm^{-1})	2040.0192(6)[e]	2040.589
	B (cm^{-1})	0.435704(19)[e]	0.43112
	D (10^{-5} cm^{-1})	0.4328(31)[e]	0.38
		$^{12}C_2{}^{13}C$	
(00^00)	B_0 (cm^{-1})	0.413743(21)[f]	
	D_0 (10^{-5} cm^{-1})	0.1398(42)[f]	
(00^01)	ν_0 (cm^{-1})	2027.2078(5)[f]	
	B (cm^{-1})	0.418743(23)[f]	
	D (10^{-5} cm^{-1})	0.1398(42)[f]	
		$^{13}C_3$	
(00^00)	B_0 (cm^{-1})	0.39024(15)[f]	
	D_0 (10^{-5} cm^{-1})	0.1220(33)[f]	
	r_0 (Å)	1.2890(1)[f]	
(00^01)	ν_0 (cm^{-1})	1961.9488(3)[f]	
	B (cm^{-1})	0.4101376(16)[f]	
	D (10^{-5} cm^{-1})	0.3470(45)[f]	

[a] Numbers in parentheses are uncertainties in the last digits. [b] Theoretical values are from a potential energy surface calculated at the CCSD(T)/177cGTO level using the discrete variable representation.[40] [c] Tunable far-infrared laser spectroscopy.[154] [d] SEP spectroscopy.[89] [e] Infrared diode laser spectroscopy.[153] [f] Infrared diode laser spectroscopy.[163]

Szczepanski and Vala measured the $\nu_1 + \nu_3$ combination mode of C_3 and its isotopomers trapped in solid Ar and Kr using FTIR spectroscopy.[157] The frequency of the $^{12}C_3$ band was 3245 cm^{-1} in Ar and 3243 cm^{-1} in Kr. From a normal-mode analysis of several isotopomers, the authors concluded that C_3 was bent in Ar and Kr matrices with a bond angle of 160.0°. This analysis also predicted a ν_2 frequency for C_3 in the matrix of 82 cm^{-1}, which agrees with a phosphorescence measurement of $2\nu_2 = 175$ cm^{-1} in solid Ne,[151] but is about 20% larger than the gas-phase value. The large matrix shifts of both the ν_1 and the ν_2 frequencies, as well as the negligible shift observed for ν_3, were also rationalized in terms of a bent structure. The authors found support for a bent geometry observed in these matrices in ab initio calculations by Kraemer et al.[155] and a MORBID analysis of rovibronic data by Jensen.[158] However, both of these works have since been superseded by more rigorous experimental and theoretical studies, in which the equilibrium structure is found to be linear, with a flat potential minimum, to be discussed in the next section.[159,160] Therefore, it seems that the agreement between the matrix structure and these earlier studies is simply fortuitous. The matrix behavior of C_3 appears to be similar to that of triplet C_4, also discussed below. In that case, all theoretical and experimental evidence support a linear structure

for gas-phase C_4, whereas ESR studies of triplet C_4 trapped in Ar and Ne was interpreted in terms of a slightly bent structure.[161,162] This interesting matrix effect deserves further investigation.

Finally, Moazzen-Ahmadi and McKellar have reported infrared diode laser observations of the ν_3 fundamental and the $(\nu_3 + \nu_2) - \nu_2$ hot band of $^{13}C_3$, as well as the ν_3 fundamental of $^{12}C^{12}C^{13}C$ in the gas phase.[163] Table 4 presents molecular constants obtained for these isotopomers.

C. Electronic Spectroscopy

1. The $^1\Sigma_u^+$ Ground State

The $A^1\Pi_u - X^1\Sigma_g^+$ band system of C_3 has been studied extensively for many years. Weltner and Van Zee[1] described early gas-phase and matrix studies of this band, which characterized the ground-state vibrational frequencies for several bending levels and stretch−bend combination levels. From these studies, it was recognized that C_3 possesses a very unusual ground-state potential surface, characterized by floppy bending motion and strong stretch−bend coupling interactions. The data seemed to indicate that the molecule may be quasilinear, with a barrier to the linear configuration that increases upon excitation of the antisymmetric stretch and decreases as the symmetric stretch is excited. Jensen used a MORBID Hamiltonian to analyze the bending potential, whereby parameters of an effective potential were fitted to experimentally determined vibronic energy levels.[158] This study yielded a barrier to linearity of 16.5 cm^{-1} and an equilibrium bond angle of 165.2°, which was also in agreement with ab initio calculations performed by Kraemer et al.[155]

Dispersed fluorescence (DF) and stimulated emission pumping (SEP) measurements of C_3 seeded in a molecular beam, performed by Rohlfing and Goldsmith[101] and Northrup and Sears,[89] have greatly increased the number of measured ground-state vibronic levels. Rohlfing and Goldsmith measured a large number of vibronic transitions using the DF technique after excitation to the $A^1\Pi_u$ state and a higher-lying UV state. Assignment of the DF spectra yielded frequency positions and molecular constants for ground state (ν_1, ν_2, ν_3) energy levels up to 17 000 cm^{-1}. These included states for which the vibrational quantum numbers were in the range $0 \le \nu_1 \le 8$, $0 \le \nu_2 \le 37$, and $0 \le \nu_3 \le 4$. SEP studies were then used to measure high resolution (0.08 cm^{-1}) spectra of the $(0\nu_2 1)$ ($\nu_2 = 1-13$) and $(6\nu_2 1)$ ($\nu_2 = 1-5$) states in the ground state of the UV band system. Similar measurements were performed on the $(0\nu_2 2)$ ($\nu_2 = 0-8$) and $(0\nu_2 4)$ ($\nu_2 = 0-14$) antisymmetric stretch−bend combination levels in the ground state of the $A^1\Pi_u - X^1\Sigma_g^+$ system. In a parallel study, Northrup and Sears measured SEP spectra of the pure bending levels $(0\nu_2 0)$ ($\nu_2 = 0-34$) and the symmetric stretch−bend combination levels $(1\nu_2 0)$ ($\nu_2 = 0-8$) and $(3\nu_2 0)$ ($\nu_2 = 4-8$).

This new DF and SEP data sampled regions of the potential energy surface that were much higher in energy than the data set that had been available previously. Therefore, a more accurate fit of the ground-state potential was possible. Northrup et al. used this extensive data set, along with the infrared and far-infrared results to fit an effective bending potential using the semirigid bender analysis.[39] The results of this analysis revealed that C_3 is *not* quasilinear in its ground state as had previously been thought, but rather possesses an extremely flat, broad potential minimum. A barrier to linearity appears when the antisymmetric stretch is excited, which increases upon further excitation. Excitation of the symmetric stretch, on the other hand, results in a more rigid linear configuration. Figure 8 displays the effective potentials obtained from this analysis for the pure bending levels and the stretch−bend combination levels.

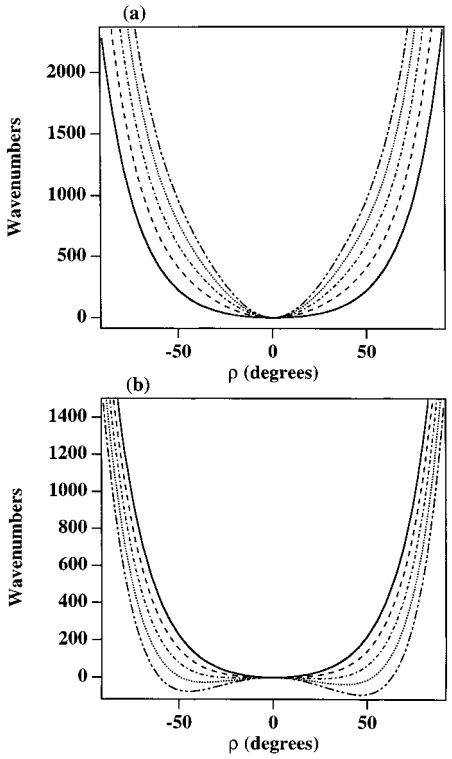

Figure 8. (a) Effective bending potentials from a semirigid bender analysis for $X^1\Sigma_g^+C_3$ plotted vs ρ, the supplemental bond angle.[39] The solid line is the zero point bending potential ($\nu_1 = 0$, $\nu_3 = 0$). The dotted curves are due to excitation of the ν_1 symmetric stretch: (- - -) $\nu_1 = 1$; (- · · ·) $\nu_1 = 2$; (· · ·) $\nu_1 = 3$; (- · · -) $\nu_1 = 4$. (b) Effective bending potentials due to increasing the ν_3 antisymmetric stretch. The solid curve is the zero point bending potential and the dotted curves are for $\nu_3 = 1-4$. The curve styles for each ν_3 level are the same as above. (Produced from data in ref 39.)

Several recent ab initio studies have been performed over the past few years that address the nature of this rather remarkable ground-state potential. The CISD study of Kraemer et al.,[155] which revealed a quasilinear bending potential for C_3, was superseded by the work of Jørgensen et al.[164] These authors performed a CASSCF calculation of the ground-state potential energy surface and the dipole moment surface. Later, Jensen et al. repeated this calculation using the full-valence CASSCF.[156] The qualitative features of the potential energy surface obtained were in agreement with the semirigid bender analysis, in that the equilibrium structure

was found to be linear with a flat, broad potential minimum. Also, the calculations correctly predicted the emergence of a barrier to linearity upon ν_3 excitation and the increased harmonicity of the potential with excitation of ν_1.

More recently, Mladenovic et al. investigated the C_3 equilibrium geometry, potential energy surface, and rovibrational energies using the CCSD(T) method with large basis sets of contracted Gaussian-type orbitals (cGTO).[40] The highest level of theory employed was CCSD(T)/255 cGTO, which was used to calculate the equilibrium geometry, yielding an equilibrium C=C bond length of 1.294 52(30) Å. An effective zero-point bending potential was obtained using a 222 cGTO basis set that corroborated the experimental potential. Finally, an analytical ground-state potential energy function for all three normal modes was calculated by fitting 108 energy points calculated at the CCSD(T)/177 cGTO level. This potential energy function was then used to calculate the term energies for energy levels up to 3000 cm^{-1}. Much more quantitative agreement with experiment was achieved with the CCSD(T) method, as compared to the CASSCF calculations, and the strong stretch−bend coupling was dealt with more adequately. Table 4 compares these theoretical calculations with the experimental parameters for the ground-state fundamental vibrations. A complete set of experimental and theoretical parameters can be found in ref 40.

2. The $A^1\Pi_u$ State

In addition to the unusual dynamics present in the ground state of the $A^1\Pi_u-X^1\Sigma_g^+$ band, the excited state was also found to exhibit its own unique properties. Many of the low-lying energy levels of the $A^1\Pi_u$ state were assigned in the 1965 work of Gausset et al.[147] Subsequently, numerous gas-phase and matrix experiments have been performed to characterize the band system. According to Weltner and Van Zee,[1] the vibrational frequencies of the symmetric stretch and the bending modes in the $A^1\Pi_u$ state were measured as $\nu_1' = 1085.8$ cm^{-1} and $\nu_2' = 307.9$ cm^{-1}.[1] Such a large increase in the excited electronic state bending frequency was thought to be due to the occupation of the π_g antibonding orbital, which stabilizes the linear configuration. The interaction of the bending vibration with the excited electronic configuration produces a strong Renner−Teller effect that splits the degeneracy of the electronic state into positive and negative symmetry components.[152] This effect is particularly intriguing in C_3 due to the large amplitude of the bending mode. Thus, the $A^1\Pi_u$ state has become a prototype system for studying Renner−Teller interactions in linear polyatomic molecules.[152]

While most of the recent effort to study the $A^1\Pi_u-X^1\Sigma_g^+$ band system has focused on the ground state, significant progress on the upper state has also been made. At the time of Weltner and Van Zee's review, no definitive assignment of the ν_3' frequency had been made. The nature of the antisymmetric stretch vibration in the $A^1\Pi_u$ state has been the source of some controversy over the intervening years and has only been resolved recently. Earlier estimates placed this frequency somewhere between 650 and 900 cm^{-1}. Recent attempts to measure ν_3' included the work of Balfour et al.,[98] whose tentative assignment of $2\nu_3'$ suggested a frequency of 808 cm^{-1}. Also, Baker et al. proposed an assignment of the (001)−(001) transition, leading to an estimate of 890.2 cm^{-1} for ν_3'.[165] All of these estimates place ν_3' substantially lower than the ν_3'' frequency in the ground state, indicating a large increase in the anharmonicity of the antisymmetric stretch in the $A^1\Pi_u$ state. However, a consensus on the exact value of the upper state frequency was reached only after the recent work of Izuha and Yamanouchi.[166] These authors observed new vibronic bands in the $A^1\Pi_u-X^1\Sigma_g^+$ system by laser induced fluorescence of C_3 clusters produced in a laser vaporization−supersonic expansion source. In particular, a series of vibronic bands in the 389−337 nm region were found to exhibit rotational structure characteristic of $^1\Sigma_u^+-{}^1\Sigma_g^+$ symmetry. $^1\Sigma_g^+$ vibronic symmetry in the $A^1\Pi_u$ state can occur through the Herzberg−Teller interaction with a higher-lying $^1\Sigma_u^+$ state and is realized only when both the $\nu_2^{+\prime}$ and the ν_3' quantum numbers take odd values. (The ν_2' states are labeled with + or − signs according to the symmetry of the Renner−Teller state.) Therefore, the lowest energy vibronic band in this region was assigned as the $(01^+1)-(000)$ transition in the $A^1\Pi_u-X^1\Sigma_g^+$ system. Given the known frequency of the $(01^+0)-(000)$ transition, it was then possible to estimate ν_3' to be about 539 cm^{-1}. This result was in conflict with the study by Baker et al.,[165] who assigned hot band transitions arising from the (001) ground state. One of these hot bands was tentatively assigned as the (001)−(001) transition, leading to the estimate of 890.2 cm^{-1} for ν_3' as mentioned above. Izuha and Yamanouchi's measurement implied a (001)−(001) transition frequency of 23 174 cm^{-1}, which is lower than the band assigned by Baker et al by 352 cm^{-1}. A direct measurement of the (001)−(001) transition by Izuha and Yamanouchi revealed a transition frequency of 23 177.174 cm^{-1}, leading to a ν_3' frequency of 541.7 cm^{-1}.[166] Furthermore, these authors reassigned the band observed by Baker et al. to the $(02^-1)-(001)$ transition. Izuha and Yamanouchi's work placed the ν_3' frequency lower than any previous estimate and implied an even larger anharmonicity along the antisymmetric stretch coordinate in the $A^1\Pi_u$ state than previously thought. Selected molecular parameters for the $A^1\Pi_u$ state are given in Table 5. A complete list of all the observed transitions in the $A^1\Pi_u$ state can be found in refs 98 and 166.

3. The $^1\Sigma_u^+$ State

$^1\Sigma_u^+$ is the next excited state above $A^1\Pi_u$ in the singlet manifold. Although the oscillator strength of the $^1\Sigma_u^+-X^1\Sigma_g^+$ band system is predicted to be very large ($f \sim 0.92$), it has been notoriously difficult to observe. Extrapolation of the $^1\Sigma_u^+-X^1\Sigma_g^+$ band origins that have been measured for C_7 through C_{15}[167] down to C_3 leads to a value of ~170 nm for this band. Chang and Graham tentatively assigned a series of

Table 5. Molecular Parameters of C_3 in the $A^1\Pi_u$, $a^3\Pi_u$, and $b^3\Pi_g$ States[a]

	parameter	experiment	theory[b]
$A^1\Pi_u$	T (cm^{-1})	24675.5[c]	24676
(000)	B_0 (cm^{-1})	0.4124[c]	
	r_0 (Å)	1.305[c]	
(010) Σ_g^-	ν_0 (cm^{-1})	136[c]	136
	B (cm^{-1})	0.4159[c]	
(010) Δ_g	ν_0 (cm-1)	259[c]	260
	B (cm^{-1})	0.4154[c]	
(010) Σ_g^+	ν_0 (cm-1)	480[c]	480
	B (cm^{-1})	0.4083[c]	
(100)	ν_0 (cm-1)	1085[c]	1085
	B (cm^{-1})	0.4094[c]	
(001)	ν_0 (cm-1)	541.7(1)[d]	
	B (cm^{-1})	0.41105(6)[d]	
	q (cm^{-1})	0.00402(3)[d]	
$a^3\Pi_u$	T (cm^{-1})	16930[c]	
(000)	A_0 (cm^{-1})	13.360(13)[e]	
	B_0 (cm^{-1})	0.416904(17)[e]	
	D_0 (10^{-5} cm^{-1})	0.030(2)[e]	
	λ_0 (cm^{-1})	−0.053(5)[e]	
	γ_0 (cm^{-1})	−0.0046(8)[e]	
	r_0 (Å)	1.2980(1)[e]	
$b^3\Pi_g$	T (cm^{-1})	$T(a^3\Pi_u)$+6482.3903(32)[f]	
(000)	A_0 (cm^{-1})	13.919(44)[f]	
	B_0 (cm^{-1})	0.424524(22)[f]	
	D_0 (10^{-5} cm^{-1})	0.0575(7)[f]	
	λ_0 (cm^{-1})	0.040(7)[f]	
	γ_0 (cm^{-1})	−0.0022(8)[f]	
	r_0 (Å)	1.2863(1)[f]	

[a] Numbers in parentheses are uncertainties in the last digits. [b] From a theory of the Renner−Teller effect.[152] [c] LIF spectroscopy.[98] [d] LIF spectroscopy.[166] [e] Infrared diode laser spectroscopy.[171] [f] Distributed feedback diode laser spectroscopy.[169]

absorption transitions observed in an Ar matrix near 189 nm to the $^1\Sigma_u^+-X^1\Sigma_g^+$ band of C_3, although this assignment has not been confirmed.[168] Part of the reason for the difficulties in observing this band may be due to strong interactions of the $^1\Sigma_u^+$ state with other excited electronic states, including $A^1\Pi_u$, as discussed above, as well as states in the triplet manifold. These interactions may distribute the intensity of the band over a very large energy range.

4. The $a^3\Pi_u$ and $b^3\Pi_g$ States

The metastable $a^3\Pi_u$ state was first observed through the $a^3\Pi_u-X^1\Sigma_g^+$ phosphorescence transition in Ar and Ne matrices.[148] The mechanism for populating the $a^3\Pi_u$ state was intersystem crossing from the (000) level of the $A^1\Pi_u$ state. Recently, Sasada et al.[169] detected the $b^3\Pi_g-a^3\Pi_u$ band system in the gas phase by measuring absorption from the $a^3\Pi_u$ state using a distributed-feedback diode laser spectrometer with a precision of about 0.001 cm^{-1}. Emission from the $b^3\Pi_g$ state was also observed with a Fourier transform spectrometer. C_3 molecules were prepared in the excited triplet states in a hollow cathode acetylene discharge. The lifetime of the $a^3\Pi_u$ state in the discharge cell was estimated to be about 50 μs as compared to a lifetime of 20 ms observed in the neon matrix. The rovibronic spectrum, centered at 6482.4 cm^{-1}, displayed splitting patterns characteristic of a triplet electronic state and also showed evidence for perturbation of the b state. Analysis of the band yielded the molecular constants for both the a and b states, some of which are shown in Table 5. Although a definitive vibrational assignment could not be made for this band, there was no evidence for bending excitation in either state, due to the absence of Renner−Teller splittings.

Smith et al. performed a more recent FTIR study of the $a^3\Pi_u$ state in order to assign some of the vibrational structure both within the a state and in transition to the b state.[170] In these experiments, the $a^3\Pi_u$ state was populated by laser excitation of C_3 trapped in solid Ar or Ne to the $A^1\Pi_u$ state, followed by intersystem crossing. Direct FTIR absorption spectra were then recorded from the a state. Several vibrational transitions within the a state were observed, including a band at 1455.3 cm^{-1}, which was assigned as ν_3, and a band at 2609 cm^{-1}, assigned as $\nu_1 + \nu_3$. Further evidence was provided for these assignments using isotopic substitution. $b^3\Pi_g-a^3\Pi_u$ vibronic transitions were observed as well. In particular, the matrix studies confirmed that the band measured in the gas phase by Sasada et al.[169] was the vibrationless origin. Tentative assignment of a band in the b state at 1303 cm^{-1} to the ν_1 stretch was also made. The assignment by Smith et al. of the ν_3 mode in the $a^3\Pi_u$ state was recently confirmed by the gas-phase measurements of Hwang et al.[171] These authors used infrared diode laser spectroscopy of $a^3\Pi_u$ C_3 produced in a hollow cathode discharge to observed the rotationally resolved ν_3 absorption spectrum centered at 1449.5255(22) cm^{-1}. Rotational and centrifugal distortion constants, spin−spin and spin−rotation interaction constants, Λ-doubling parameters, and spin−orbit coupling constants were all determined from the rotational analysis. Molecular parameters for C_3 in the vibrationless levels of the $a^3\Pi_u$ and $b^3\Pi_g$ can be found in Table 5.

Recently, Tokaryk and Civis observed $b^3\Pi_g \rightarrow a^3\Pi_u$ gas-phase emission spectra that involved transitions between excited bending vibrational energy levels in both the ground and upper states.[172] C_3 was prepared in the excited states using a methane discharge, and a Fourier transform spectrometer with a precision of 0.005 cm^{-1} was used to record the spectra. Both $^{12}C_3$ and $^{13}C_3$ bands were observed. These experiments afforded the authors a rare opportunity to study the Renner−Teller effect in a triplet electronic state, which was found to be large in both states. The following bands and their vibronic symmetries were analyzed in this work: $(010)^3\Sigma_u^+-(010)^3\Sigma_g^+$, $(010)^3\Sigma_u^--(010)^3\Sigma_g^+$, $(010)^3\Delta_u-(010)^3\Delta_g$, $(020)^3\Phi_g-(020)^3\Phi_u$, and $(030)^3\Gamma_u-(030)^3\Gamma_g$. Since these were all sequence bands, the Renner−Teller splittings and the bending vibrational energies for the two states could not be measured directly. However, an analysis of the spin−orbit parameters for the transitions yielded the value for the upper state Renner parameter $\epsilon' = +0.447$ and $\epsilon'' = +0.566$ for the lower state. These large, positive values for the Renner parameters are an indication of significant coupling between the bending vibrational and electronic angular momenta. From the Renner parameters, it was possible to estimate ν_2 for the upper and lower state. For the a state ν_2'' was found to be ∼505 cm^{-1}, and for the b state ν_2' was ∼345 cm^{-1}. Again, the analysis of the b state was complicated

by perturbations, the nature of which are as yet undetermined.

5. Other Band Systems

Lemire et al. observed a UV band system in the 266−302 nm region using resonant two photon ionization spectroscopy of C_3 produced in a pulsed supersonic expansion by laser ablation.[173] Dispersed fluorescence and SEP measurements due to excitation to this upper electronic state were discussed earlier in the description of Rohlfing and Goldsmith's work.[101] The vibronic symmetry of the band system was found to be $^1\Sigma_u^+-^1\Sigma_g^+$ with the bands arising from the (000) level of the ground electronic state. Lifetimes of the upper state vibronic levels ranged from 0.4 to 2.5 μs, which is consistent with a spin allowed transition. However, the low oscillator strength that was observed ($f \sim 0.001$) indicated that the transition was electric dipole forbidden. Thus, the authors proposed that the upper state was either $^1\Pi_g$ or $^1\Delta_g$ or possibly both. Oscillator strength for this band system was thought to result from mixing with the nearby $^1\Sigma_u^+$ state through the Herzberg−Teller interaction.

D. C_3 in the Interstellar Medium

Emission due to the $A^1\Pi_u-X^1\Sigma_g^+$ band of C_3 was first detected in the tail of a comet as early as 1882, and its ν_3 infrared absorption spectrum was observed more recently in the circumstellar shell of a carbon star,[2] as mentioned above. Recent efforts have been devoted to detecting the molecule in cold interstellar molecular clouds. Since numerous carbon chain molecules have been detected in these sources, it has been speculated that pure carbon clusters are present as well. However, since C_3 is nonpolar, the standard millimeter wave astronomy methods cannot be used to detect these clusters. Rather, we have sought to exploit the low-frequency bending vibration to perform far-infrared astronomy measurements. Precise laboratory far-infrared measurements of the ν_2 bending mode of C_3[154] were used to design a far-infrared astronomy search using a heterodyne detector on board the Kuiper Airborne Observatory.[5] Figure 9 displays the spectrum that was observed toward the Sagittarius B2 star forming region. The weak absorption signal at 63.7 km s^{-1} relative to the local standard of rest (LSR) has been tentatively identified as the R(2) transition of the C_3 bending mode. An LSR velocity near 63 km s^{-1} is characteristic of molecules near the core of Sgr B2.

Haffner and Meyer studied optical emission spectra from a translucent molecular cloud toward the star HD 147889.[6] They observed a weak emission feature at 4051.6 Å, which was tentatively assigned as blended Q-branch transitions of the $A^1\Pi_u-X^1\Sigma_g^+$ spectrum of C_3. P- and R-branch lines were not observed due to spectral congestion. From these two studies, it appears that C_3 is indeed present in the cold interstellar medium, although it is clearly difficult to detect. Unless larger carbon clusters are more abundant than C_3 in these sources, improvements in the signal-to-noise ratio may be necessary before detection of the larger species becomes feasible.

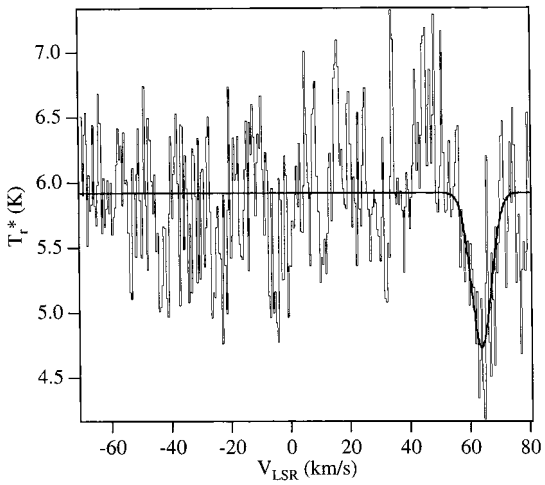

Figure 9. Far-infrared spectrum observed toward SgrB2 using the Kuiper Airborn Observatory. The weak absorption feature occurring at 63.7(6) km/s has been tentatively assigned as the R(2) transition in the ν_2 bending mode of C_3 at 1968.495 GHz. The solid curve is from a Gaussian fit to the absorption feature, yielding a fwhm peak width of 7.9(8) km/s. The observed LSR velocity and line shape are characteristic of molecular species near the core of SgrB2. (Reprinted from ref 5. Copyright 1995 Astronomical Society of the Pacific.)

E. C_3^-

Theoretical calculations predict that C_3^- is linear with a $^2\Pi_g$ ground electronic state.[174−176] Raghavachari calculated structures, atomization energies, and vibrational frequencies at the QCISD(T)/6-31G* level.[174] In particular, he predicted that the ν_2 bending vibration should occur at 399 cm^{-1}, which is substantially larger than the bending frequency for neutral C_3. This is indicative of a much more harmonic bending frequency for the anion due to the added stability imparted to the linear configuration by an additional electron in the π shell. More recently, Schmatz and Botschwina carried out large-scale coupled cluster calculations to study the linear ground state of C_3^-.[57] These authors determined the equilibrium bond length to be 1.3070 Å and the ν_1 symmetric stretch frequency to be 1177 cm^{-1} at the RCCSD(T)/255 cGTO level.

Until very recently, the only experimental technique used to measure ground-state vibrational frequencies of carbon cluster anions was the analysis of hot band transitions in anion photoelectron spectroscopy. Arnold et al. used this technique to measure a ν_1 symmetric stretch frequency of 1075 ± 100 cm^{-1} for C_3^-,[41] in good agreement with the RCCSD(T) prediction.[57] Szczepanski et al. have recently reported direct infrared absorption spectroscopy measurements of linear carbon cluster anions trapped in Ar matrices.[177,178] The clusters were formed by depositing laser vaporized graphite in the matrix and then irradiating with an electron beam or an Ar plasma to form anions. Figure 10 displays a region of the infrared spectrum obtained in this way. The authors assigned an absorption band at 1721.8 cm^{-1} to the ν_3 antisymmetric stretch. Measurements of

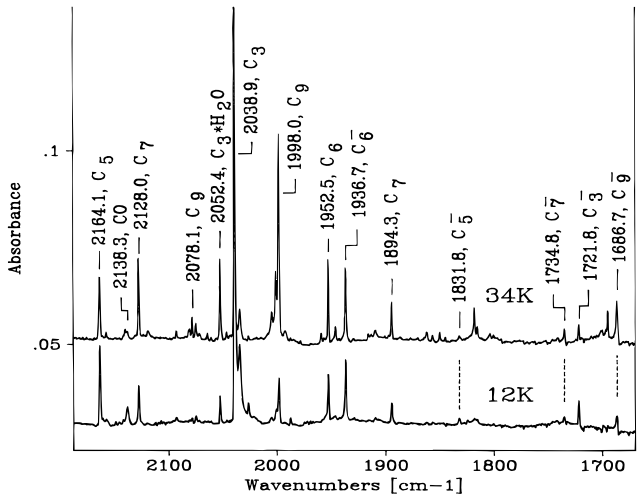

Figure 10. Infrared spectra of carbon clusters and carbon cluster anions trapped in an Ar matrix at 12 K (lower spectrum) and 34 K (upper spectrum). Anions were produced by irradiating the matrix with a low-energy electron source. (Reprinted from ref 177. Copyright 1997 American Chemical Society.)

all possible ^{13}C-substituted isotopomers confirmed this assignment,[178] which is also in agreement with Raghavachari's prediction of 1754 cm^{-1} for this band.[174]

F. C_3^+

C_3^+ is one of the magic number peaks observed in laser vaporization/mass spectra of carbon cluster cations. Nevertheless, experimental information regarding the structural and spectroscopic properties of this ion is extremely sparse. The only experimental data for C_3^+ was provided by Faibis et al. using Coulombic explosion imaging techniques.[179] These authors found that the ion possessed a bent geometry, although later analysis revealed that these results could also be interpreted in terms of a floppy linear structure.[180] All of the latest ab initio calculations agree that the ground state is a bent C_{2v} structure with a $^2B_2$ electronic state.[181−184] A bond length of 1.324 Å and a bond angle of 67.8° was calculated at the CCSD(T)/[4s3p2d1f] level of theory.[184] A $^2\Sigma_u^+$ linear structure was found to lie 6.8 kcal/mol higher in energy at this same level. Horgreve recently used configuration interaction methods to calculate the properties of the C_3^{2+} dication.[185] A linear $^1\Sigma_g^+$ structure with a bond length of 2.43 Å was predicted to be the ground state.

VII. C_4

A. Theory

Ab initio calculations predict that the even-numbered carbon clusters C_4, C_6, and C_8 possess two low-energy structural isomers, a linear chain with a $^3\Sigma_g^-$ ground electronic state, and a ^1A_g cyclic ring. An enormous number of theoretical studies have appeared in the literature on the C_4 cluster. These calculations have addressed the geometric structural parameters of various isomers, relative stabilities, vibrational frequencies and intensities, electronic structure, and thermodynamic properties. Most theoretical predictions agree on the two lowest energy structures, the cumulenic linear chain, and a bicyclic rhombic structure. (See Figure 1.) However, there has been considerable disagreement over which of these structures is the true global minimum. Theoretical calculations that have appeared since the Weltner and Van Zee review include a configuration interaction study of the electronic structure of linear C_4, C_6, C_8, and C_{10} by Liang and Schaefer.[186] In addition, Andreoni et al. used the Car−Parrinello method to obtain optimized structures for C_4 and C_{10}.[187] Adamowicz used first-order correlation orbitals to calculate electron affinities for both isomers of C_4 at the coupled cluster level.[85] Lammertsma et al. investigated the unusual nature of the cross-ring bond of the rhombic isomer using MP4 calculations.[188] Nygren and Pettersson used an internally contracted averaged coupled pair functional method to predict the lowest dipole allowed electronic transition of rhombic C_4,[189] finding a $^1B_{1u}-{}^1A_g$ transitions to occur at about 16 000 cm^{-1}.

Martin et al. studied the geometries, energetics, and vibrational frequencies of C_4 ab initio.[190] The geometry and frequency calculations were performed at the MP2 level, and the relative energies were obtained at the QCISD(T) level. They found the linear−cyclic energy difference to be 4.23 kcal/mol in favor of the rhombic structure. On the basis of their harmonic frequency calculations, these authors tentatively assigned a matrix absorption at 1284 cm^{-1} to cyclic C_4. Parasuk and Almlöf studied geometric and electronic structures and relative energies of the cumulenic and polyacetylenic linear chains and the rhombic structure at the CASSCF and MRCI levels.[70] These authors found the cumulenic linear structure to be slightly lower in energy than the rhombus. However, the relative energies were strongly influenced by the size of the basis set used, and larger basis sets tended to lower the energy of the rhombic structure. The linear acetylenic structure was found to occur at higher energies. They also investigated the possibility that linear C_4 may be slightly bent, as suggested by ESR studies,[161,162] by calculating a potential function for bending. They found the potential function to be very harmonic, indicating that triplet C_4 is linear and relatively (with respect to C_3) rigid.

The largest scale calculations that have been performed on C_4 to date are those of Watts et al. at the CCSD(T) level of theory.[71] These authors employed large basis sets, which included *f* and *g* functions, to calculate structures, vibrational frequencies, and relative energies for the ground electronic states of the cumulenic chain and the bicyclic ring. Geometries, frequencies, and IR intensities were obtained using various basis sets, the largest and most complete being the PVTZ basis. For the linear isomer, the calculated bond lengths were 1.284 and 1.306 Å for the inner and outer bond lengths, respectively, at this level. The authors attempted to characterize the effect of the basis set on the relative isomer energies by performing the calculations over

a range of basis sets. They found the relative energies to be extremely sensitive to the size of the basis and the type of basis employed, although the effect of increasing the polarization of the basis functions, as well as inclusion of triple excitations, tended to favor the rhombus. The highest level calculations performed (CCSD(T)/PVTZ) revealed the rhombic isomer to be the lowest energy structure, but only by about 1 kcal/mol.

Martin and Taylor recently studied the isomers of C_2-C_{10} at the CCSD(T) level using correlation consistent basis sets.[58] The aim of this study was to examine, in detail, the vibrational spectra and to attempt assignments of some of the unknown transitions in the spectrum of carbon clusters trapped in matrices. More recently, Martin et al. reevaluated their earlier assignment of the 1284 cm^{-1} matrix band to the ν_6 band of cyclic C_4.[191] The authors constructed a quartic force field at the CCSD(T) level and found a strong Fermi resonance interaction between the ν_6 mode and the $\nu_3 + \nu_5$ combination mode. This interaction raised the perturbed band origin to 1320 ± 10 cm^{-1}, casting doubt on the earlier assignment.[190]

Given the remarkable sensitivity of the linear−cyclic energies, as well as the spectroscopic parameters, to the details of the calculation, it is quite apparent that experimental constants are badly needed for the cyclic system.

B. Experiment

1. The Rhombic Isomer

The goal of characterizing the rhombic isomer of C_4 by direct high-resolution spectroscopic measurements continues to elude researchers. Evidence for a rhombic C_4 isomer has been obtained by researchers using Coulomb explosion imaging.[192,193] In this technique, carbon cluster anions are produced by Cs ion sputtering of a graphite surface. The ions are then mass selected and accelerated to 12 MeV, and the electrons are photodetached by a UV laser intersecting the beam. The neutral clusters are then atomized in an "explosion" that results from electron stripping in a high-field region. From the spatial distribution of the charged fragments, it is possible to infer the structure of the molecule before the explosion occurred. Algranati et al. observed the rhombic C_4 cluster using this technique.[192] Later, Kella et al. used a combination of Coulomb explosion imaging and laser photodetachment to characterize the isomers of C_4.[193] The observation of three distinct photodetachment wavelengths was taken as evidence for three different structural isomers for the anions and the neutrals. Coulomb explosion after photodetachment at each wavelength revealed the three structures to be linear, rhombic, and three dimensional. The three-dimensional structure was assumed to be tetrahedral, although no other experimental or theoretical evidence exists for this isomer. A weakness in the Coulomb explosion approach is the lack of knowledge of the vibrational state distribution of the neutral fragment prior to the explosion. Vibrational excitation in these floppy systems could obscure the analysis of the fragmentation pattern.[180]

2. The Linear Isomer

Much progress has been made toward the characterization of linear C_4 since the publication of Weltner and Van Zee's review. Linear C_4 was first observed using electron spin resonance (ESR) spectroscopy of carbon clusters trapped in solid Ne and Ar matrices by Graham et al.[194] The results were consistent with a linear $^3\Sigma$ structure. Later, Cheung and Graham observed ESR spectra of C_4 trapped in an Ar matrix, in which the clusters were produced by UV photolysis of C_4H_2.[161] Under these conditions, the ESR line widths were more than 10 times narrower than had been observed in the previous experiments, revealing splittings to the xy_1 and xy_2 lines that were interpreted as evidence for a slightly bent structure. The authors ruled out the possibility that the splitting could arise from nonequivalent matrix sites since no changes in the splittings were observed after annealing the matrix. Jiang and Graham later repeated the ESR measurements for C_4 trapped in a Ne matrix.[162] Since the same splittings were observed in Ne as in Ar, the authors reasoned that, if the observed splittings were caused by interactions with the matrix, then these interactions should change for the different matrices. Otherwise, the bent structure might be an intrinsic property of the molecule. However, no evidence for a bent structure of gas-phase C_4 has been obtained, either from ab initio theory, as discussed above, or from subsequent gas-phase measurements. Additional support for a bent structure in matrices was initially claimed by Shen et al. from the assignment of an IR absorption band at 1699.8 cm^{-1} to the $\nu_2 + \nu_5$ stretch−bend combination band of *cis*-bent C_4 in an Ar matrix.[195] However, this band was recently reassigned to the ν_3 antisymmetric stretch of the C_4^- carbon cluster anion.[196]

Prior to the Weltner and Van Zee review, numerous infrared absorption transitions had been observed from polyatomic carbon clusters trapped in cryogenic matrices, but there was great confusion as to the assignments of these bands. For example, Thompson et al. tentatively assigned a matrix absorption at 1544 cm^{-1} to linear C_5 and a band at 2164 cm^{-1} to linear C_4.[197] Subsequent ab initio calculations suggested a much lower frequency for C_4 and recommended that these assignments be reversed.[198] Later, the 2164 cm^{-1} band was reassigned to C_5, based on isotopic substitution measurements by Vala et al.,[199] while Shen and Graham confirmed the assignment of the 1544 cm^{-1} band to the ν_2 antisymmetric stretch of linear C_4.[200] More recently, Withey et al. performed Fourier transform far-infrared spectroscopy of C_4 in an Ar matrix in an attempt to observe the ν_5 bending frequency.[201] An absorption band at 172.4 cm^{-1} was observed that could be assigned to the C_4 bending mode based on isotope substitution. Besides the ν_2 band of C_3 discussed above[154] this measurement represents the only bending mode of a linear carbon cluster to be observed directly in the infrared.

Linear C_4 was first detected and characterized in the gas phase by Heath and Saykally, who measured

the ν_3 antisymmetric stretch using tunable infrared diode laser spectroscopy.[202] The clusters were produced by pulsed UV laser vaporization of graphite and expanded into an Ar jet. Fourteen rovibrational transitions were assigned to the ν_3 fundamental. The observed band origin of 1549 cm^{-1} confirmed the assignment of the matrix band, which was slightly red-shifted from the gas-phase value due to the matrix perturbation effect. Triplet splitting was observed only in the transition arising from the lowest rotational level, but the spin splitting was not analyzed due to the low signal-to-noise ratio for this transition. Moazzen-Ahmadi et al. performed diode laser spectroscopy measurements on this same band by producing the clusters in a hollow cathode acetylene discharge, wherein the observed rovibrational transitions were extended out to $N = 35$ in both the P- and the R-branch.[203] These authors found that the rotational assignment of Heath and Saykally was slightly in error and presented a corrected assignment. From the revised rotational constant, a value of 1.30055(5) Å was obtained for the average ground-state C═C bond length, in excellent agreement with the averaged CCSD(T)/PVTZ result of 1.2999 Å.[71] The average bond length obtained from experiment confirms that linear C_4 exists in a cumulenic bonding configuration. Bond lengths for the acetylenic structure were calculated at the CISD/DZP level to be 1.213 and 1.374 Å for the triple and single bonds, respectively, yielding an average bond length of 1.267 Å, which is significantly smaller than the experimental value.[190] At this same level of theory, the average bond length for the cumulene was 1.300 Å, again in agreement with experiment.

In addition to the fundamental band, Moazzen-Ahmadi et al. also observed $(\nu_3 + \nu_5) - \nu_5$ hot band transitions.[203] On the basis of their measurement of q_5, the *l*-type doubling constant for the ν_5 bending mode, it was possible to estimate the lowest bending frequency. This estimated value was 160 ± 4 cm^{-1}, in reasonable agreement with the matrix work of Withey et al.[201] Because of the high temperature of the discharge, the lower rotational lines, for which triplet splittings might be observable, were not measured. Therefore, the spin−spin and spin−rotation interactions have not yet been characterized in the gas phase. Recently, the $(\nu_3 + \nu_4) - \nu_4$ hot band was also observed by Moazzen-Ahmadi and Thong.[37] From these measurements, the frequency of the ν_4 bending mode was estimated to be 352 ± 15 cm^{-1}. Representative experimental data are displayed in Figure 11. Molecular constants for the fundamental vibrations of C_4 are presented in Table 6. All of the gas-phase spectra that have been observed are consistent with that of a relatively rigid linear molecule. The very large amplitude bending motion that was present for C_3 is not evident for C_4, and there is no evidence for a bent structure in the gas phase. We are left to conclude that the bent structure observed in Ne and Ar matrices is due to some unusual matrix interaction that is apparently present in both matrices.

Additional spectroscopic information for gas-phase linear C_4 was provided by the anion photoelectron spectroscopy measurements of Arnold et al.[41] Carbon cluster anions produced by laser vaporization of graphite were mass selected using time-of-flight techniques. The electrons were then photodetached from the negative ions, and their kinetic energies were measured. Peaks in the electron kinetic energy distribution corresponded to transitions between vibronic states of the anions and the neutrals. Figure 12 displays the photoelectron spectra observed for the even-numbered C_4−C_8 cluster anions. From these data it was possible to measure vibrational frequencies of the neutral species. In some cases, tentative

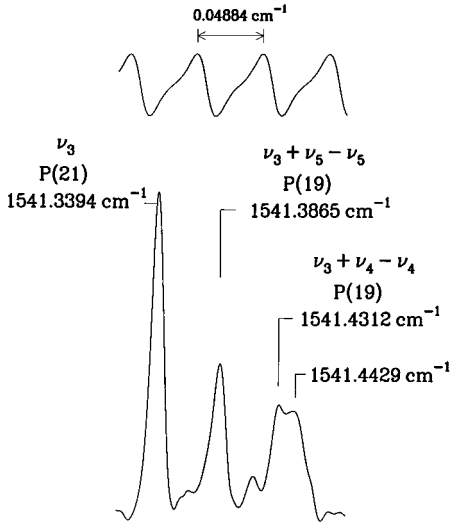

Figure 11. Infrared rovibrational transitions of the ν_3 antisymmetric stretch and associated hot bands of linear C_4 (lower trace). A hollow cathode discharge was used to produce the clusters, and a tunable diode laser spectrometer was used to record the spectrum. The upper trace shows the fringe spectrum of an Etalon used for wavenumber calibration. (Reprinted with permission from ref 37. Copyright 1995 Elsevier Science B.V.)

Table 6. Molecular Parameters of $X^3\Sigma_g^-$ C_4[a]

	parameter	experiment	theory
	B_0 (cm^{-1})	0.166111(7)[b]	
	D_0 (10^{-7} cm^{-1})	0.282(14)[b]	
	λ_0 (cm^{-1})	0.128(3)[c]	
	γ_0 (cm^{-1})	−0.0006(2)[c]	
	$\bar{r}_0$ (Å)	1.30055(5)[b]	1.306 1.284[d]
$\nu_1(\sigma_g)$	ν_0 (cm^{-1})	2032(50)[e]	2156[f] 2082.7[g]
$\nu_2(\sigma_g)$	ν_0 (cm^{-1})		936[f] 911.3[g]
$\nu_3(\sigma_u)$	ν_0 (cm^{-1})	1548.6128(4)[b] 1543.4[h]	1600 [316][f]
	B (cm^{-1})	0.165406(66)[b]	
	D (10^{-7} cm^{-1})	0.279(14)[b]	
$\nu_4(\pi_g)$	ν_0 (cm^{-1})	339(55)[e] 352(15)[i]	447[f]
	B (cm^{-1})	0.166808(70)[j]	
	D (10^{-7} cm^{-1})	0.239(25)[j]	
	q (cm^{-1})	0.000184(6)[j]	
$\nu_5(\pi_u)$	ν_0 (cm^{-1})	160(4)[k] 172.4[l]	203 [46][f]
	B (cm^{-1})	0.166862(58)[b]	
	D (10^{-7} cm^{-1})	0.265(16)[b]	
	q (cm^{-1})	0.000366(4)[b]	

[a] Numbers in parentheses are uncertainties in the last digits. Numbers in brackets are calculated IR intensities [km/mol]. [b] Infrared diode laser spectroscopy.[203] [c] ESR spectroscopy in an Ar matrix.[200] [d] CCSD(T)/PVTZ, outer and inner equilibrium bond lengths.[71] [e] Anion photoelectron spectroscopy.[41] [f] CCSD(T)/cc-pVTZ.[58] [g] RCCSD(T)/256 cGTO.[57] [h] Ar matrix.[200] [i] Estimated from the *l*-type doubling constant.[37] [j] Infrared diode laser spectroscopy.[37] [k] Estimated from the *l*-type doubling constant.[203] [l] Ar matrix.[201]

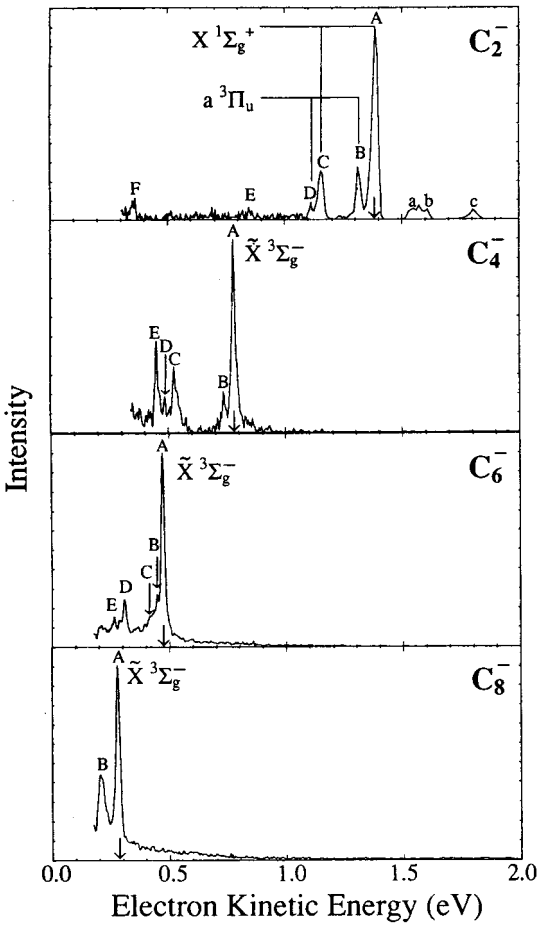

Figure 12. Photoelectron spectra of even-numbered C_2^-–C_8^- at 266 nm. Arrows indicate the electron affinity. (Reprinted with permission from ref 41. Copyright 1991 American Institute of Physics.)

assignments of excited electronic states for the anions and the neutrals were made as well. Photoelectron spectroscopy measurements are complimentary to infrared absorption experiments in that only symmetric vibrational states are observed for the linear carbon clusters, as opposed to direct absorption, which only measures antisymmetric vibrations. The photoelectron spectra observed for C_4 were consistent with linear structures for both the anion and the neutral. Vibrational frequencies for neutral C_4 that were deduced from the spectra were 2032 ± 50 cm^{-1} for the ν_1 symmetric stretch and 339 ± 55 cm^{-1} for the ν_4 bending mode. This latter result was consistent with the estimate for ν_4 deduced from Moazzen-Ahmadi and Thong's hot band analysis.[37]

C. Excited Electronic States

Three electronic states can be derived from the ground electron configuration of linear C_4, the ground $^3\Sigma_g^-$ state, a $^1\Delta_g$, and a $^1\Sigma_g^+$ state. Theoretical predictions for the excitation energies of these states as well as two low-lying $^3\Pi$ states can be found in Weltner and Van Zee's review.[1] More recently, Liang and Schaefer calculated the energies of the $^3\Sigma_g^-$ ground states, the two symmetry components of the $^1\Delta$ states, and a state that results from mixing of the $^1\Delta$ and the $^1\Sigma_g^+$ states, denoted as $^1(\Sigma D)$ for the even-numbered linear C_4–C_{10} clusters.[186] These calculations were performed at the SCF and CISD levels of theory using the DZP basis. Theoretical predictions for the low-lying electronic states of the rhombic isomer were also given by Weltner and Van Zee. The only calculation on the electronic states of the rhombic isomer to appear since their review is that of Nygren and Petterson mentioned above.[189]

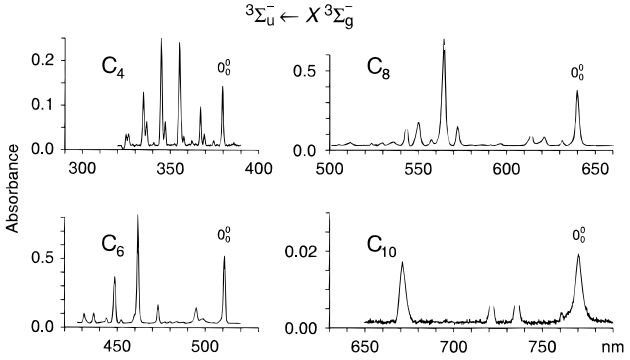

Figure 13. $^3\Sigma_u^- \leftarrow X^3\Sigma_g^-$ electronic absorption spectra of mass-selected, even-numbered linear C_4–C_{10} deposited in Ne matrices at 5 K. (Reprinted with permission from ref 46. Copyright 1997 Royal Society of Chemistry.)

Several low-lying excited electronic states of C_4 were recently assigned by Neumark and co-workers using photoelectron spectroscopy of mass-selected C_4^-, produced in a pulsed electric discharge/supersonic molecular beam source.[42] These were the $^1\Delta_g$, $^1\Sigma_g^+$, $^3\Pi_g$, $^3\Pi_u$, $^1\Pi_u$, and $^1\Pi_g$ states, with term energies of 0.332, 0.93, 0.82, 0.93, 1.16, and 1.41 ($\pm\sim$0.02) eV, respectively.

Numerous optical and UV transitions have been observed for carbon clusters trapped in rare gas matrices, which are due to clusters larger than C_3.[204,205] Assignments for most of these transitions are very tentative. The most conclusive experimental data on the electronic spectra of linear carbon clusters trapped in matrices has been provided since 1995 by Maier and co-workers.[167,206–208] These authors used mass selection of carbon cluster anions, produced either in a hot cathode discharge or a Cs ion sputter source. The mass-selected ions were then deposited in a solid Ne matrix. UV/visible and IR absorption spectra of both anionic and neutral carbon clusters in the matrix were then recorded. Neutral carbon clusters were produced from the anions by irradiating the matrix with the output of a medium-pressure Hg lamp. For example, researchers from this group have measured $^3\Sigma_u^- \leftarrow X^3\Sigma_g^-$ vibronic transitions for even-numbered linear carbon clusters in the C_4–C_{10} size range.[206–208] Figure 13 displays the observed spectra. A near linear dependence of the band origin wavelength on the cluster size has been observed, as would be predicted by the free electron molecular orbital model. The C_4 origin was observed at $26\,323 \pm 15$ cm^{-1},[208] which contradicts an earlier assignment of a 22 600 cm^{-1} band discussed in Weltner and Van Zee's review.[1] At the same time, the authors also observed the 1547.2 cm^{-1} vibrational transition.[208]

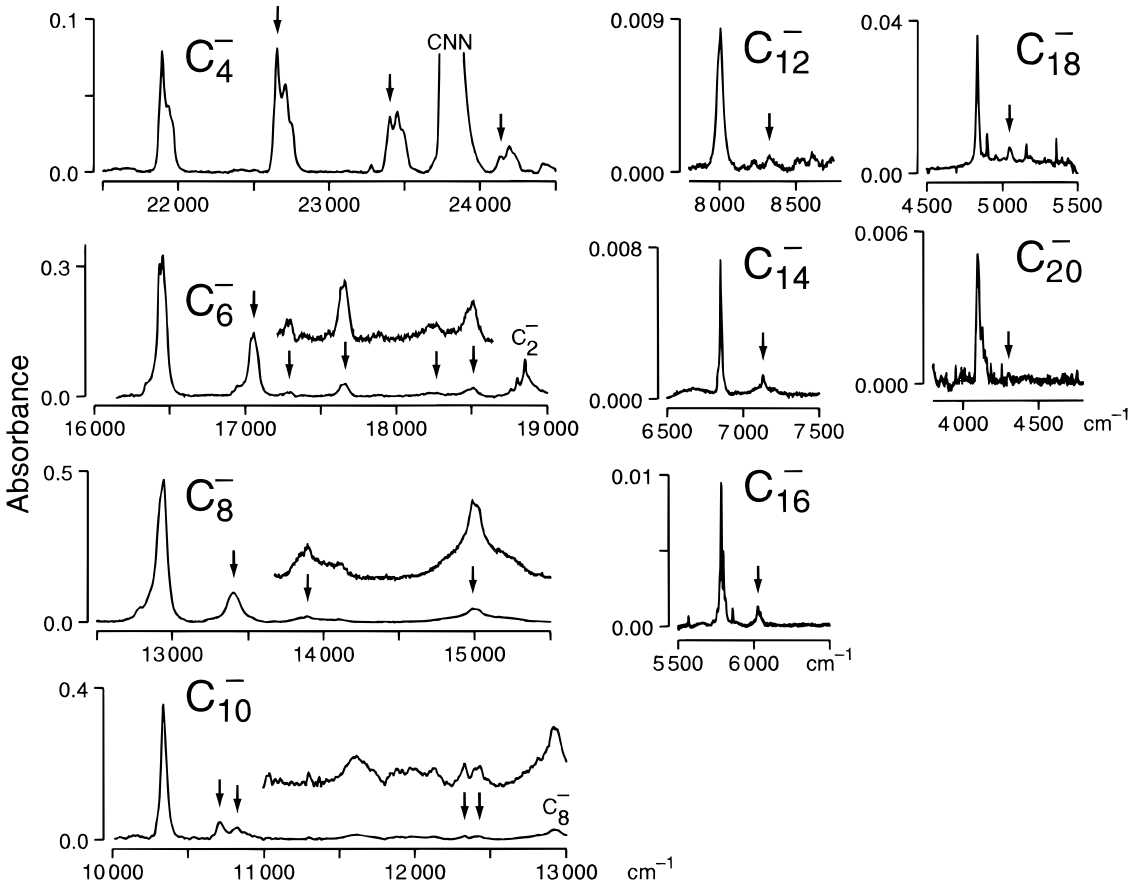

Figure 14. $C^2\Pi-X^2\Pi$ electronic absorption spectra of mass-selected, even-numbered C_4^-−C_{20}^- deposited in Ne matrices at 5 K. (Reprinted with permission from ref 207. Copyright 1995 American Institute of Physics.)

D. C_4^-

The C_4^- cluster ion is predicted to be linear with a $^2\Pi_g$ ground electronic state. Using coupled cluster techniques, Watts et al. found the linear isomer to be 30 kcal/mol more stable than the rhombic structure.[209] This is in contrast to both the neutral species and the cation, for which the rhombus and the linear chain are nearly isoenergetic. The linear ground state of C_4^- has been studied using the first-order correlation orbital method (FOCO), SCF, MBPT, and coupled cluster techniques.[57,176,209,210] Schmatz and Botschwina used large-scale coupled cluster calculations to determine values for the ground-state equilibrium bond lengths of 1.336 and 1.277 Å for the inner and outer bond lengths, respectively at the RCCSD(T)/256 cGTO level of theory.[57] Symmetric stretch vibrational frequencies were predicted to be 2082.7 and 911.3 cm^{-1} for ν_1 and ν_2, respectively. In addition, these authors calculated molecular parameters for three bound excited electronic states in the doublet manifold.

Linear carbon cluster anions are particularly interesting because they possess excited electronic states that are stable with respect to electron autodetachment. This makes them amenable to study by various electronic spectroscopy techniques. Maier and co-workers have measured electronic spectra for mass-selected carbon cluster anions deposited in Ne matrices in the C_4^- to C_{20}^- size range.[206,207,211−214] Figure 14 displays the $^2\Pi-X^2\Pi$ spectra observed for these clusters. For C_4^-, the $C^2\Pi_u-X^2\Pi_g$ vibrationless origin occurs at 21 896 cm^{-1}.[207] A more recent study reported observations of the $A^2\Sigma_g^+-X^2\Pi_g$, the $B^2\Sigma_u^+-X^2\Pi_g$, the $(2)^2\Pi_u-X^2\Pi_g$, and the $(3)^2\Pi_u-X^2\Pi_g$ transitions.[212] Vibrationless origins for these transitions were measured to be 8293, 10 789, 26 069, and 28 868 cm^{-1}, respectively. Schäfer et al. measured the $C^2\Pi_u-X^2\Pi_g$ emission spectra of mass-selected C_4^- in a Ne matrix to determine lower state fundamental vibrational frequencies.[211] Their measurements of the ν_1 and ν_2 symmetric stretch frequencies of 2047 ± 20 and 936 ± 20 cm^{-1}, respectively, were in excellent agreement with the calculations of Schmatz and Botschwina.[57] The ν_4 symmetric bending frequency was also observed at 396 ± 20 cm^{-1}.

Zhao et al. have studied the electronic spectra of gas-phase carbon cluster anions using resonant two-photon photodetachment (R2PD) techniques.[48,215] Carbon cluster anions produced in a pulsed discharge/supersonic expansion source were mass selected and then photodetached using one and two-color R2PD. The $C^2\Pi_u-X^2\Pi_g$ vibronic spectrum of C_4^- was observed with a vibrationless origin of 21 872 cm^{-1},[215] which agreed well with the Ne matrix work.[207] By minimizing the power broadening of the photodetachment transitions, Zhao et al. were able to resolve the rotational structure of the $C^2\Pi_u-X^2\Pi_g$ R2PD spectrum,[215] making C_4^- the largest carbon cluster ion for which a rotationally resolved spectrum has been recorded. Figure 15 displays the experimental data, and Table 7 presents selected molecular parameters derived from the rotational analysis. Very

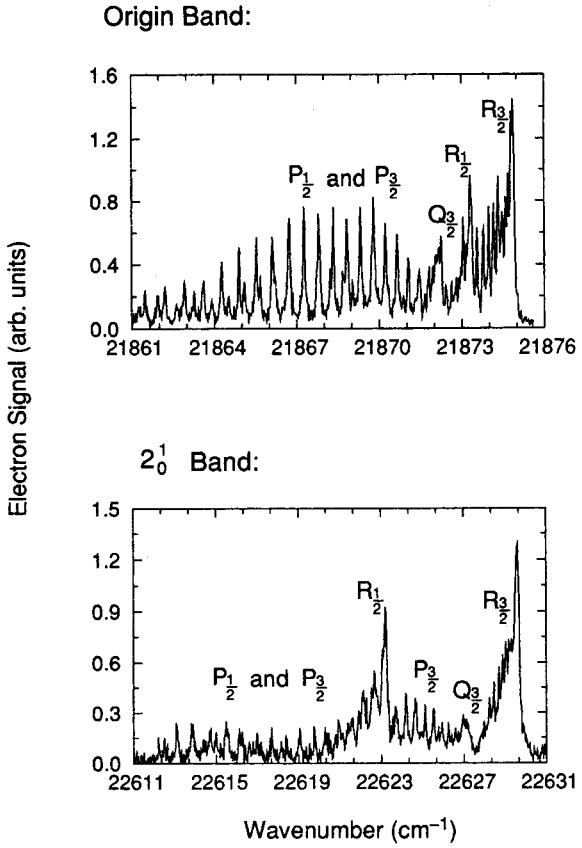

Figure 15. High-resolution $C^2\Pi_u - X^2\Pi_g$ two-color resonant multiphoton detachment spectrum of C_4^-. (Reprinted with permission from ref 215. Copyright 1996 American Institute of Physics.)

Table 7. Molecular Parameters for the Ground Vibrational States of the $X^2\Pi_g$ and $C^2\Pi_u$ Electronic States of C_4^-[a,b]

parameter	$X^2\Pi_g$	$C^2\Pi_u$
T_0 (cm^{-1})	0.0	21871.525(7)
B_0 (cm^{-1})	0.16663(22)	0.15651(25)
A_0 (cm^{-1})	−39(9)	−37(9)

[a] Adapted from ref 215. [b] Numbers in parentheses are uncertainties in the last digits.

recently, Tulej et al. observed the $(2)^2\Pi_u - X^2\Pi_g$ and $(3)^2\Pi_u - X^2\Pi_g$ transitions in the gas phase using two-color photodetachment spectroscopy, with band origins of 25 989 and 28 717 cm^{-1}, respectively.[50]

As mentioned above, Szczepanski et al. have recently identified an infrared absorption band at 1699.8 cm^{-1}, observed in an Ar matrix, as the ν_3 antisymmetric stretch of C_4^-.[196] This new assignment was based on isotopic substitution measurements as well as the different behavior observed for this band, with respect to the 1544 cm^{-1} band of neutral C_4, after irradiating the matrix with an electron beam.

E. C_4^+

In contrast to C_4^-, there is very little information available about the C_4^+ cation. Raghavachari performed HF and MP4 calculations on the structural isomers of C_2 through C_6 and their ions.[216] His results for C_4^+ predicted that, like the neutral, a linear chain and a rhombic isomer were nearly isoenergetic. The linear and rhombic isomers were found to possess $^2\Pi_g$ and $^2B_{1u}$ ground electronic states, respectively.

VIII. C_5

A. Theory

The ab initio calculations of Raghavachari and Binkley were the first to consider relative energies for linear and cyclic isomers of C_5.[67] These calculations concluded that the ground-state structure was a $^1\Sigma_g^+$ linear cumulene and was more stable than the lowest energy cyclic isomer by over 60 kcal/mol. More recent calculations support this prediction.[217] C_5 is the largest carbon cluster to be detected in an astrophysical source, having been observed in the circumstellar shell of the carbon star IRC+10216 via its ν_3 infrared absorption spectrum.[3] A large body of theoretical work on C_5 already existed prior to the Weltner and Van Zee review. Most of this work concentrated on the ground-state geometry, vibrational frequencies and intensities, and thermodynamic functions. More recent work has extended this treatment to higher levels of sophistication. Kurtz and Adamowicz calculated bond lengths and vibrational frequencies using first-order correlation orbitals along with coupled cluster techniques[217] and at the MP2/6-31G* level.[218] Botschwina and Sebald used the CEPA-1 (coupled electron pair approximation) approach with basis sets of contracted Gaussian-type orbitals.[219] One of the purposes of this study was to calculate the frequency and intensity of the ν_3 mode, which had just been measured in the gas phase[220] and in IRC+10216.[3] On the basis of their intensity calculation, the authors recommended a value of 5×10^{13} cm^{-2} for the column density of C_5 in IRC+10216.

Recently, Botschwina reported the largest scale calculation that has been performed on the C_5 cluster to date.[74] He used the CCSD(T) method with all electrons correlated and a very large basis set of 275 cGTO's (cc-pVQZ) to calculate the ground-state geometry and the harmonic vibrational frequencies. SCF, MP2, and CCSD calculations were also performed using the same basis set for comparison. The estimated accuracy of bond lengths calculated at the CCSD(T)/cc-pVQZ level is 0.001 Å. For C_5, Botschwina obtained 1.2896 and 1.2819 Å for the inner and outer equilibrium bond lengths, respectively. Force constants, the equilibrium rotational constant, and the frequencies of the ν_1 and ν_2 modes were also calculated.

Martin and Taylor calculated bond lengths, vibrational frequencies, and intensities at the CCSD(T)/cc-pVDZ level of theory.[58] By scaling the calculated vibrational frequencies for several linear carbon chains with known experimental values, the authors predicted the frequency of the ν_4 antisymmetric stretch to be 1442.5 ± 28 cm^{-1}, which is in agreement with a matrix study by Kranze and Graham.[221]

B. Experiment

C_5 was first identified by its 2164 cm^{-1} ν_3 infrared absorption transition in a rare gas matrix.[199] In a

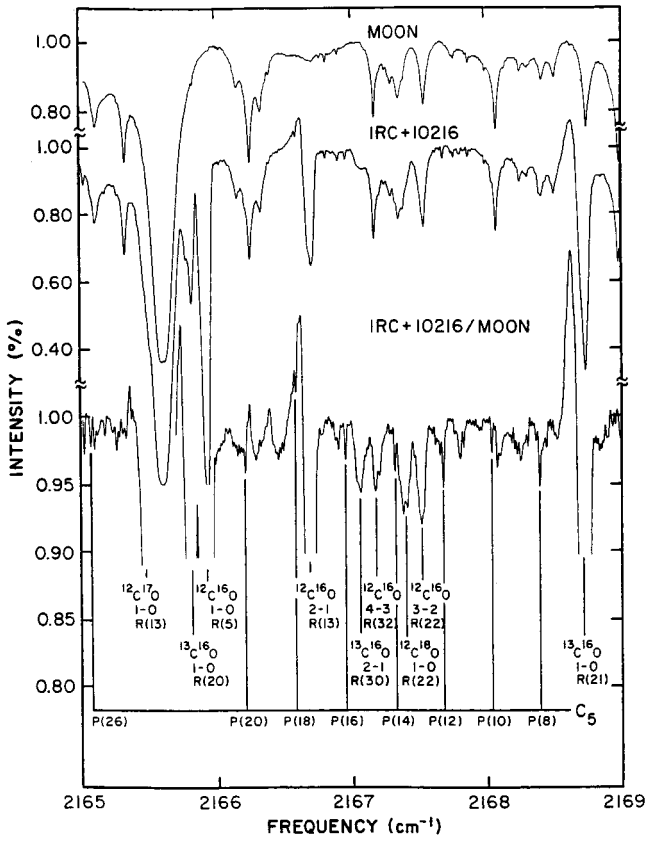

Figure 16. Part of the infrared absorption spectrum of the moon, IRC+10216, and the ratio IRC+10216/moon. The spectra were obtained using the 4-m telescope and the Fourier transform spectrometer at the Kitt Peak National Observatory. The lower spectrum displays several rovibrational transitions of the ν_3 antisymmetric stretch of C_5. The frequency scale has not been corrected for the earth's velocity. (Reprinted with permission from ref 3. Copyright 1989 American Association for the Advancement of Science.)

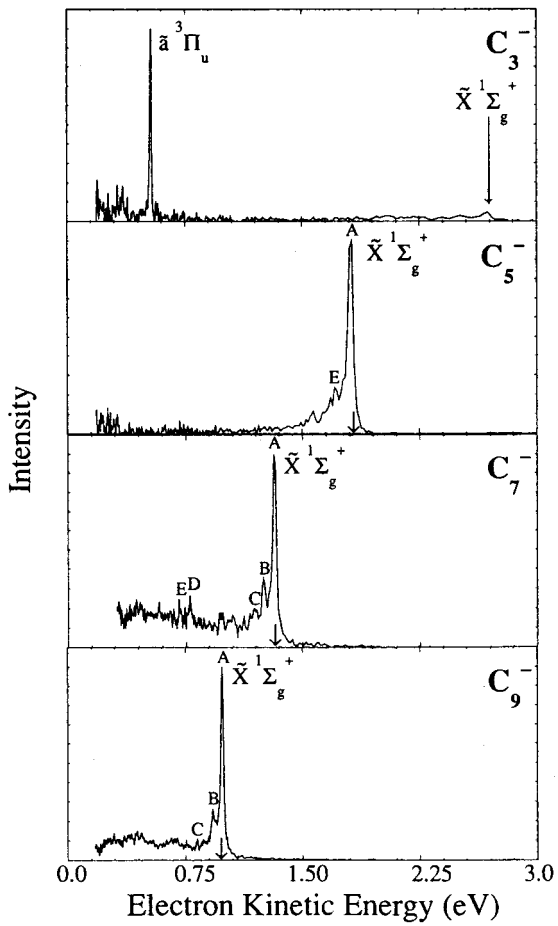

Figure 17. Photoelectron spectra of odd-numbered C_3^-–C_9^- at 266 nm. Arrows indicate the electron affinity. (Reprinted with permission from ref 41. Copyright 1991 American Institute of Physics.)

more recent study, Kranze and Graham assigned a much weaker Ar matrix absorption at 1446.6 cm^{-1} to the ν_4 antisymmetric stretch.[221] Szczepanski et al. recently assigned Ar matrix absorptions at 2939.9 and 4327.8 cm^{-1} to the $\nu_2 + \nu_3$ combination band and the $2\nu_3$ overtone, respectively.[113] These assignments were based on similar annealing behavior with respect to the known ν_3 transition and must be regarded as tentative, since isotopic substitution experiments were not performed. On the basis of the latter result, the authors obtained a value of -0.1 cm^{-1} for the x_{33} anharmonicity constant.

The ν_3 absorption spectrum of C_5 was first detected in the gas phase simultaneously by Bernath et al., who observed a series of rovibrational transitions with a resolution of 0.010 cm^{-1} in the carbon star IRC+10216,[3] and in the laboratory by Heath et al. using a laser vaporization–supersonic cluster beam source to produce the clusters and infrared diode laser spectroscopy to record the spectra.[220] These studies represented the first observation of rotationally resolved spectra for a polyatomic carbon cluster larger than C_3, and provided the most detailed structural information ever obtained for a cluster of this size. Figure 16 displays the C_5 absorption transitions observed toward IRC+10216. In their laboratory study, Heath et al. observed P- and R-branch transitions out to $J = 40$ with a precision in the frequency positions of $\sim$0.002 cm^{-1}. From the relative intensities of the transitions, they estimated a rotational temperature of 10 K. Moazzen-Ahmadi et al. later observed the ν_3 spectrum of C_5 using infrared diode laser spectroscopy of a hollow cathode acetylene discharge.[99,222] The number of fundamental transitions observed by these authors was extended out to $J = 72$.[222] Due to the high temperature of the acetylene discharge, several hot bands arising from low-frequency bending modes of $^{12}C_5$ were also observed. Hot bands that were analyzed were $(\nu_3 + \nu_7) - \nu_7$, $(\nu_3 + 2\nu_7) - 2\nu_7$, and $(\nu_3 + \nu_5) - \nu_5$. From the *l*-type doubling constants, q_7 and q_5, the authors estimated frequency positions of 118 ± 3 cm^{-1} for the lowest ν_7 bending frequency and 218 ± 13 cm^{-1} for ν_5. As with C_4, there is no evidence for exceptionally large amplitude bending motion in the lowest bending coordinate. Although perturbations to some of the rovibrational energy levels were observed, C_5 can generally be considered a well-behaved semirigid linear molecule with a cumulenic bonding configuration. Researchers from this same group also observed the ν_3 band of the $^{13}C_5$ isotopomer.[223]

Figure 17 displays photoelectron spectra observed for the odd-numbered C_5–C_9 clusters by Arnold et al.[41] These authors measured the $2\nu_5$, $2\nu_6$, and $2\nu_7$,

Table 8. Molecular Parameters of $X^1\Sigma_g^+C_5$[a]

	parameter	experiment	theory
	B_0 (cm^{-1})	0.0853133(29)[b]	
	D_0 (10^{-8} cm^{-1})	0.537(43)[b]	
	$\bar{r}_0$ (Å)	1.28323(4)	1.28959 1.28190[c]
$\nu_1(\sigma_g)$	ν_0 (cm^{-1})		1967[d] 2008[c]
$\nu_2(\sigma_g)$	ν_0 (cm^{-1})	779(5)[e]	770[d] 786.2[c]
$\nu_3(\sigma_u)$	ν_0 (cm^{-1})	2169.4410(2)[b] 2164[f]	2269 [2536][g] 2212[d]
	B (cm^{-1})	0.0848933(29)[b]	
	D (10^{-8} cm^{-1})	0.544(43)[b]	
$\nu_4(\sigma_u)$	ν_0 (cm^{-1})	1446.6[h]	1498 [123][g] 1436[d]
$\nu_5(\pi_g)$	ν_0 (cm^{-1})	216(5)[e] 218(13)[i]	280[g] 215[j]
	B (cm^{-1})	0.0856547(37)[b]	
	D (10^{-8} cm^{-1})	0.821(80)[b]	
	q (cm^{-1})	0.0000788(29)[b]	
$\nu_6(\pi_u)$	ν_0 (cm^{-1})	535(5)[e]	676 [3 × 2][g] 533[50][j]
$\nu_7(\pi_u)$	ν_0 (cm^{-1})	107(5)[e] 118(3)[i]	139 [15 × 2][g] 116[36][j]
	B (cm^{-1})	0.0856235(23)[b]	
	D (10^{-8} cm^{-1})	0.427(40)[b]	
	q (cm^{-1})	0.000132(2)[b]	
$^{13}C_5$[k]			
$\nu_3(\sigma_u)$	ν_0 (cm^{-1})	2085.7691(2)	
	B_0 (cm^{-1})	0.07872(2)	

[a] Numbers in parentheses are uncertainties in the last digits. Numbers in brackets are IR intensities [km/mol]. [b] Infrared diode laser spectroscopy.[222] [c] CCSD(T)/275cGTOs.[74] [d] CCSD(T)/cc-pVDZ.[58] [e] ZEKE spectroscopy.[224] [f] Ar matrix.[199] [g] B3LYP/cc-pVDZ.[62] [h] Ar matrix.[221] [i] Estimated from the *l*-type doubling constants.[222] [j] DFT(BLYP).[60] [k] Infrared diode laser spectroscopy.[223]

bending transitions and the ν_2 symmetric stretch of C_5. From these measurements, they estimated the following vibrational frequencies: $\nu_5 = 222$ cm^{-1}, $\nu_6 = 512$ cm^{-1}, $\nu_7 = 101$ cm^{-1}, and $\nu_2 = 798$ cm^{-1}, with uncertainties in the frequency positions of 45 cm^{-1}. The ν_5 and ν_7 frequencies are in agreement with the estimated values of Moazzen-Ahmadi et al.[222] Kitsopoulos et al. later measured vibrational frequencies with much higher precision by selectively detecting only the zero kinetic energy (ZEKE) electrons as a function of the photodetachment frequency.[224] Ground-state vibrational frequencies for both the anion and the neutral were obtained from this study. For the neutral, the authors obtained the following vibrational frequencies: $\nu_2 = 779$ cm^{-1}, $\nu_5 = 216$ cm^{-1}, $\nu_6 = 535$ cm^{-1}, and $\nu_7 = 107$ cm^{-1} with uncertainties of about 5 cm^{-1}. Evidence for an excited electronic state of neutral C_5 was obtained as well and will be discussed below. Experimental and theoretical molecular parameters for C_5 are presented in Table 8.

C. Excited Electronic States

The electronic spectrum of linear C_5 is analogous to that of C_3. A $^1\Pi_u - X^1\Sigma_g^+$ transition was predicted to occur at 428 nm by Kolbuszewski using MRD-CI/5s3p1d[225] compared to the 405-nm transition for C_3. This transition was recently measured by Forney et al. from mass-selected C_5 clusters trapped in solid Ne.[167] The observed band origin was 19599 cm^{-1} (510.2 nm). Kolbuszewski also predicted a $^1\Pi_g$ state at 2.85 eV and a $^3\Pi_g$ state lying 0.8 eV lower in energy.[225] No transitions involving these energy levels have been observed experimentally. Kitsopoulos et al. observed a series of peaks in their threshold photodetachment experiment 0.26 eV above the origin band.[224] These peaks were tentatively assigned to transitions to a low-lying $^3\Pi_g$ state, which was consistent with the selection rules of negative ion photodetachment and with the line width broadening observed when compared to the ground-state transitions. However, this assignment is in conflict with the calculations of Kolbuszewski who predicted a term energy of 2.03 eV for this state.[225]

D. C_5^-

The C_5^- carbon cluster anion is linear with a $^2\Pi_u$ ground electronic state.[176,226] Equilibrium bond lengths of 1.309 and 1.269 Å were calculated at the ROHF/DZP level of theory for the inner and outer bond lengths, respectively.[176] C_5^- has been studied experimentally using anion photoelectron spectroscopy,[41] zero electron kinetic energy (ZEKE) spectroscopy,[224] multiphoton photodetachment spectroscopy,[47] gas-phase ion mobility studies,[227] and infrared[177,228] and electronic[214] absorption spectroscopy in rare gas matrices.

Kitsopoulos et al. observed a hot band transition in their ZEKE spectra of C_5^- that they attributed to the ν_7 antisymmetric bending vibration, measured to be 200 ± 50 cm^{-1}.[224] Until very recently, this was the only measurement of a fundamental vibration in the electronic ground state of C_5^-. Two groups have recently reported observations of an antisymmetric stretch mode of C_5^- trapped in rare gas matrices. Szczepanski et al. assigned a transition at 1831.8 cm^{-1} in an Ar matrix, observed after irradiating the matrix with an electron beam, to the ν_3 vibration (see Figure 10).[177] This assignment was made on the basis of density functional theory calculations performed by the authors. Freivogel et al. observed this same band from mass-selected C_5^- deposited in a Ne matrix. In this case, the transition frequency was measured to be 1822.3 cm^{-1}.[228]

It has long been recognized that the even-numbered carbon cluster anions possess bound excited electronic states, due to the high electron affinities

of the linear triplets.[175,176,210] Recent experimental studies have revealed that the odd-numbered anions also possess bound electronic states,[47,49,214] despite earlier theoretical predictions to the contrary.[226] Ohara et al. accomplished the first observation of a gas-phase electronic spectrum of a polyatomic carbon cluster anion.[47] These authors observed two broad peaks in their resonance-enhanced multiphoton photodetachment spectrum of C_5^- produced in a laser vaporization−supersonic expansion source, which were assigned as transitions to the $A^2\Pi_g$ excited electronic state. The $A^2\Pi_g-X^2\Pi_u$ spectrum was also measured by Forney et al. from mass-selected C_5^- in a Ne matrix.[214] The band origin was measured to be 20 200 cm^{-1} (495.1 nm). The line widths observed for these transitions was about 0.2 cm^{-1}, which was narrower than the gas-phase line widths by about a factor of 35. Forney et al. also observed a band system assigned as the $B^2\Pi_g-X^2\Pi_u$ spectrum of C_5^-.[204] The observed band origin was 27 847 cm^{-1} (359.1 nm).

E. C_5^+

As with C_4^+, there is very little structural and spectroscopic information available for C_5^+. Raghavachari found two low-lying electronic states for the linear ground state—a $^2\Sigma_u^+$ state and a $^2\Pi_g$ state using HF and MP4 theoretical techniques.[216] He found the $^2\Sigma_u^+$ state to be lower in energy by 0.4 eV.

IX. C_6

A. Theory

Like C_4, C_6 is predicted to exist as two low-energy structural isomers, a cumulenic linear $^3\Sigma_g^-$ form and a planar ^1A_g monocyclic ring. The lowest energy cyclic structure is a distorted hexagon ring of D_{3h} symmetry. (See Figure 1.) As expected on the basis of experience with C_4, the calculated relative energies of the two isomers are extremely sensitive to the ab initio technique. The first high-level ab initio calculation to address relative isomer energies of C_6 were those of Raghavachari et al., who performed calculations at several different levels of theory, the highest one being MP4/6-31G*.[67,229] These authors studied energies of the linear cumulene and acetylene structures and four different cyclic isomers, including a symmetric D_{6h} ring, a distorted D_{3h} ring and the chair conformation. From a vibrational analysis, they found that the two linear structures and the D_{3h} structures were minima on the potential energy surface, while the remaining isomers represented saddle points. The $^3\Sigma_g^-$ structure was found to be the lowest energy linear form but was about 19.3 kcal/mol higher in energy than the D_{3h} isomer. Parasuk and Almlöf studied similar structures using MCSCF and MRCI methods.[69] These calculations concluded that the cumulenic chain was more stable than the D_{3h} isomer by over 40 kcal/mol, in stark contrast to the earlier results of Raghavachari et al. Even the polyacetylene structure, which was less stable than the cumulene by about 20 kcal/mol, was more stable than the ring.

Two recent theoretical studies addressed the discrepancies between the calculations of Raghavachari et al. and those of Parasuk and Almlöf. Pless et al. performed a detailed investigation of the effect of electron correlation on the energy separation between the linear and cyclic isomers.[73] These calculations were performed using the MRD-CI, CASPT2, and CCD methods with ANO basis functions. The authors found that correlation of all 24 valence electrons was critical for obtaining reliable relative energies. In Parasuk and Almlöf's study, only 10 valence electrons were correlated at the MR-CI level. Furthermore, the theoretical technique used to take correlation effects into account is also critical. Very sophisticated techniques, like CCSD(T) and MRD-CI that take into account high order correlation effects, must be employed for clusters of this complexity. At the MRD-CI level, Pless et al. predicted that the D_{3h} structure is the ground state, with the linear cumulene lying 7 kcal/mol higher in energy. The symmetric D_{6h} structure was found to be a saddle point, lying 5 kcal/mol above the ground state. Hutter and Lüthi performed a similar study using CCSD(T) calculations with ANO basis functions.[72] These authors also studied electron correlation effects and arrived at the same conclusion reached by Pless et al., that all valence electrons must be correlated at a high level of theory to achieve convergence of the relative energies. At the CCSD(T) level, the D_{3h} structure was again found to be the ground state by 10.7 kcal/mol over the cumulene.

Schmatz and Botschwina performed large-scale calculations on the ground electronic state parameters of linear C_6 in conjunction with their ab initio study of the excited electronic states of linear C_6^-.[75] Open-shell coupled cluster methods, which take into account triple excitations, were used with a basis set of 207 cGTO's. At the RCCSD(T) level of theory, these authors obtained the following equilibrium bond lengths for linear C_6: 1.2738, 1.2861, and 1.3011 Å for the inner, middle, and outer bonds, respectively. Martin and Taylor included the C_6 cluster as part of their study of the structures and vibrational spectra of C_2-C_9.[58] C_6 calculations were performed at the CCSD(T) level using cc-pVDZ and cc-pVTZ basis sets. The authors found the energy splitting between the linear and cyclic isomers to be 13 ± 2 kcal/mol, also in favor of the ring at the CCSD(T)/cc-pVTZ level. On the basis of their vibrational analysis, the authors predicted that the most intense infrared active vibrational mode of cyclic C_6 should occur in the region of 1700−1800 cm^{-1}. Matrix absorption peaks at 1695 and 1715 cm^{-1} were suggested as possible candidates for this mode. The former prediction was recently confirmed experimentally, as will be discussed below. For linear C_6, the infrared spectrum was dominated by a very intense antisymmetric stretch (ν_4) with an unscaled CCSD(T)/cc-pVDZ frequency of 1991 cm^{-1}, while the weaker ν_5 antisymmetric stretch band was predicted to occur at 1197 cm^{-1}. Two infrared active bending transitions with very weak intensities were predicted to occur in the far-infrared region.

B. Experiment

1. The Cyclic Isomer

Zajfman et al. reported evidence for a nonlinear isomer of C_6, based on the observation that significant electron photodetachment cross sections for C_6^- were measured at energies below the known electron affinity of the linear isomer.[230] This observation was interpreted as a linear anion to nonlinear neutral photodetachment transition. Similar results were also obtained from $C_4^- - C_8^-$ photodetachment cross section measurements.[230,231] Recently, however, Neumark and co-workers have shown that these apparently low photodetachment cross sections were most likely the result of multiphoton processes.[48,215] These authors performed a study of the spectroscopy and electron detachment dynamics of C_4^-, C_6^-, and C_8^- using resonant multiphoton detachment spectroscopy. They found that, for all three ions, efficient resonant multiphoton detachment occurred at the low photon energies reported by Zajfman et al.

Two groups recently reported the first spectroscopic identification of a small cyclic carbon cluster. Presilla-Marquez et al.[43] and Wang et al.[44] have simultaneously and independently assigned an infrared absorption transition at 1695 cm^{-1} to the $\nu_4(e')$ fundamental transition of cyclic C_6 trapped in an Ar matrix at 10 K. This assignment was supported by density functional theory calculations[62] and by good agreement between the observed and calculated frequency shifts of the ^{13}C-substituted isotopomers. This is a very significant result, given the great importance of experimentally characterizing the cyclic isomers of small carbon clusters. It is hoped that these initial measurements will eventually lead to a more detailed characterization of cyclic C_6 by high-resolution gas-phase spectroscopy.

2. The Linear Isomer

The $^3\Sigma_g^-$ form of C_6 was first identified by its ESR spectrum in an Ar matrix.[232,233] Later, Vala et al. used isotopic substitution techniques to assign an Ar matrix absorption at 1952 cm^{-1} to the ν_4 antisymmetric stretch.[234] From a normal coordinate analysis of numerous ^{13}C-substituted isotopomers, the authors suggested that C_6 is probably slightly bent in the Ar matrix due to packing stress induced by the matrix. A more extensive set of isotopomer frequencies of linear C_6 in an Ar matrix were reported by Kranze and Graham.[235] This study confirmed the assignment of the ν_4 mode to the absorption at 1952.0 cm^{-1}. A weaker absorption at 1197.3 cm^{-1} was also assigned as the ν_5 antisymmetric stretch. Szczepanski et al. recently assigned the following combination bands measured in an Ar matrix:[113] $\nu_1 + \nu_5 = 3247.6$ cm^{-1}, $\nu_3 + \nu_4 = 2579.8$ cm^{-1}, and $\nu_2 + \nu_5 = 2863.0$ cm^{-1}.[105] The $2\nu_4$ overtone band was also assigned to an absorption at 3905.6 cm^{-1}, yielding a value for x_{44} of 0.3 cm^{-1}. Again, these tentative results await confirmation by isotopic substitution or gas-phase measurements.

The ν_4 rovibrational spectrum of C_6 was observed in the gas phase by Hwang et al. using diode laser spectroscopy of a supersonic beam.[236] Transitions

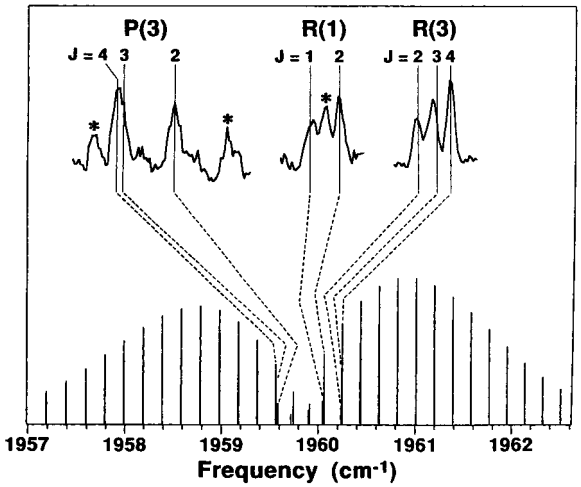

Figure 18. Experimental data and a simulated stick spectrum showing rovibrational transitions and triplet fine structure of the ν_4 antisymmetric stretch of linear C_6. The rotational temperature was 20 K. A laser vaporization–supersonic molecular beam source was used to produce the clusters, and a tunable diode laser spectrometer was used to record the spectra. Peaks labeled with asterisks are unassigned transitions. (Reprinted from ref 236. Copyright 1993 Taylor & Francis.)

with N up to 37 were observed with an estimated rotational temperature of 20 K. Uncertainties in the frequency positions were $\sim$ 0.001 cm^{-1}. The spectrum was characteristic of a centrosymmetric linear molecule in a triplet electronic state. Figure 18 shows experimental data along with a calculated stick spectrum. Triplet splittings were observed for the P(5)–R(7) transitions, permitting analysis of the spin–spin interaction. Analysis of these transitions yielded the vibrational frequency, the rotational constants, and the spin–spin coupling constant. (See Table 9.) The band origin of 1959.858 52(18) confirms the assignment of the matrix absorption at 1952 cm^{-1}. The spin coupling constant, λ_v is compared to the corresponding values observed by ESR spectroscopy of C_6 in Ar and Ne matrices.[232,233] As expected, the gas-phase value is larger than the matrix values due to the matrix perturbation effect. The spin–rotation interaction was not resolved in the data set, and the constant γ_v was fixed to the ESR value. The average C=C bond length of 1.2861(1) Å is consistent with cumulenic-like bonding, and is in excellent agreement with the RCCSD(T) calculations of Shmatz and Botschwina.[75] At the MRCI level, average bond lengths were predicted to be 1.275 and 1.284 Å for the acetylenic and cumulenic structures, respectively.[69] Thus, although the experimental value most closely resembles the cumulene, the difference between the average carbon–carbon bond lengths of the cumulenic and acetylenic forms of C_6 is not as obvious as it is for C_4. In any case, no infrared active transitions are predicted to occur above 1200 cm^{-1} for the acetylenic form of C_6,[229] whereas the vibrational frequency reported here is in excellent agreement the value predicted for the cumulene,[58] providing further support for cumulenic bonding in linear C_6.

Upon the basis of the symmetry of the highest occupied molecular orbital of C_6, we might expect this

Table 9. Molecular Parameters of $X^3\Sigma_g^-$ C_6[a]

	parameter	experiment	theory
	B_0 (cm^{-1})	0.048479(10)[b]	
	D_0 (10^{-7} cm^{-1})	0.22(9)[b]	
	λ_0 (cm^{-1})	0.1875(16)[b] 0.1815(5)[c] 0.1655(5)[d]	
	γ_0 (cm^{-1})	−0.0001[c,d]	
	$\bar{r}$ (Å)	1.2868(1)[b]	1.2801 1.2861 1.3011[e]
$\nu_1(\sigma_g)$	ν_0 (cm^{-1})	2061(10)[f]	2129[g] 2142.3[h]
$\nu_2(\sigma_g)$	ν_0 (cm^{-1})	1694(50)[i]	1695[g] 1696.9[h]
$\nu_3(\sigma_g)$	ν_0 (cm^{-1})	637(50)[i]	654[g] 653.0[h]
$\nu_4(\sigma_u)$	ν_0 (cm^{-1})	1959.85852(18)[b] 1952.0[j]	1991[g] 2037 [1073][k]
	B (cm^{-1})	0.048410(9)[b]	
	D (10^{-7} cm^{-1})	0.30(8)[b]	
	λ (cm^{-1})	0.1854(16)[b]	
$\nu_5(\sigma_u)$	ν_0 (cm^{-1})	1197.3[l]	1197[g] 1233 [95][k]
$\nu_6(\pi_g)$	ν_0 (cm^{-1})		551[m] 665[k]
$\nu_7(\pi_g)$	ν_0 (cm^{-1})	246(50)[i]	223[m] 234[k]
$\nu_8(\pi_u)$	ν_0 (cm^{-1})		432 [0.6][m] 434 [6 × 2][k]
$\nu_9(\pi_u)$	ν_0 (cm^{-1})	90(50)[i]	108 [22][m] 108 [15 × 2][k]

[a] Numbers in parentheses are uncertainties in the last digits. Numbers in brackets are calculated IR intensities [km/mol]. [b] Infrared diode laser spectroscopy.[236] [c] ESR spectroscopy in a Ne matrix.[232,233] [d] ESR spectroscopy in an Ar matrix.[232,233] [e] Inner, middle, and outer (respectively) equilibrium bond lengths calculated at the RCCSD(T)/204cGTO level.[75] [f] ZEKE spectroscopy.[237] [g] CCSD(T)/cc−pVDZ.[58] [h] RCCSD(T)/204cGTO.[75] [i] Photoelectron spectroscopy.[42] [j] Ar matrix.[234,235] [k] B3LYP/cc−pVDZ.[62] [l] Ar matrix.[235] [m] MP2/6−31G*.[244]

cluster to undergo large amplitude motion in its lowest-frequency bending coordinate. Like C_3, C_6 possesses a π_u HOMO, as opposed to C_4, and C_5 which possess π_g HOMO's. To date, no rotationally resolved spectra of C_6 that sample the lowest frequency bending mode have been assigned. Therefore, it is not currently possible to definitively characterize the bending dynamics. However, for very floppy molecules, the centrifugal distortion tends to be unusually large due to the high density of bending vibrational states that can interact with the antisymmetric stretch through the Coriolis effect. For C_6, the centrifugal distortion constant, D_v, is about 1 order of magnitude larger than expected for a semirigid molecule of this size, which may be an indication of a floppy bending potential. There is no evidence for quasilinearity in the bending potential upon excitation of the antisymmetric stretch, as is the case for C_3.

The symmetric stretch vibrations of C_6 were assigned at low resolution using anion photoelectron spectroscopy (see Figure 12),[41] and at higher resolution using threshold photodetatchment spectroscopy by Neumark and co-workers.[237] The threshold photodetatchment spectra were characteristic of linear geometries for both the anion and the neutral. The following symmetric stretch frequencies were assigned: $\nu_1 = 2061$ cm^{-1}, $\nu_2 = 1322$ cm^{-1}, and $\nu_3 = 489$ cm^{-1}. Uncertainties in these frequencies were ± 10 cm^{-1}. The latter two assignments are in conflict with the recent coupled cluster results of Schmatz and Botschwina.[75] Their force field calculations at the RCCSD(T) level predicted the harmonic frequencies of ν_2 and ν_3 to occur at 1683 and 649 cm^{-1}, respectively. Assignment of the $\nu_2 + \nu_5$ absorption in an Ar matrix by Szczepanski et al., which implies a value for ν_2 of 1665.8 cm^{-1}, supports this theoretical prediction.[113] Hutter et al. suggested that the peak assigned to ν_2 might be due to a low-lying $^1\Delta_g$ state.[72] In more recent experiments, Xu et al. measured much more detailed photoelectron spectra for C_6^- than had been observed previously.[42] Transitions that were separated from the origin by 1694 ± 50 and 637 ± 50 cm^{-1} were observed and assigned to ν_2 and ν_3, in better agreement with theoretical predictions.

C. Excited Electronic States

Liang and Schaefer calculated term energies for the low-lying $^1\Delta_g$ and $^1(\Sigma\Delta)$ states of cumulenic linear C_6.[186] At the CISD/DZP level, with all valence electrons correlated, including Davidson's correction, the term energy of the $^1\Delta_g$ state was 0.15 eV. Parasuk and Almlöf also predicted the relative energy of the $^1\Delta_g$ state using CASSCF and configuration interaction methods.[69] At the CISD/ANO level, with 14 valence electrons correlated and with the inclusion of Davidson's correction, the authors predicted the $^1\Delta_g$ state to lie at 0.19 eV. The term energy of the $^1\Delta_g$ state was recently measured by Xu et al., using photoelectron spectroscopy of C_6^-, to be 0.166 ± 0.015 eV,[42] in excellent agreement with the theoretical predictions. Other low-lying electronic states observed by these authors were the $^1\Sigma_u^+$ state and the $^3\Pi_u$ state, with term energies of 0.85 ± 0.02 and 1.10 ± 0.02 eV, respectively.

Forney et al. measured $^3\Sigma_u^- - X^3\Sigma_g^-$ vibronic transitions as part of their study of mass selected linear carbon clusters and anions trapped in solid Ne (see Figure 13).[206] The term energy of the $^3\Sigma_u^-$ state of neutral C_6 was 19558 cm^{-1}. The 1952 cm^{-1} vibrational absorption of C_6 was observed simultaneously. Three of the bands assigned to linear C_6 in this work at 511, 462, and 449 nm had been tentatively assigned to linear C_4 and C_2^- in previous studies by Graham et al.[238] and Szczepanski and Vala.[205]

D. C_6^-

A number of theoretical studies have been reported that characterized the $^2\Pi_u$ ground state and several excited electronic states of linear C_6^-.[75,175,176] The most sophisticated of these was the large-scale coupled cluster study of Schmatz and Botschwina.[75] These authors predicted values for the equilibrium bond lengths of 1.252, 1.325, and 1.275 Å for the inner, middle, and outer bond lengths, respectively, on the basis of calculations performed at the RCCSD-(T) level. Rhaghavachari studied the relative isomer energies of linear and cyclic C_6^- using HF and MP4 techniques.[216] He found the linear isomer to be more stable by about 1.4 eV. The ion mobility of C_6^- through a He drift cell was characteristic of a single linear isomer.[227,239]

Experimental techniques that have been used to study C_6^- are negative ion photoelectron spectroscopy,[41,42] ZEKE spectroscopy,[237] resonant two-photon photodetachment,[48] gas-phase ion mobility measurements,[227,239] infrared,[177,228,240] and electronic[206,207,212] absorption spectroscopy of C_6^- trapped in rare gas matrices, and matrix resonance Raman spectroscopy.[240]

Several fundamental vibrations in the C_6^- ground electronic state have been assigned. Szczepanski et al. measured the ν_1, ν_2, and ν_3 symmetric stretch modes to be 2086, 1775, and 634 cm^{-1}, respectively using resonance Raman spectroscopy of C_6^- trapped in an Ar matrix.[240] These assignments were supported by density functional theory calculations and isotopic shift measurements. The ν_4 antisymmetric stretch was observed at 1936.7 cm^{-1} in an Ar matrix (see Figure 10)[177,240] and 1938.5 cm^{-1} in Ne[228] by infrared absorption spectroscopy.

Electronic absorption spectra of C_6^- were first observed by Forney et al. by trapping the mass-selected ions in a Ne matrix (see Figure 14).[206] The $C^2\Pi_g-X^2\Pi_u$ spectrum was observed with a band origin of 16458 cm^{-1} (607.6 nm). Zhao et al. measured this same band in the gas phase using two-photon photodetachment.[48] The observed band origin was 16476 cm^{-1}. Freivogel et al. have recently reported new electronic absorption spectra of mass-selected C_6^- trapped in a Ne matrix.[212] These spectra were assigned as the $A^2\Sigma_g^+-X^2\Pi_u$, $(2)^2\Pi_g-X^2\Pi_u$, and $(3)^2\Pi_g-X^2\Pi_u$ bands, with band origins at 9352, 20064, and 22517 cm^{-1}, respectively.

E. C_6^+

Raghavachari's HF and MP4 calculations predicted a linear $^2\Pi_u$ ground state for C_6^+, although he could not give a reliable estimate for the relative stability of the cyclic isomer at this level of theory.[216] von Helden et al. performed ROMP2 and SD-CI calculations on linear and planar monocyclic ring isomers of carbon cluster cations, including C_6^+.[241] These calculations predicted that the linear and cyclic isomers are essentially isoenergetic, with the latter level of theory favoring the chain, and the former favoring the ring. Measurements of the ion mobility of C_6^+ ions through a high-pressure He drift cell were consistent with a single linear isomer.[242,243]

X. C_7

A. Theory

The most stable form of C_7 is predicted to be a linear cumulene with a $^1\Sigma_g^+$ ground electronic state, as is also the case for C_5. Martin et al. calculated structures and vibrational spectra of linear C_6-C_9 clusters in an attempt to assign some of the unknown infrared matrix absorptions.[244] Two intense antisymmetric stretch bands were found for C_7. At the RHF/6-31G* level these bands occurred with harmonic frequencies of 2281 and 2132 cm^{-1}, with the largest intensity in the higher frequency band. On the basis of these calculations, the authors suggested that two well-correlated matrix absorptions at 1893 and 2128 cm^{-1} belonged to the ν_5 and ν_4 bands of linear C_7, respectively. These assignments were confirmed when both bands were observed in the gas phase as will be discussed below.

von Helden et al. performed ab initio calculations to study the structural isomers of C_7 and its ions.[245] At the MP2 level, these authors found a C_{2v} planar ring isomer to be a local minimum of neutral C_7, lying about 19 kcal/mol above the linear ground state. Slanina et al. also studied the isomers of C_7 in an earlier study.[246] These authors obtained a cyclic minimum lying 17 kcal/mol above the linear isomer. Finally, Martin et al. studied the isomerization of C_7 using coupled cluster and density functional methods.[247] They obtained a relative energy of 14 kcal/mol in favor of the linear chain at the CCSD(T)/cc-pVDZ level of theory.

The highest level calculations to be performed on the linear ground state of C_7 are those of Schmaltz and Botschwina, who used open-shell coupled cluster techniques to study the $X^1\Sigma_g^+$ ground state and the $X^2\Pi_g$ state of C_7^-.[57] Bond lengths calculated for the neutral cluster at the MCCSD(T)/238 cGTO level were 1.290, 1.286, and 1.272 Å for the outer, middle, and inner bonds, respectively. The authors calculated an anharmonic force field involving the symmetric stretch vibrations for both the anion and the neutral. These data, along with the calculated electron affinity, were used to reproduce the photoelectron spectrum measured by Arnold et al.[41]

Martin and Taylor used CCSD(T) methods with a cc-pVDZ basis set to obtain bond lengths and harmonic vibrational frequencies of the stretching modes.[58] Bond lengths calculated at this level tended to be too long by 0.01−0.02 Å, although harmonic vibrational frequencies were adequately reproduced. The infrared spectrum was dominated by a very intense antisymmetric stretch (ν_4), with a less intense antisymmetric stretch occurring at lower frequency (ν_5).

B. Experiment

The linear C_7 cluster was first detected in a solid Ar matrix via its infrared vibrational spectrum. Absorption bands at 1893 and 2128 cm^{-1} were observed in the early work of Thompson et al., who recognized that the two bands were highly correlated from their annealing behavior, although the very

complex isotopic substitution pattern could not be analyzed at that time.[197] The authors concluded that the absorber was a large linear chain and tentatively assigned the bands to C_9. Martin et al. later suggested a reassignment of these bands to ν_5 and ν_4 of C_7 as has already been discussed.[244] These bands were reevaluated in recent matrix work by Kranze et al. to further characterize the sensitivity of vibrational frequency calculations to ^{13}C isotope substitution.[248] Szczepanski et al. assigned Ar matrix absorptions at 2709.7 and 4255.6 cm^{-1} to the $\nu_3 + \nu_4$ combination band and the $2\nu_4$ overtone, respectively.[113] A value of $x_{44} = -0.2$ cm^{-1} was obtained for the anharmonicity constant of the ν_4 mode.

C_7 was first studied in the gas phase by Heath et al., who observed the ν_4 rovibrational spectrum using tunable infrared diode laser spectroscopy of a supersonic cluster beam.[249] These authors measured rovibrational transitions out to $J = 42$ with an estimated rotational temperature of 10 K. The band origin at 2138.1951 cm^{-1} confirmed the assignment of the 2128 cm^{-1} matrix absorption. A later study by Heath and Saykally extended the number of observed fundamental transitions out to $J = 64$.[250] In addition, adjustments in the experimental conditions for producing the clusters in the laser vaporization source permitted the observation of hot band transitions, whose signal-to-noise ratio was about a factor of 10 weaker than the fundamental transitions. These hot bands were assigned to the $(\nu_4 + \nu_{11}) - \nu_{11}$ and the $(\nu_4 + 2\nu_{11}) - 2\nu_{11}$transitions, where ν_{11} is due to bending about the central carbon atom and is the lowest frequency vibration. P- and R-branch transitions out to $J = 11$ were measured for the $(\nu_4 + \nu_{11}) - \nu_{11}$ band, while for the $(\nu_4 + 2\nu_{11}) - 2\nu_{11}$ band only R-branch transitions out to $J = 20$ in the $l = 0$ component were observed. Figure 19 displays experimental data showing ν_4 fundamental and $(\nu_4 + \nu_{11}) - \nu_{11}$ hot band transitions along with a calculated stick spectrum. Heath et al. later measured rovibrational transitions of the ν_5 fundamental band out to $J = 42$.[251] The band origin was 1898.3758 cm^{-1}, which also confirmed the matrix assignment of the 1893 cm^{-1} band. The relative intensity of ν_5 was found to be about 5−7 times weaker than that of the ν_4 band. Molecular parameters resulting from analysis of the observed spectra can be found in Table 10.

C_7 possesses a filled π_u HOMO, which makes this molecule a candidate for extremely large amplitude bending motion. From the high-resolution spectroscopy data, rotational constants for the ground vibrational state and the first two excited ν_{11} bending states were obtained.[250] The rotational constant increased by 9.3% upon excitation of the first excited bending level, and 22% when the second level was excited. This extremely large increase in the rotational constant upon bending excitation is unprecedented for a strongly bound linear molecule. For example, excitation of the lowest frequency bending mode of C_5 results in a corresponding increase of the rotational constants of only 0.36% and 0.70% for the first two excited states. The enormous increase in the rotational constant observed for C_7 results from large amplitude motion in the ν_{11} bending coordinate.

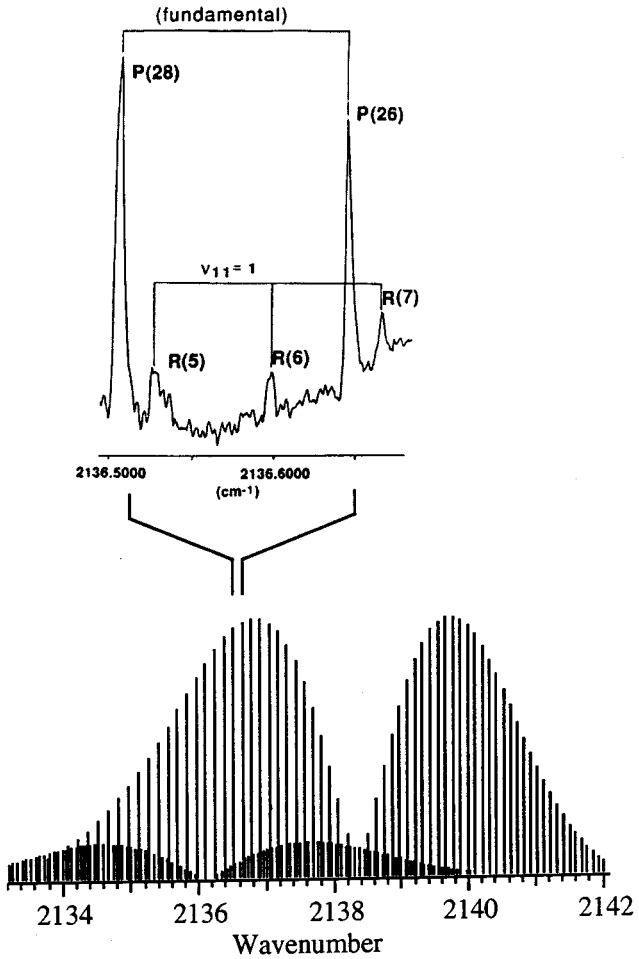

Figure 19. Rovibrational transitions of the ν_4 antisymmetric stretch and the $(\nu_4 + \nu_{11}) - \nu_{11}$ hot band of C_7. The clusters were produced in a laser vaporization−supersonic expansion source, and the spectra were recorded using a tunable diode laser spectrometer. (Reprinted from ref 250. Copyright 1991 American Institute of Physics.)

Theoretical calculations predict a harmonic bending frequency of ν_{11} that is in the far-infrared region of the spectrum.[244] However, the true bending potential is likely to be very anharmonic, which would probably result in a much lower frequency bending mode than the calculations predict. Further evidence for unusual behavior in the vibrational dynamics of C_7 arose from the centrifugal distortion parameters. These constants were large and negative for both the ground state and the excited state, which may be due to Coriolis perturbations occurring between the stretching and bending modes. There was no evidence for quasilinearity in the potential surface of C_7 however, since excitation of the antisymmetric stretch fundamental resulted in the expected decrease of the rotational constant.

The negative ion photoelectron spectrum of C_7 was difficult to interpret due to the large spectral congestion that resulted from the low-frequency bending modes and the lower instrument resolution at higher electron kinetic energies (see Figure 17).[41] Only two vibrational modes of the neutral were tentatively assigned, the ν_3 symmetric stretch at 548 ± 90 cm^{-1} and the ν_7 bend at 496 ± 110 cm^{-1}. This assignment of the ν_3 symmetric stretch was consistent with the

Table 10. Molecular Parameters of $X^1\Sigma_g^+C_7$[a]

	parameter	experiment	theory
	B_0 (cm^{-1})	0.030613(14)[b]	
	D_0 (10^{-7} cm^{-1})	−0.233(85)[b]	
	$\bar{r}_0$ (Å)	1.2800(6)[b]	1.272 1.286 1.290[c]
$\nu_1(\sigma_g)$	ν_0 (cm^{-1})		2154[d] 2163[e]
$\nu_2(\sigma_g)$	ν_0 (cm^{-1})		1547[d] 1557[e]
$\nu_3(\sigma_g)$	ν_0 (cm^{-1})	548(90)[f]	569[d] 572[e]
$\nu_4(\sigma_u)$	ν_0 (cm^{-1})	2138.3152(5)[b] 2128[g]	2198[d] 2258 [4652][h]
	B (cm^{-1})	0.030496(14)[b]	
	D (10^{-7} cm^{-1})	−0.251(91)[b]	
$\nu_5(\sigma_u)$	ν_0 (cm^{-1})	1898.3758(8)[i] 1893[g]	1914[d] 1988 [1307][h]
	B (cm^{-1})	0.030556(15)[i]	
	D (10^{-7} cm^{-1})	−0.16(11)[i]	
$\nu_6(\sigma_u)$	ν_0 (cm^{-1})		1077[d] 1119 [16][h]
$\nu_7(\pi_g)$	ν_0 (cm^{-1})	496(110)[f]	574[h]
$\nu_8(\pi_g)$	ν_0 (cm^{-1})		190[h]
$\nu_9(\pi_u)$	ν_0 (cm^{-1})		708 [6 × 2][h]
$\nu_{10}(\pi_u)$	ν_0 (cm^{-1})		293 [6 × 2][h]
$\nu_{11}(\pi_u)$	ν_0 (cm^{-1})		80 [10 × 2][h]
	B (cm^{-1})	0.033583(40)[b]	

[a] Numbers in parentheses are uncertainties in the last digits. Numbers in brackets are calculated IR intensities [km/mol]. [b] Infrared diode laser spectroscopy.[250] [c] Inner, middle, and outer equilibrium bond lengths calculated at the RCCSD(T)/238cGTOs level.[57] [d] CCSD(T)/cc-pVDZ.[58] [e] RCCSD(T)/238cGTOs.[57] [f] Anion photoelectron spectroscopy.[41] [g] Ar matrix.[244] [h] B3LYP/cc-pVDZ.[62] [i] Infrared diode laser spectroscopy.[251]

subsequent coupled cluster calculations of Schmaltz and Botschwina.[57]

C. Excited Electronic States

The $^1\Pi_u-X^1\Sigma_g^+$ transition of C_7 that is analogous to the 405-nm C_3 band was predicted by Kolbuszewski to occur at 469 nm at the MRD-CI/5s3p1d level.[225] The excitation energy of the $^1\Sigma_u^+-X^1\Sigma_g^+$ state was predicted to be 223.8 nm. These bands were observed by Forney et al. by electronic absorption spectroscopy of mass selected C_7 trapped in a Ne matrix with band origins of 18 444 (542.3 nm) and 39 556 cm^{-1} (252.8 nm), respectively.[167] The $^1\Sigma_u^+-X^1\Sigma_g^+$ band had been observed previously by Szczepanski and Vala in an Ar matrix.[205]

D. C_7^-

The C_7^- anion is a linear chain with a $^2\Pi_g$ ground electronic state.[57,176,245] Schmatz and Botschwina calculated the equilibrium bond lengths at the RCCSD(T)/238 cGTO level to be 1.279, 1.307, and 1.279 Å for the inner, middle, and outer bond lengths, respectively.[57] C_7^- has been studied experimentally using anion photoelectron spectroscopy,[41] resonance-enhanced multiphoton electron detachment (REMPED),[49] ion mobility measurements,[227,239] and infrared[177,228] and electronic[214] absorption spectroscopy. Ion mobility studies revealed no evidence for a cyclic isomer of C_7^-.[227,239]

Szczepanski et al. tentatively assigned a vibrational transition observed at 1734.8 cm^{-1} in an Ar matrix to the ν_5 antisymmetric stretch of C_7^- (see Figure 10).[177] Their density functional theory calculations supported this assignment. This same transition was observed by Freivogel et al. at 1736.4 cm^{-1} from mass-selected C_7^- deposited in a Ne matrix,[228] confirming the assignment of Szczepanski et al. Ohara et al. observed REMPED spectra of gas-phase C_7^-, C_9^-, and C_{11}^-.[49] They measured an electronic band of C_7^- whose band origin occurred at 15950 cm^{-1}. Forney et al. recently observed this same transition at 15954 cm^{-1} from mass-selected C_7^- in a Ne matrix, which they assigned as the band origin of the $A^2\Pi_u-X^2\Pi_g$ band.[214]

There have been several reports of the detection of metastable carbon cluster dianions as small as C_7^{2-}.[104,252,253] Earlier theoretical studies had found C_8^{2-} to be the smallest stable dianion with a linear chain structure.[176,254] However, more recent calculations have predicted that a trigonal planar isomer of C_7^{2-} is stable with respect to electron loss.[255,256]

E. C_7^+

Ion−molecule reactions between carbon cluster cations and D_2, O_2, HCN, and small hydrocarbons, studied by ICR/FTMS, revealed that C_7^+, C_8^+, and C_9^+ existed in two different isomeric forms—a reactive form, postulated to be linear, and an unreactive form, presumed to be cyclic.[257−259] These assumptions were confirmed by the gas-phase ion chromatography experiments of von Helden et al.[241−243,260] Mass-selected carbon cluster ions were passed through a high-pressure (1−5 Torr) He drift cell under the influence of a 2−20 V/cm electric field. Temporal separation of different structural isomers occurred in the drift cell, due to the dependence of the ion mobilities on the geometric structures. Cyclic isomers possess higher mobilities than linear isomers, so that the cyclic clusters moved through the cell at a faster rate. A short pulse of ions is injected into the drift cell, and the arrival time distribution (ATD) of these ions is measured at a detector after they exit the cell. Different peaks in the ATD for each cluster size correspond to different structural isomers.

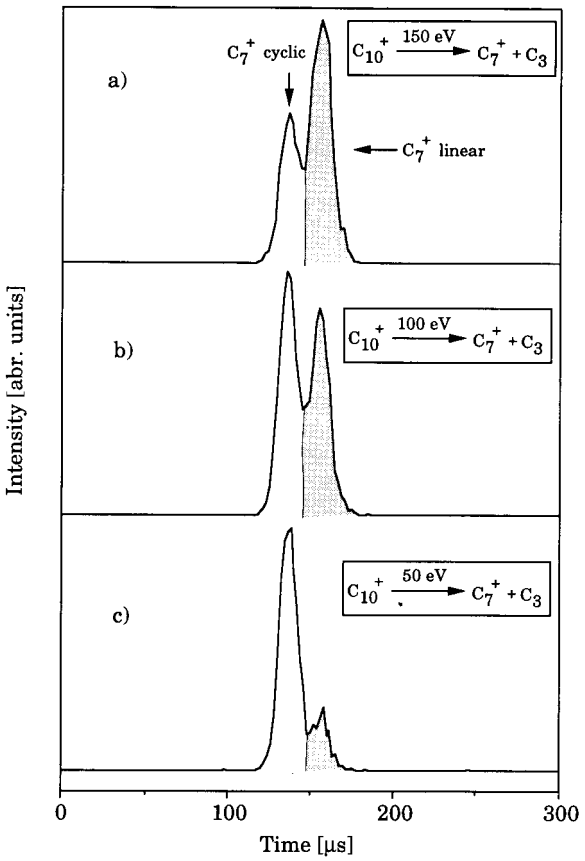

Figure 20. A series of arrival time distributions for C_7^+, measured using gas-phase ion chromatography, for different injection energies of C_{10}^+ into the He drift cell. The peaks at longer times correspond to the linear isomer and the peaks at shorter times to the cyclic isomer. (Reprinted with permission from ref 260. Copyright 1993 Elsevier Science B.V.)

For C_7^+, two peaks were observed in the ATD.[242,243] Theoretical modeling of the ion mobilities for different structural isomers revealed that the faster peak was due to a planar monocylic ring isomer, and the slower peak to the linear chain. Information about the relative stabilities of the two isomers was obtained through annealing studies.[260] Mass-selected C_{10}^+ ions were injected into the drift cell at kinetic energies up to 150 eV to induce fragmentation of a fraction of the ions into C_7^+ and C_3 products. Figure 20 displays the ATD's observed for the C_7^+ products at three different injection energies. Raising the injection energy increased the fraction of linear C_7^+ isomers, revealing this to be the higher energy isomeric form. This observation was supported by theoretical calculations that predicted a C_s $^2A'$ planar monocyclic ring to be the ground-state structure of C_7^+,[245] lying 20 kcal/mol lower in energy than the linear chain. The transition state between the linear and cyclic minima was also calculated and found to lie about 58 kcal/mol above the ground state.[245] We have already seen that the addition of an electron to the π shell of a carbon cluster to form an anion stabilizes the linear configuration relative to the cyclic form.[216] The opposite occurs when an electron is removed from the π shell to form a cation. A consequence of this is that the transition point at which cyclic isomers become more stable than the linear forms takes place at a smaller cluster size for the cations than for the neutral and anionic clusters. For the cations, this transition appears to occur at C_7^+, compared to C_{10} for the neutrals[67,68] and somewhere between C_{10}^- and C_{15}^- for the anions.[227]

The ion mobility results obtained for C_7^+ can be generalized to explain the isomeric distributions of other carbon clusters that possess low-energy linear and cyclic forms. Despite the apparently large energy difference between the C_7^+ ring and chain isomers, linear chains are still experimentally observed. This is also the case for C_4, C_6, C_{10}, and larger clusters that possess cyclic ground states. At the high temperatures under which carbon clusters typically form, entropy favors the linear isomer even when the ring is significantly more stable. Because of the high barriers that exist between rings and chains, there is often no chance for the clusters to anneal to their most stable forms, so that the metastable linear isomers are "frozen out." This may partly explain the scarcity of experimental data for the cyclic isomers of neutral carbon clusters.

XI. C_8

A. Theory

C_8 is analogous to C_4 and C_6 in that both a cyclic structure and a $^3\Sigma_g^-$ linear chain are believed to be low-energy isomeric forms. The early SCF calculations of Raghavachari and Binkley predicted that a planar monocyclic ring of C_{4h} symmetry was the ground-state structure (see Figure 1).[67] The linear structure was studied by Martin et al. at the UHP/6-31G* level as part of their study of structures and harmonic frequencies of C_6−C_9.[244] These authors argued that the assignment of the 1998 cm^{-1} matrix absorption to linear C_8 was in error,[234] upon the basis of their frequency predictions and from the annealing behavior of this band. They suggested that this band was more likely due to C_9 while the most intense C_8 absorption probably occurred at higher frequency. One of the unresolved transitions near 2075 cm^{-1} was suggested as the most likely candidate for C_8. The linear structure was also studied at the MP2/6-31G* level by Kurtz and Adamowicz.[218] More recently, Schmatz and Botschwina used large-scale open-shell coupled cluster methods with 272 cGTO's to study geometries and symmetric vibrational frequencies for two electronic states of linear C_8^- and the ground state of linear C_8.[76] Equilibrium bond lengths of C_8, obtained at the RCCSD(T) level (after a standard 0.007 Å correction), were 1.2969, 1.2879, 1.2726, and 1.2788 Å for the outer to inner bonds.

The nature of the cyclic minimum has recently been the subject of some controversy. As stated above, Raghavachari and Binkley found a planar monocyclic ring structure of C_{4h} symmetry to be the minimum at the SCF/6-31G* level.[67] However, using an MP2/6-31G* technique, Slanina et al. located a nonplanar ring of D_{2h} symmetry, possessing a boat-like conformation, 13 kcal/mol lower in energy than the C_{4h} planar ring.[261,262] In this study, the planar structure was actually a saddle point on the potential surface. Upon the basis of previous experience with

the C_6 cluster, however, these results should be viewed with some skepticism. Recall that for C_6, it was found that only techniques which take electron correlation into account at high order produce reliable predictions of the relative energies.[72,73] Martin and Taylor investigated these structures at the CCSD(T)/6-31G* level.[58] Their findings indicated that the planar monocyclic ring of C_{4h} symmetry is indeed a minimum on the potential surface (see Figure 1). The nonplanar D_{2d} structure was found to lie 4.1 kcal/mol above the planar minimum. At this level of theory, the linear isomer was predicted to be the global minimum, lying 11.3 kcal/mol below the cyclic isomer. By expanding the basis set to cc-pVTZ quality, the linear−cyclic energy splitting was reversed, such that the cyclic form became the global minimum by 10.1 kcal/mol. In any case, as Martin and Taylor pointed out, relative energy calculations performed at the MP2 level on clusters of this size produce numerous artifacts and should be viewed with caution.

B. Experiment

1. The Cyclic Isomer

Wang et al. have recently reported the detection of cyclic C_8 trapped in an Ar matrix at 10 K.[45] These authors assigned an infrared absorption transition at 1844.2 cm^{-1} to the $\nu_{12}(e_u)$ fundamental transition of cyclic C_8. This assignment was made based upon agreement between the frequency and isotopomer frequency shifts and the results of density functional theory calculations.

2. The Linear Isomer

The linear triplet form of C_8 was first detected via its ESR spectrum in a solid Ar matrix.[233] Szczepanski et al. recently made tentative assignments of two infrared Ar matrix absorptions as being due to the ν_6 (2071.5 cm^{-1}) and ν_5 (1710.5 cm^{-1}) antisymmetric stretch bands of linear C_8.[113] These assignments were based on similarities in the annealing behavior of the two bands and agreement with the density functional theory calculations of Hutter et al.[60] These same bands were observed from mass-selected C_8 deposited in a Ne matrix at 2067.8 and 1707.4 cm^{-1},[228,263] which further supports the assignment of these transitions to ν_6 and ν_5, respectively.

C_8 is the only carbon cluster in the C_2-C_9 size range for which the linear isomer has not been characterized by high-resolution spectroscopy. Infrared diode laser searches in the regions of 1690−1720 and 2050−2100 cm^{-1} yielded no spectra that could be attributed to linear C_8. It would appear that the number density of linear C_8 molecules produced in the laser vaporization source is below the detection limit of the diode laser spectrometer. Previous experiments on C_4[202] and C_6[236] have shown that the even-numbered triplets are produced in less abundance than the odd singlets. In addition, the infrared intensities of the triplet bands are predicted to be significantly smaller than those of the singlets.[62] These factors may have thus far precluded detection of the antisymmetric stretch bands of C_8.

Very little information on C_8 was obtained from the negative ion photoelectron spectra observed by Arnold et al., due to its high electron affinity.[41] Only two peaks were resolved with a separation of 565 cm^{-1}. This separation was tentatively assigned as the ν_4 symmetric stretch, although assignment to a low-lying electronic state could not be ruled out. A much more complete picture of C_8 has emerged from more recent photoelectron spectroscopy experiments by Xu et al.[42] In particular, the band previously assigned to ν_4 was reassigned as the origin of the $^1\Delta_g$ electronic spectrum. In addition, two peaks lying 1928 and 1361 cm^{-1} from the origin were observed and found to be consistent with the ν_1 and ν_3 symmetric stretch fundamentals.

C. Excited Electronic States

Liang and Schaefer calculated term energies for the $^1\Delta_g$ and the $^1(\Sigma\Delta)$ states of linear C_8 to be 0.141 and 0.010 eV, respectively.[186] The calculation was performed at the CISD/DZP level using Davidson's correction. Xu et al. recently measured the term energy of the $^1\Delta_g$ state to be 0.071 ± 0.015 eV (605 cm^{-1}) using photoelectron spectroscopy of C_8^-.[42] These authors also observed the $^1\Sigma_g^+$, the $^3\Sigma_u^+$, and (tentatively) the $^3\Pi_g$ states with term energies of 0.115 ± 0.015 (927 cm^{-1}), 0.78 ± 0.02, and 1.03 ± 0.02 eV, respectively. $^3\Sigma_u^-$−$X^3\Sigma_g^-$ vibronic transitions, with a band origin of 15630 cm^{-1}, were observed by Freivogel et al. for mass-selected C_8, using the same electronic spectroscopy technique that was applied to C_4 and C_6 (see Figure 13).[207]

D. C_8^-

The C_8^- anion is linear with a $^2\Pi_g$ ground electronic state.[76,176] The ground-state equilibrium geometry was calculated at the RCCSD(T)/272 cGTO level by Schmatz and Botschwina.[76] An equilibrium rotational constant of 0.0202 cm^{-1} was derived from the calculated bond lengths. As was also the case for C_6^- and C_7^-, there was no evidence for a cyclic isomer of C_8^- in the ion mobility experiments.[227,239] Freivogel et al. observed a transition at 1796.0 cm^{-1} from mass-selected C_8^- deposited in a Ne matrix that they assigned as the ν_6 antisymmetric stretch.[228] The $C^2\Pi_u-X^2\Pi_g$ electronic spectrum has been measured for C_8^- trapped in a Ne matrix, with a band origin of 12 933 cm^{-1},[207] and in the gas phase by resonant two-photon photodetachment at 12 963 cm^{-1}.[48] More recently, Freivogel et al. measured the $^2\Sigma_u^+-X^2\Pi_g$ and the $(2)^2\Pi_u-X^2\Pi_g$ bands of mass-selected C_8^- in a Ne matrix.[213] The band origins were 9545 and 16 295 cm^{-1}, respectively.

E. C_8^+

Ion mobility experiments have shown that C_8^+ exists in two isomeric forms—a planar monocyclic ring and a linear chain.[241−243] Annealing studies similar to those described for C_7^+ revealed that C_8^+ possesses a cyclic ground-state geometry.[241] von Helden et al. used a simple kinetic model to estimate the energy difference between the cyclic and linear

isomers to be 23 ± 8 kcal/mol. The ground-state structure of the cyclic isomer was predicted to be a C_{4h} planar monocyclic ring with a $^2A''$ electronic state at the ROHF/6-31G(d) level of theory.[241] The ground electronic state of the linear isomer was $^4\Sigma^-$ at this same level.

XII. C_9

A. Theory

C_9 is the largest neutral carbon cluster for which the ground-state structure is predicted to be a linear chain. The properties of the $^1\Sigma_g^+$ ground electronic state have been calculated at numerous levels of theory. Martin et al. calculated harmonic vibrational frequencies and intensities at the HF/6-31G* level.[244] As has already been discussed, their calculations led to a reassignment of the matrix absorption at 1998 cm^{-1} to the ν_6 antisymmetric stretch of C_9. The assignment was based on harmonic frequency predictions and upon observed annealing behavior. The authors reasoned that the strong annealing behavior observed for the 1998 cm^{-1} band was most consistent with stepwise condensation of C_3 in the matrix. Kurtz and Adamowicz calculated minimum energy structures and vibrational spectra at the MBPT(2)/6-31G* level.[218] For C_9 they found that the equilibrium geometry was slightly bent from the linear configuration, with angles between adjacent bonds of 177−179°. Although these bending angles were most likely due to artifacts, the authors claimed that the harmonic frequencies calculated at this level were still valid.

Martin and Taylor have performed more recent calculations at the CASSCF[264] and the CCSD(T)[58] levels of theory using the cc-pVDZ basis set. Again the main focus of these calculations was to study the vibrational spectrum. The authors noted that, for linear carbon clusters, as the size of the chain increases, such treatments as HF, SCF, and MP2 become less reliable, producing results that deviate more strongly from experiment. This is due to nondynamical correlation effects, which for smaller systems, are effectively dealt with using coupled cluster techniques. However, for systems larger than C_9, the coupled cluster methods are prohibitively costly at present. Therefore, the authors used C_9 to test the utility of CASSCF calculations for larger linear chains. They obtained reliable results for the harmonic frequencies of C_9, although relative intensities at this level were not predicted correctly. The CCSD(T)/cc-pVDZ study of Martin and Taylor are the largest scale calculations to be performed on C_9 to date.[58] The authors used these calculations to predict bond lengths and harmonic stretching frequencies. They noted that bond lengths calculated at this level are consistently too long by as much as 0.01 to 0.02 Å, although harmonic frequencies are the most accurate that can be obtained for a system this large.

In addition to the very intense ν_6 band, the ν_5 and ν_7 bands were also predicted to have appreciable infrared intensities.[58] By scaling the calculated harmonic frequencies for C_3−C_9 with known experimental values, the authors predicted the ν_5 band to occur at 2101 ± 14 cm^{-1} and the ν_7 band at 1607 ± 12 cm^{-1}. Recent experimental measurements of these two bands are in satisfactory agreement with these predictions and will be discussed below.[38,265]

Slanina et al. recently investigated the possibility of a cyclic isomer for C_9. They obtained a C_s nonplanar structure, lying just 6 kcal/mol above the linear ground state, at the MP2/6-31G* level.[266] However, more recent calculations by Martin et al. showed the cyclic structure to be a planar monocyclic ring of C_{2v} symmetry, for which the relative energy was 9 kcal/mol above the chain.[58] Once again, the MP2 results were shown to be artifactual. Finally, Wu et al. calculated the cyclic−linear energy spacings of C_9 using HF, MP2, and DFT techniques, in connection with their theoretical study of the LaC_9^+ ion.[267]

B. Experiment

After reassignment of the 1998 cm^{-1} matrix absorption to the ν_6 vibration of C_9 by Martin et al.,[244] Heath and Saykally discovered this band in the gas phase using diode laser spectroscopy of a supersonic cluster beam.[268] Rovibrational transitions were measured with J values as large as $J = 80$. In a later diode laser spectroscopy study by Van Orden et al., the ν_6 fundamental transitions were remeasured after improvements in the sensitivity of the spectrometer.[269] Due to the improved signal-to-noise ratio, the lowest energy rovibrational transitions, P(2) and R(0), were observed, which facilitated an unambiguous rotational assignment. It was found that the original assignment by Heath and Saykally was in error by two units in J. In addition, the precision of the frequency positions was improved by more than a factor of 4, from 0.0035 to 0.0008 cm^{-1}. Thus, some of the anomalous behavior reported by Heath and Saykally, including perturbations of the low-J transitions and large, negative values for the centrifugal distortion constants, were determined to be artifacts of the lower precision measurements and the incorrect rotational assignment. The gas-phase frequency of ν_6 was measured as 2014.277 96(7) cm^{-1}, which represents a 16 cm^{-1} red-shift of the same band in the Ar matrix.

In addition to the improvements in the analysis of the ν_6 fundamental transitions, Van Orden et al. also observed hot band transitions arising from the lowest frequency ν_{15} bending mode.[269] The $(\nu_6 + \nu_{15}) - \nu_{15}$ band with J values up to 57 and the $(\nu_6 + 2\nu_{15}) - 2\nu_{15}$ band with J up to 34 were observed in the region of the antisymmetric stretch. The signal-to-noise ratio of the $(\nu_6 + \nu_{15}) - \nu_{15}$ transitions were about 10 times less than the fundamental peaks. Experimental hot band and fundamental transitions are shown in Figure 21. Molecular parameters obtained from the analysis of these bands are shown in Table 11. There was no evidence for large amplitude motion in the bending coordinate from these data, although there was evidence for Coriolis-type perturbations to the symmetry components of the $(\nu_6 + \nu_{15}) - \nu_{15}$ band due to large centrifugal distortion constants. Excitation of the bending vibrations resulted in an increase in the rotational constant that is characteristic of a

Table 11. Molecular Parameters of $X^1\Sigma_g^+C_9$[a]

	parameter	experiment	theory
	B_0 (cm^{-1})	0.0143214(10)[b]	0.01412[c] 0.01378[d]
	$\bar{r}_0$ (Å)[i]	1.27863(9)[b]	
$\nu_1(\sigma_g)$	ν_0 (cm^{-1})		2276[c] 2212[d]
$\nu_2(\sigma_g)$	ν_0 (cm^{-1})		1970[c] 1898[d]
$\nu_3(\sigma_g)$	ν_0 (cm^{-1})	1258(50)[e]	1294[c] 1247[d]
$\nu_4(\sigma_g)$	ν_0 (cm^{-1})	484(48)[e]	464[c] 449[d]
$\nu_5(\sigma_u)$	ν_0 (cm^{-1})	2079.67358(17)[b]	2217 [4077][c] 2148[d] 2239 [3675][f]
	B (cm^{-1})	0.0142889(10)[b]	
$\nu_6(\sigma_u)$	ν_0 (cm^{-1})	2014.27800(18)[b] 1998[g]	2132 [6520][c] 2061[d] 2132 [17810][f]
	B (cm^{-1})	0.0142962(11)[b]	
	D (10^{-8} cm^{-1})	0.107(30)[b]	
$\nu_7(\sigma_u)$	ν_0 (cm^{-1})	1601[h]	1670 [394][c] 1607[d] 1696 [423][f]
$\nu_8(\sigma_u)$	ν_0 (cm^{-1})		895 [0.19][c] 864[d] 906 [5.8][f]
$\nu_9(\pi_g)$	ν_0 (cm^{-1})		642[c]
$\nu_{10}(\pi_g)$	ν_0 (cm^{-1})		303[c]
$\nu_{11}(\pi_g)$	ν_0 (cm^{-1})		129[c]
$\nu_{12}(\pi_u)$	ν_0 (cm^{-1})		744 [7 × 2][c]
$\nu_{13}(\pi_u)$	ν_0 (cm^{-1})		519 [0.3 × 2][c]
$\nu_{14}(\pi_u)$	ν_0 (cm^{-1})		225 [10 × 2][c]
$\nu_{15}(\pi_u)$	ν_0 (cm^{-1})		51 [7 × 2][c]
	B^{1f} (cm^{-1})	0.014311(15)[i]	
	B^{1e} (cm^{-1})	0.014353(12)[i]	

[a] Numbers in parentheses are uncertainties in the last digits. Numbers in brackets are calculated infrared intensities [km/mol]. [b] Infrared diode laser spectroscopy.[38] [c] B3LYP/cc-pVDZ.[62] [d] CCSD(T)/cc-pVDZ.[58] [e] Anion photoelectron spectroscopy.[41] [f] CCSD/6-31G*.[265] [g] Ar matrix.[244] [h] Ar matrix.[265] [i] Infrared diode laser spectroscopy.[269]

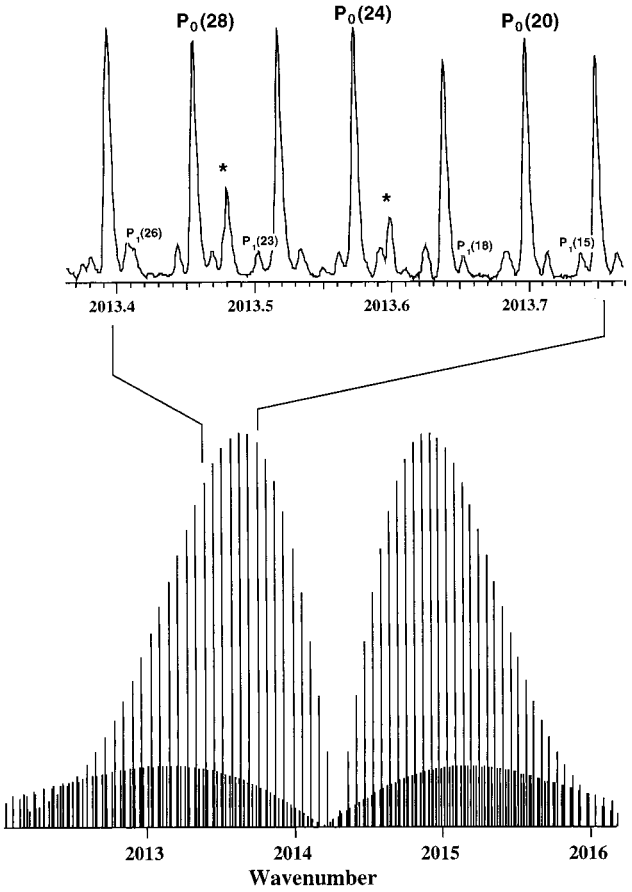

Figure 21. Rovibrational spectra and a simulated stick spectrum of the ν_6 fundamental (strong peaks) and (ν_6 + ν_{15}) − ν_{15} hot band of linear C_9 near 2014 cm^{-1} at 30 K. Subscripts on the P- and R-branch labels indicate the bending excitation level of the lower state. Asterisks mark unassigned peaks. (Modified from ref 269.)

semirigid linear molecule. In addition, the magnitude of the centrifugal distortion constant of the ν_6 = 1 state and the small redshift in the (ν_6 + ν_{15}) − ν_{15} band origin also characterized the molecule as a fairly well-behaved semirigid linear chain.

Recently, the two other infrared active stretching frequencies were observed experimentally. Kranze et al. confirmed that an Ar matrix absorption at 1601.0 cm^{-1} corresponds to the ν_7 band of C_9.[265] These authors used extensive isotopic substitution experiments along with density functional theory calculations to predict isotope shifts, confirming the carrier of the band. Van Orden et al. observed the gas-phase rovibrational spectrum of the ν_5 band at 2079.6736(2) cm^{-1}.[38] A diode laser spectrometer was used to observe 28 rovibrational transitions with J values up to 42. Table 11 displays molecular constants obtained from a simultaneous fit of the ν_5 and ν_6 spectra. By comparing the absorbance of ν_5 and ν_6 transitions, the authors measured the relative IR intensity of ν_5 to be 0.11 ± 0.01 compared to ν_6. Large disparities were found between this measured value and the relative IR intensities calculated at various levels of theory,[62] underscoring the difficulty encountered when calculating IR intensities for a molecule of this size.

More recently, matrix absorptions at 2081.1 cm^{-1} (Ne) and 2078 cm^{-1} (Ar) were assigned to the ν_5 vibration of C_9 by Maier and co-workers[228,263] and Szczepanski et al.,[113] respectively. The latter authors also assigned the ν_4 + ν_5 combination band (2525.7 cm^{-1}) and the $2\nu_5$ (3996.5 cm^{-1}) and $2\nu_6$ (4156.2 cm^{-1}) overtone bands. On the basis of the latter two results, anharmonicity constants of x_{55} = 0.0 cm^{-1} and x_{66} = 0.25 cm^{-1} were obtained. Finally, two of the symmetric stretch frequencies of C_9 were measured by Arnold et al. using anion photoelectron spectroscopy.[41] The ν_3 mode was found to occur at 1258 ± 50 cm^{-1} and the ν_4 mode was measured at 484 ± 48 cm^{-1}.

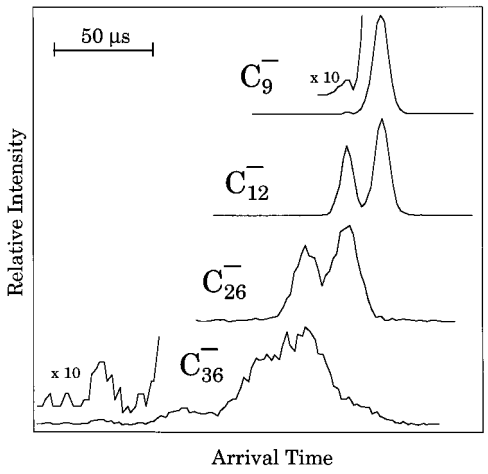

Figure 22. Arrival time distributions (ATDs) for C_9^-, C_{12}^-, C_{26}^-, and C_{36}^- measured using gas-phase ion chromatography. The large peak in the ATD of C_9^- is due to the linear isomer. For C_{12}^-, the peak at shorter time is due to the monocyclic ring and the peak at longer time to the linear chain. For C_{26}^-, the two peaks are due to the monocyclic ring at longer time and the bicyclic ring at shorter time. Five isomers are present for C_{36}^-. The broad feature at longer time is due to monocyclic, bicyclic, and tricyclic rings. The peak at shorter time is the graphitic isomer, and the peak shown on the expanded scale is the fullerene isomer. (Reprinted with permission from ref 227. Copyright 1995 Elsevier Science B.V.)

C. Excited Electronic States

By extrapolating the term energies calculated for odd-numbered C_3-C_9, Kolbuszewski predicted the $^1\Sigma_u^+$ state of C_9 to lie at 5.16 eV.[225] This corresponds to a $^1\Sigma_u^+-X^1\Sigma_g^+$ transition wavelength of 240.3 nm. Kurtz and Huffman observed a strong correlation in the annealing behavior between the IR Ar matrix absorption at 1998 cm^{-1},[204] which was later assigned to C_9, and a UV band at about 310 nm. This same correlation was observed by Szczepanski and Vala.[205] Assignment of this transition to C_9 was recently confirmed by Forney et al.[214] These authors measured the band origin of the $^1\Sigma_u^+-X^1\Sigma_g^+$ band of mass-selected C_9 in a Ne matrix to be 33 895 cm^{-1} (295.0 nm).

D. C_9^-

C_9^- is a linear chain with a $^2\Pi_u$ ground electronic state.[176] The arrival time distribution (ATD) measured after mass-selected C_9^- clusters passed through a He drift tube is shown in Figure 22.[241] The ATDs of C_{12}^-, C_{26}^-, and C_{36}^- are also shown for comparison and will be discussed later. The ATD of C_9^- is dominated by a peak corresponding to the linear isomer, although a weak shoulder appearing at earlier times provides evidence for a very small fraction of cyclic isomers that might also be present. All other experimental information concerning C_9^- relates to the linear isomer. Other experimental techniques that have been used to study C_9^- are anion photoelectron spectroscopy,[41] resonance-enhanced multiphoton electron detachment (REMPED),[49] and infrared[177,228] and electronic[214] absorption spectroscopy of C_9^- trapped in rare gas matrices.

Szczepanski et al. tentatively assigned two Ar matrix absorptions at 1686.7 and 1583.3 cm^{-1} to the ν_6 and ν_7 transitions of C_9^-, respectively.[177] The former band was also observed at 1692.6 cm^{-1} from mass-selected C_9^- deposited in a Ne matrix. Ohara et al. measured a REMPED spectrum of gas-phase C_9^-, corresponding to an electronic band whose origin occurred at 13 020 cm^{-1}.[49] This same band was observed with an origin of 13082 cm^{-1} from mass-selected C_9^- deposited in a Ne matrix and assigned as the $A^2\Pi_g-X^2\Pi_u$ spectrum.[214] Other bands observed in this way were the $B^2\Pi_g-X^2\Pi_u$, $C^2\Pi_g-X^2\Pi_u$, and $D^2\Pi_g-X^2\Pi_u$ spectra, with band origins of 16 468, 29 446, and 34 536 cm^{-1}, respectively.

E. C_9^+

Both linear and monocyclic ring isomers were observed for C_9^+ in the gas-phase ion chromatography experiments of von Helden et al., as was also the case for C_7^+ and C_8^+.[241-243] Annealing studies showed that the cyclic isomer was more stable than the linear chain by 17 ± 8 kcal/mol.[241] The cyclic ground state was found to be a planar monocyclic C_2 structure at the ROHF/6-31G(d) level of theory.[241] A $^2\Sigma^+$ state was found to be the ground electronic state of the linear isomer using this same technique.

XIII. C_{10}

A. Theory

The C_{10} molecule has long been recognized as a geometric transition point for small neutral clusters, which generally prefer linear geometries, and larger clusters, which are believed to form planar monocyclic ring structures, due to reduced angle strain for larger rings.[67] The cyclic C_{10} cluster is also of interest because it satisfies Huckel's rules for aromaticity, which may impart added stability to the ring. Experimental evidence for the unusual stability of cyclic C_{10} was provided very recently by Wakabayashi et al.[270] These authors used tandem IR and UV pulsed laser irradiation of graphite to produce molecular beams of carbon cluster anions, which were then detected using time-of-flight mass spectrometry. Under conditions in which the separation between the IR and UV pulses was between 50 and 200 μs, it was found that C_{10}^- ions were formed almost exclusively. The authors took this result as evidence for preferential formation of neutral C_{10}, presumed to be cyclic, under these conditions, since the anions were thought to form as products of the reaction between neutral clusters and photoelectrons in the cluster source.

In the SCF calculations of Raghavachari and Binkley, a cyclic structure of D_{5h} symmetry was determined to be the ground state of C_{10}.[67] Liang and Schaefer performed calculations at the CISD/DZP level to study the relative isomer energies of the cumulenic and acetylenic triplet states of the linear chains as well as three monocyclic rings.[68] The ring structures investigated were a cumulenic D_{10h} structure, a D_{5h} isomer, in which cumulenic double bonding occurs, and a D_{5h} isomer with acetylenic bonding.

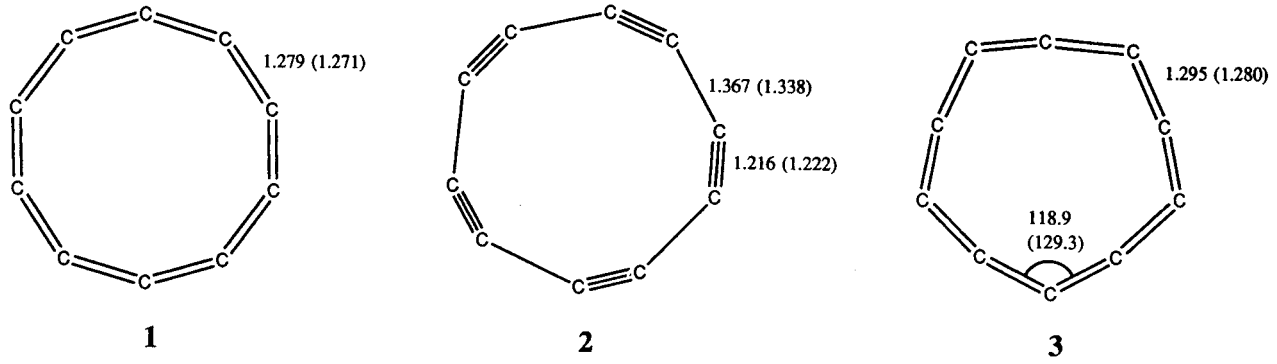

Figure 23. SCF/DZP and SCF/3-21G (parentheses) optimized geometries of cyclic C_{10}. Bond lengths are in angstroms and bond angles are in degrees. (Reprinted with permission from ref 68. Copyright 1990 American Institute of Physics.)

These structures are labeled as 1, 2, and 3, respectively, in Figure 23. At the highest level of theory considered (CISD/DZP including Davidson's correction), the cumulenic D_{5h} ring was found to be the global minimum, lying 67 kcal/mol below the lowest energy linear structure. The relative energies of the linear structures depended strongly upon the level of theory and the basis set. Liang and Schaefer investigated these effects by performing calculations at the SCF and CISD levels using both the DZP and the 3-21G basis sets. The acetylenic structure of linear C_{10} was actually the lowest energy form for the lower levels of theory. Only after the Davidson correction was applied at the CISD/DZP level did the cumulenic structure emerge as the most stable linear chain by 4.9 kcal/mol. Similar effects were observed in the relative energy calculations of the monocyclic rings. At the CISD/3-21G level, the acetylenic D_{5h} structure was lowest in energy, while calculations at the CISD/DZP level with the Davidson correction found this structure to be least stable. Electron correlation effects had a strong influence on the energy spacing between the D_{5h} and the D_{10h} cumulenic isomers. While the D_{5h} structure was lower in energy, increasing the level of electron correlation systematically reduced the relative energy. Thus, the authors could not confirm that the D_{5h} structure would still be the global minimum at higher levels of theory.

Watts and Bartlett studied the structures and energetics of cyclic C_{10} isomers at higher levels of electron correlation using coupled cluster methods.[271] The D_{5h} cumulene, the D_{5h} acetylene, and the D_{10h} cumulene were again investigated, this time at the CCSD+T(CCSD) and the CCSD(T) levels, using the cc-pVDZ basis set. They also reported SCF and second-, third-, and fourth-order MBPT results for comparison, although these methods were generally found to be artifactual for studying a system of this size. The DZP and 4s3p1d basis sets were used to study basis set effects on the relative energies. At the CCSD(T)/cc-pVDZ level of theory, the D_{5h} cumulene was the lowest energy isomer, lying 2.4 kcal/mol lower in energy than the D_{10h} structure. However, when the basis set was expanded to 4s3p1d quality, the CCSD(T) level of theory predicted an energy separation that was reduced to within the expected errors of the calculation. A vibrational analysis of the three structures indicated that the D_{5h} structure was a local minimum. The D_{10h} structure was most likely a transition state along a ring deformation coordinate of the D_{5h} structure, in which the vibrational motion interconverts the molecule between two equivalent minima. Force constant calculations indicated that this vibration of the D_{5h} isomer was very floppy. Because of the large zero point energy of cyclic C_{10}, it is most likely that the effective vibrationally averaged structure that would be observed experimentally would be the D_{10h} ring.

Martin and Taylor investigated the relative energies of the D_{5h} and D_{10h} cumulenes as part of their coupled cluster study of the vibrational spectrum of small carbon clusters.[58] They confirmed that the D_{10h} structure is a transition state at the CCSD(T)/cc-pVTZ level, lying an estimated 1.0 ± 0.1 kcal/mol above the D_{5h} minimum. Again it was predicted that the vibrationally averaged structure would possess D_{10h} symmetry. The harmonic frequencies of the three vibrationally active e_1' modes were calculated at the CCSD(T)/cc-pVDZ level of theory. The most intense transition was predicted to occur at 2011 cm^{-1}, which the authors speculated may correspond to a matrix absorption at 1915 cm^{-1}. This peak grows very strongly with annealing as would be expected for a cyclic carbon cluster.

B. Experiment

Despite the theoretical predictions that the most stable form of C_{10} should be cyclic, the only experimental data that exist for the neutral cluster is for the linear isomer. This is also the case for C_{11}, C_{13}, and C_{15}, to be discussed below. It is interesting to note that, even for the extremely large linear−cyclic energy splitting that has been predicted for C_{10}, the linear chain still seems to be the favored isomer under experimental conditions. The ESR spectrum of $^3\Sigma_g^-$ C_{10} was detected in solid Ar along with those of linear C_4, C_6, and C_8.[232,233] The zero field splitting parameter, $|D|$, for C_{10} was the lowest value observed for these clusters, which was anomalous since $|D|$ increased with cluster size for C_4-C_8. It was suggested that this relatively low zero field splitting may be due to a nonlinear structure.

Freivogel et al. have recently reported observation of two infrared transitions at 2074.5 and 1915.4 cm^{-1} that were present after a Ne matrix containing mass-selected C_{10}^- was irradiated with UV light.[228] These

bands were tentatively assigned as antisymmetric stretches of linear C_{10}, although assignment of one of these bands to the cyclic isomer cannot be ruled out, since theoretical calculations predict that an infrared active transition should occur in this region.[62]

C. Excited Electronic States

Liang and Schaefer's CISD/DZP predictions, including Davidson's correction, for the low-lying singlet states of linear C_{10} were 2.71 kcal/mol for the $^1\Delta_g$ state and −2.28 kcal/mol for the $^1(\Sigma\Delta)$ state.[186] The $^1(\Sigma\Delta)$ state was actually found to be lower in energy than the $^3\Sigma_g^-$ state, although the experimental ESR measurements support a $^3\Sigma_g^-$ ground state. Freivogel et al. measured three vibronic transitions that were assigned to the $^3\Sigma_u^- - X^3\Sigma_g^-$ band of linear C_{10} in a Ne matrix, whose origin occurred at 13 596 cm^{-1}.[207] However, in more recent work this band was attributed to the $(2)^2\Pi_g - X^2\Pi_u$ spectrum of linear C_{10}^-.[213] A new band measured at 12 985 cm^{-1} has now been attributed to the $^3\Sigma_u^- - X^3\Sigma_g^-$ band origin of neutral C_{10} (see Figure 13).[213]

D. C_{10}^-

C_{10}^- is the smallest carbon cluster anion for which a significant fraction of the planar monocyclic ring isomer is observed in the ATD of the ion chromatography experiments.[227,239] Both the linear and cyclic forms are present, and, depending upon experimental conditions, one isomer can be made to dominate over the other. Annealing experiments performed to determine the relative stabilities of the linear and cyclic anions were significantly more difficult to interpret than for the cations.[227] This is due to the lower barriers that are thought to exist between the linear and cyclic minima of the anions. Increasing the energy at which the ions were injected into the He drift cell was found to favor the formation of linear isomers for cluster anions in the $C_{10}^- - C_{15}^-$ size range. For example, the isomer distribution of C_{10}^- was shifted to almost 100% linear at an injection energy of 100 eV. One possible explanation for this observation could be that the ground-state structures of these clusters are the linear chains. Alternatively, the formation of linear isomers at increased injection energies could be due to their higher density of states at these energies. Bowers and co-workers favor the latter explanation and consider the cyclic isomers to be the ground states for these clusters,[227] although the energy differences between the two isomers are probably quite small (≤5 kcal/mol). Theoretical calculations that address these issues would be of great value.

C_{10}^- has been studied experimentally by photoelectron (PE) spectroscopy[41,77,78,272,273] and infrared[228] and electronic[207,213] absorption spectroscopy of mass-selected C_{10}^- deposited in a Ne matrix. Evidence for a linear to cyclic transition at C_{10}^- was provided by the photoelectron spectroscopy experiments of Yang et al.[77,78] and more recently, by the PE studies of Handschuh et al. on annealed cluster ions.[273] Arnold et al. observed broad, unresolved features in their anion photoelectron spectra of C_{10}^- that they attributed to transitions between nonlinear isomers of the anion and/or the neutral cluster.[41] However, Achiba et al. reported evidence for both cyclic and linear isomers of $C_{10}^- - C_{20}^-$ in their photoelectron spectra in which the clusters were formed under different experimental conditions.[272] The disparity between these observations underscores the complex competition between linear and cyclic isomers observed by Bowers and co-workers.[227,239]

Electronic absorption spectroscopy of mass-selected cluster ions deposited in Ne matrices has been used to measure the $C^2\Pi_g - X^2\Pi_u$, the $(2)^2\Pi_g - X^2\Pi_u$, and the $B^2\Sigma_g^+ - X^2\Pi_u$ bands of linear C_{10}^-.[207,213] The band origins were at 10 338, 13 596, and 8964 cm^{-1}, respectively. Freivogel et al. observed an infrared absorption at 2094.5 cm^{-1} in the Ne matrix that they attributed to an antisymmetric stretch vibration of linear C_{10}^-.[228]

E. C_{10}^+

Ion chromatography experiments indicated that C_{10}^+ is formed overwhelmingly as a planar monocyclic ring.[241−243] Only a very small fraction of the ions were present in the linear form. Annealing studies showed that the cyclic isomer was about 47 ± 8 kcal/mol more stable than the linear chain.[241] An ROHF/6-31G(d) calculation predicted that the ground state was a C_{2v} structure with a $^2A''$ electronic state.[241]

XIV. C_{11} and Beyond

A. Theory

Clusters in the C_{11} to ~C_{20} size range are predicted to exist predominantly as monocyclic rings. At this size, the angle strain associated with closing the ring is small, while added stability arises from forming an additional carbon−carbon bond. Unfortunately, very high level ab initio techniques such as coupled cluster methods are currently too costly to be performed on clusters of this size. While perturbative methods such as MP2 have been performed for C_{11},[274] C_{13},[275] and larger systems[276] to calculate structures and linear−cyclic energy spacings, we have already addressed the limitations of these techniques from results on the smaller clusters. The highest level calculations to be performed on clusters in this size range are the CASSCF studies applied to linear C_{11} and C_{13} by Martin et al.[264] In general, theoretical calculations for clusters of this size must be viewed with caution, as we have seen the importance of treating electron correlation at high levels of theory, which is difficult to accomplish for these larger species.

Density functional theory (DFT) has recently emerged as a technique that can be applied to much larger systems than more accurate ab initio methods such as coupled cluster, due to its lower CPU time dependence on the size of the system. In general, DFT calculations of the structures and vibrational frequencies of smaller clusters are in excellent agreement with more sophisticated coupled cluster calculations and with experiment.[60,62] However, the ac-

curacy of these techniques has not been verified for systems larger than C_{10}. Hutter et al. used the BLYP level of DFT to calculate structures, relative isomer energies, and vibrational frequencies for C_2-C_{18}.[60] For the small C_2-C_9 clusters, this technique reproduced structural parameters and harmonic frequencies that were generally in good agreement with coupled cluster calculations.[58] The exceptions were that a bent equilibrium structure was obtained for C_3, and a C_{2h} structure was found to be the lowest ring isomer of C_8. For the relative isomer energies of C_4, C_6, and C_8, the density functional treatment was found to overestimate the stability of the linear triplet states. Thus, quantitative agreement with the higher levels was not achieved, although in all cases the chain and the ring were close in energy. For the odd-numbered clusters in the $C_{11}-C_{17}$ size range, the authors found that planar, monocyclic rings were lower in energy than the chains. However, imaginary vibrational frequencies were calculated for all these clusters, leading the authors to conclude that the true ground states should have three-dimensional structures. For the even-numbered $C_{12}-C_{18}$ clusters, the planar monocyclic rings were also more stable than the chains. While C_{12} and C_{14} were both local minima, C_{16} and C_{18} had imaginary frequencies.

Martin et al. used the more sophisticated B3LYP level of DFT to study the even-numbered $C_{12}-C_{18}$.[62] They also performed calculations on C_2-C_{10} for comparison with higher level results. Better structural agreement with the coupled cluster calculations was achieved in that the structures of C_3 and cyclic C_8 were predicted correctly. The vibrational frequencies of these smaller clusters were of the same level of accuracy for predicting experimental values as the CCSD(T)/cc-pVDZ predictions, although linear−cyclic energy spacings for the even clusters showed a bias toward the linear triplets when compared to higher level results. For the larger clusters, this study found that the planar monocyclic rings of $C_{12}-C_{18}$ were all local minima, in contrast to the work of Hutter et al.[60] Cyclic C_{4n+2} clusters, including C_6 and C_{10}, were predicted to be doubly aromatic, such that the valence electrons are delocalized in two perpendicular systems of π orbitals, one in the plane of the ring, and the other out of the plane.[62] Martin et al. found that the most stable structures for these clusters were of $D_{(2n+1)h}$ symmetry with cumulenic bonding configurations. In contrast, the cyclic C_{4n} clusters, including C_8, existed in planar rings of $C_{(2n)h}$ symmetry. The acetylenic forms of these C_{4n} rings were determined to be lower in energy than the cumulenic forms.

More recently, Martin et al. have used density functional theory methods to examine structural properties, infrared spectra, and linear−cyclic isomerism of the odd-numbered C_{2n+1} clusters in the C_5-C_{15} size range.[247] CCSD(T)/cc-pVDZ methods were also used to calculate the relative isomer energies for the smaller linear and cyclic C_5-C_{11} systems. Not surprisingly, these results found that the linear isomers were strongly favored for clusters smaller than C_{10}, although the energy difference dropped sharply with increasing cluster size, from 60 kcal/mol for C_5, 14 kcal/mol for C_7, and 9 kcal/mol for C_9, as already discussed. For C_{11}, the ring structure was predicted to be more stable by 27 kcal/mol at this level. For C_{13}, the B3PW91 level of density functional theory was considered to be the best substitute for coupled cluster methods in the calculation of relative isomer energies. At this level, the monocyclic ring isomer was predicted to be more stable than the linear chain by 28 kcal/mol. Thus, according to the latest density functional theory results, linear isomers of clusters larger than C_{11} are not expected to be energetically competitive with planar monocyclic rings. Despite these predictions, linear chains continue to be experimentally observed for clusters in this size range.

For clusters larger than $\sim C_{20}$, numerous low-energy structural isomers have been predicted to exist. These include linear chains, monocyclic and polycyclic rings, closed-cage fullerenes, graphitic sheets, and bowl-shaped isomers to be discussed below. Many of these isomers have been observed for carbon cluster ions larger than $\sim C_{30}$ in the gas-phase ion chromatography experiments of Bowers and co-workers.[227,242,243,277] Examples of the kinds of structures that have been observed are shown in Figure 24, which depicts several isomers of C_{36}^-, deduced from ion chromatography experiments.[227] DFT calculations have been used to study the isomers of C_{20},[59,63,278] C_{24},[61] and C_{28}.[64] In particular, these calculations predict that fullerene, graphitic, and bowl-shaped structures are the lowest energy isomers of these clusters, although the ion chromatography experiments have found no evidence for fullerene or graphitic structures for cluster ions this small, and no evidence for bowl-shaped isomers of any size.[227,242,243,277] These issues will be discussed in more detail below with respect to the C_{20} cluster. More recently, Jones and Seifert have used local spin density and gradient corrected DFT to study the isomers of $C_{14}-C_{24}$.[65] For all clusters in this size range, the authors found numerous stable isomers, including linear chains, planar monocyclic and polycyclic rings, graphitic fragments, and closed-cage fullerene-like isomers. Again, there is no experimental verification for any structures besides linear chains and planar rings in this size range.

B. C_{20}

An interesting question regarding clusters in the C_{11} to $\sim C_{30}$ size range is, at what size does the closed cage fullerene-like structure begin to emerge as a stable isomer? This has been a difficult question to answer definitively because of the experimental and theoretical challenges posed by systems of this size. While it is fairly well established that, for even-numbered clusters above C_{32}, fullerenes are the most stable isomers, it is not certain precisely where the transition from ring structures to fullerenes occurs. The ion mobility experiments by Bowers and co-workers revealed more than one isomer to be present for cluster ions larger than C_{20}, with structures ranging from chains to polycyclic rings, although there was no evidence for fullerene structures smaller than C_{30}.[227,242,243,277] However, as alluded to above, several theoretical studies have shown that fullerene-

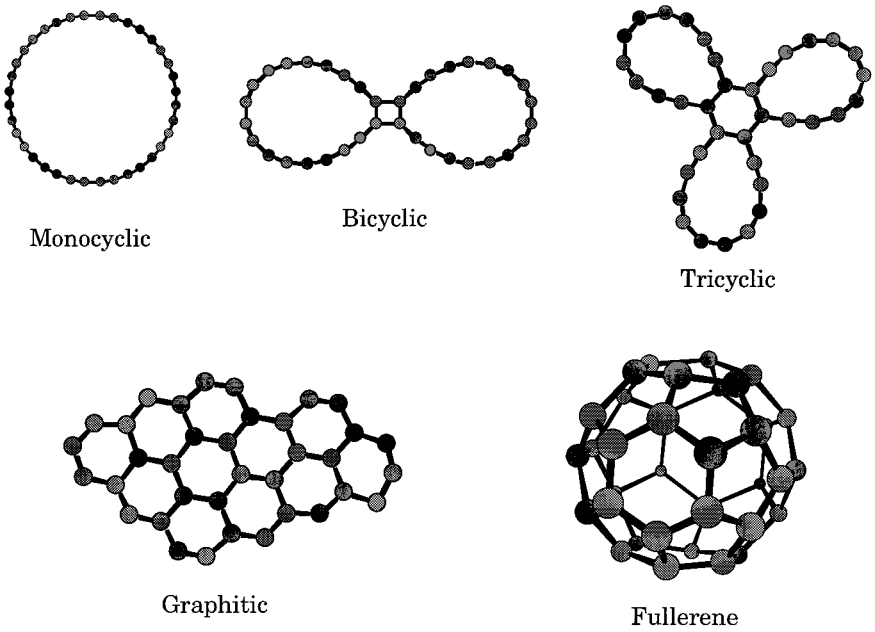

Figure 24. Structural isomers of C_{36}^- observed in gas-phase ion chromatography experiments. The structures were deduced from semiempirical quantum chemistry methods and theoretical modeling of the observed arrival time distributions. Different isomers of the bi- and tricyclic rings could not be ruled out from the data. (Reprinted with permission from ref 227. Copyright 1995 Elsevier Science B.V.)

like closed-cage isomers may be low in energy for clusters as small as C_{20} or smaller.[59,61,63,65,276,278−282]

C_{20} has received a lot of attention with regard to its possible role as the smallest fullerene.[279] Ion mobility experiments have indicated that C_{20} cations produced by laser vaporization of graphite exist exclusively as monocyclic rings.[242,243,277] For the anions, a small quantity of linear chains and polycyclic rings also coexisted with the predominant monocyclic isomer.[227,239,277] There was no evidence for a fullerene isomer or a bowl-shaped structure. Three structural isomers have been considered as low-energy forms of C_{20}—a planar monocyclic ring, a curved graphitic bowl, and a closed-cage fullerene in the theoretical calculations. These isomers are diagramed in Figure 25. Brabec et al. used the local density approximation to study the annealing behavior of C_{20} at various temperatures.[278] As the annealing temperature increased, the favored structures changed from the fullerene to a bowl-shaped corrannulene-like structure to the monocyclic ring. Parasuk and Almlöf studied the relative energies of three planar monocyclic ring isomers and the fullerene with SCF and MP2 ab initio methods.[279] At the SCF level, an acetylenic D_{10h} ring was predicted to be the ground state, with the fullerene lying over 100 kcal/mol higher in energy. However, inclusion of electron correlation at the MP2 level resulted in a reversal of the relative energies, with the fullerene lying over 60 kcal/mol lower in energy than the nearest ring. Raghavachari et al. used the BLYP level of density functional theory to study the monocyclic ring, the fullerene cage and the corrannulene structures.[59] The BLYP level includes a gradient correction in the density functional treatment that was found to have a major effect on the relative energies. Without the gradient correction, the cage isomer was significantly lower in energy than the ring and the corrannulene

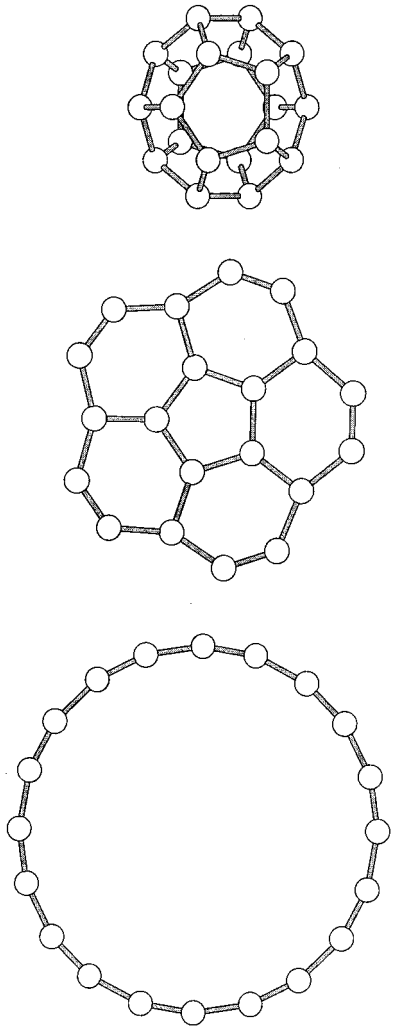

Figure 25. Fullerene, corranulene-like bowl, and monocyclic ring isomers of C_{20}. (Reprinted with permission from ref 281. Copyright 1995 Elsevier Science B.V.)

forms. However, inclusion of the gradient correction yielded the monocyclic ring as the ground state by 3.44 eV over the fullerene.

More recent theoretical studies have predicted the bowl-shaped isomer to be the ground state of C_{20}, with the fullerene structure lying close in energy and the ring at substantially higher energies. Grossman et al. used quantum Monte Carlo methods to predict the relative energies of a monocyclic ring, a corrannulene-like bowl, and a cage structure at high levels of electron correlation.[280] The structures investigated were those that had been optimized at the HF level. This work emphasized the importance of accurately treating electron correlation, finding that the more compact cage and bowl structures emerged as the lowest energy forms at this level of accuracy. Martin et al. used the B3LYP level of DFT to optimize the ring, bowl, and cage structures and to calculate relative energies and vibrational frequencies.[63] The most stable ring isomer was a polyacetylenic C_{10h} structure which was estimated to lie 48.1 kcal/mol above the bowl and 38.4 kcal/mol above the cage. Taylor et al. used CCSD(T) calculations to study the three C_{20} isomers, making this the largest carbon cluster, and the only cluster larger than C_{11}, for which coupled cluster techniques at this level have been applied.[281] The calculations were limited to ring, bowl, and cage structures that were fixed to SCF-optimized geometries. The structures considered are shown in Figure 25. The modest sized cc-pVDZ basis set was the smallest that could be used without sacrificing meaningful results. Even with these limitations, the calculation approached the limit of what can be achieved with modern supercomputers, making geometry optimization and exploration of basis set effects out of the question at this level. The energy calculations found that the bowl-shaped and cage isomers were nearly isoenergetic, with the ring lying 39 kcal/mol higher in energy.

It is interesting to note that the bowl-shaped isomer predicted to be the ground state of C_{20} is the smallest of the so-called "pentagon road" structures.[283] These types of structures have been predicted to be low-energy isomeric forms for a number of larger carbon clusters as well.[284] The "pentagon road" mechanism is a hypothesis for fullerene formation which states that the precursors to fullerene formation are highly reactive curve-shaped open cages with the carbon atoms arranged in pentagons and hexagons. "Pentagon road" structures are those that contain the maximum number of pentagons that can be arranged in such a way so that each pentagon is surrounded on all sides by five hexagons. Fullerene formation is thought to occur when conditions are such that the smaller precursors have sufficient time to anneal to their most favorable "pentagon road" structures. Growth of these structures then proceeds to C_{60}, which is the smallest cluster for which the "pentagon road" structure is a closed cage, and to larger closed-cage fullerenes such as C_{70}, C_{84}, and so on.

Despite its elegance, the "pentagon road" mechanism is difficult to rationalize in light of recent experimental ion mobility studies by Bowers and coworkers and Jarrold and co-workers. First, there are no isomers detected at any size, for which the ion mobility is consistent with these curved graphitic bowl or cup-like structures, although a recent attempt was made to produce such species from polychlorinated precursors.[285] It was clearly shown that growth of these ions proceeds through linear chains to planar rings.[52,227,242,243] Closed cages appear at C_{30} and become the dominant isomers above C_{40}, at least for the cations. Second, annealing studies of the cluster ions have shown that collisional heating of metastable cyclic isomers, followed by ejection of a small carbon fragment, is an efficient pathway to fullerene formation.[286−291] For example, the ion mobility of C_{39}^+ through the He drift cell showed that this cluster exists in several different cyclic forms.[287] Most of these isomers were metastable, however, and were produced when the high-energy laser vaporization plasma was rapidly cooled in a supersonic expansion. Annealing of the clusters took place when the ions were injected into the drift cell at 150 eV. The main products of this annealing process were the monocylic ring isomer of C_{39}^+ and the fullerene isomers of C_{38}^+ and C_{36}^+, which were accompanied by the ejection of C and C_3 fragments, respectively. Thus, a more likely mechanism is that fullerenes are formed in laser vaporization or arc discharge sources through the growth of high-energy metastable cyclic clusters that subsequently anneal to fullerenes by evaporation of smaller fragments. Further evidence for fullerene formation from the coalescence of cyclic rings was provided by Rubin et al.[109] and McElvany et al.[292] These authors showed that fullerenes could be produced by laser desorption of such cyclocarbon species as $C_{18}(CO)_6$, $C_{24}(CO)_8$, and $C_{30}(CO)_{10}$. Hunter et al. have recently proposed a detailed mechanism for the formation of fullerenes from cyclic precursors.[291]

C. Experimental Observations

1. Gas-Phase Infrared Spectroscopy of the Linear C_{13} Cluster

Most of the experimental information concerning C_{11} and larger carbon clusters has been provided by the gas-phase ion chromatography studies of carbon cluster ions to be discussed below. For the neutral species, experimental data are extremely sparse. Despite theoretical results predicting cyclic ground states for these clusters, only linear isomers have been detected experimentally. Even for clusters as large as C_{20}, the linear isomers are still competitive under experimental conditions, due to their much higher density of states, and consequently, their more favorable entropy of formation. The only definitive spectroscopic information for a cluster of this size is for linear C_{13}. This molecule is the only carbon cluster larger than C_9 for which a rotationally resolved spectrum has been recorded.[36] Giesen et al. measured 76 rovibrational absorption transitions in the frequency region between 1808.1 and 1809.7 cm^{-1} using infrared diode laser spectroscopy of a supersonic cluster beam. Figure 26 displays part of the observed spectrum. Transitions with J values up to

Table 12. Molecular Parameters of an Antisymmetric Stretch of $X^1\Sigma_g^+ C_{13}$[a]

parameter	experiment	theory
ν_0 (cm^{-1})	1808.96399(7)[b]	
B''(cm^{-1})	0.0047324(6)[b]	
B' (cm^{-1})	0.0047218(6)[b]	
$\bar{r}_0$ (Å)	1.2770(5)[b]	1.2668 1.2867 1.2581 1.2741 1.2537 1.2688[c]
		1.2717 1.2914 1.2623 1.2786 1.2679 1.2731[d]

[a] Numbers in parentheses are uncertainties in the last digits. [b] Infrared diode laser spectroscopy.[36] [c] Outer to inner equilibrium bond lengths, calculated at the MP2/6-31G* level.[275] [d] Same as *c* at the B3LYP/cc-pVDZ level.[247]

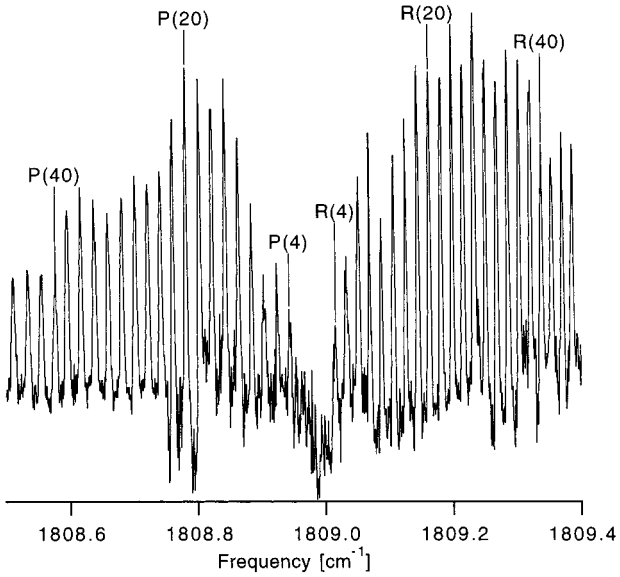

Figure 26. The infrared rovibrational spectrum of an antisymmetric stretch of linear C_{13}. The clusters were produced in a supersonic molecular beam source, and a tunable diode laser spectrometer was used to record the spectrum. (Reprinted from ref 36. Copyright 1994 American Association for the Advancement of Science.)

80 in the P-branch and 74 in the R-branch were observed. The spectrum was characteristic of a centrosymmetric linear carbon cluster in a nondegenerate vibronic state, since only even-numbered rotational states were observed, and only P- and R-branch transitions were present. Molecular parameters obtained from analysis of the data are shown in Table 12. By assuming that the carrier of these transitions was the linear C_{13} carbon cluster, an average carbon−carbon bond length of 1.2770(5) Å could be calculated from the ground-state rotational constant. C_{13} is the only cluster that reproduces the bond length within the range of about 1.27 and 1.30 Å expected for a cumulated double bond.

Observation of a linear carbon cluster of this size with a sufficient number density to be detected in a direct absorption experiment was surprising in light of theoretical predictions that the most stable form of these clusters should be cyclic. Hutter et al. found the cyclic isomer of C_{13} to be more stable than the linear form by 20−30 kcal/mol using density functional theory.[60] This result was consistent with the more recent study by Martin et al, cited above, who found the ring form to be favored by 28 kcal/mol using the B3LYP functional.[247] Bleil et al. calculated relative isomer energies of linear and cyclic C_{13} at the MP2/6-31G* level.[275] The cyclic minimum was found to be a distorted planar ring of C_{2v} symmetry and was only 6.8 kcal/mol lower in energy than the $^1\Sigma_g^+$ linear isomer. Thus, under laser vaporization conditions, these authors predicted that entropy would favor formation of the linear chain.

Vibrational frequencies were calculated for the linear isomer by Bliel et al.[275] at the MP2 level, at the CASSCF level by Martin et al,[264] and at the B3LYP/DFT level by Martin et al.[247] At the CASSCF-(8/8)/cc-pVDZ level, two extremely intense infrared active antisymmetric stretch modes were calculated to occur in the region of the observed spectrum.[264] These were the ν_9 and the ν_{10} transitions at 2003 and 1843 cm^{-1} respectively. By using a scaling factor of 0.93, derived from C_9, the ν_9 transition of C_{13} would be predicted to occur near 1850 cm^{-1}, which is somewhat close to the measured band origin of 1809 cm^{-1}. However, at the B3LYP level, there were no scaled frequencies that resembled the experimental result.[247] The closest predictions were 1944 ± 16 cm^{-1} and 1666 ± 14 cm^{-1}. Previously it was found that vibrational frequencies calculated using the B3LYP functional are in excellent agreement with more sophisticated CCSD(T) results for the smaller clusters,[62] whereas the CASSCF methods were found to produce artifacts. Therefore, Martin et al. suggested that the experimental frequency may be due to a Fermi-type resonance.[247] This would not be too surprising given the high density of states for such a large molecule.

2. Photoelectron, Optical, and Infrared Spectroscopy

C_{11} was observed in the anion photoelectron spectra of Arnold et al.[41] Three vibrational peaks, consistent with linear to linear transitions of the anion and the neutral, were measured, although no vibrational assignments were given. Broad, unresolved structure was also observed and was interpreted as transitions involving cyclic isomers for the anion and/or the neutral. Frievogal et al. observed electronic spectra of mass selected clusters deposited in a solid Ne matrix that were assigned to $^3\Sigma_u^- - X^3\Sigma_g^-$ vibronic transitions of linear C_{12} and C_{14}.[207] The origin bands fit on a linear plot of the C_4 through C_{10} origins. However, recent experiments have shown that these assignments were in error and were actually due to the $(2)^2\Pi - X^2\Pi$ transitions of the corresponding anions.[213] To date, there is no conclusive experimental data to characterize the even-numbered neutral carbon clusters larger than C_{10}. The odd-numbered C_{11}, C_{13}, and C_{15} clusters have been observed via their $^1\Sigma_u^+ - X^1\Sigma_g^+$ electronic absorption spectra in Ne matrices.[167]

Frievogel et al. assigned two infrared absorption transitions at 1938.6 and 1853.4 cm^{-1} of mass-

selected C_{11} in a Ne matrix to the ν_7 and ν_8 antisymmetric stretch vibrations of linear C_{11}.[228] A band at 2003.9 cm^{-1} was tentatively assigned to linear C_{12}.

D. Large Carbon Cluster Ions

As already pointed out, production of neutral carbon clusters is often accompanied by the formation of carbon cluster ions, which are important in growth and annealing processes. Experimentally, larger carbon cluster ions have been studied extensively using various mass spectrometric techniques, including gas-phase ion chromatography[51−53] and ion−molecule reactivity studies.[259] In addition, photoelectron spectroscopy has been used to study carbon cluster anions as large as $\sim C_{80}^-$,[49,77,78,272,273] and optical spectra have been recorded for mass-selected anions in Ne matrices as large as C_{20}^-.[46]

1. Ion Mobility Studies

Gas-phase ion chromatography has recently emerged as the most direct approach for obtaining structural information about carbon cluster ions larger than C_{10}. von Helden et al. reported studies on the structures and reactivities of carbon cluster cations from C_6^+ to C_{84}^+.[242,243] These authors identified several different families of structures that appear as the cluster size increases. For C_7^+ through C_{10}^+, linear chain structures coexisted with monocyclic rings.[241−243,260] As mentioned above, annealing studies showed that the ground states of these clusters were the ring forms, although linear chains were also present due to entropic considerations. The chain isomer disappeared at C_{10}^+, while planar monocyclic rings were the only isomers present for C_{10}^+ through C_{20}^+. As the cluster size increased beyond C_{20}^+, several different isomers were found to coexist. The mobilities of these isomers were consistent with planar monocyclic, bicyclic, and tricyclic rings. Above C_{30}^+, closed cage fullerene structures were also present, as well as a graphitic fragment. For clusters larger than C_{40}^+, fullerenes became the dominant structures for even-numbered clusters and were the only isomers present above C_{60}^+. For the odd-numbered clusters, closed caged fullerenes dominated above C_{49}^+, although ring isomers continued to coexist with the cages at larger sizes. Annealing studies indicated that, of the planar rings in the C_{20}^+ to C_{40}^+ size range, the monocyclic isomers were the most stable.[286,289,290,293] It was also found that fullerenes could be formed from larger ring isomers after C, C_2, or C_3 dissociation.[287,288] Graphitic fragments were a very minor component of the isomer distribution for C_{20}^+ to C_{40}^+, and "pentagon road" structures were not observed. Figure 27 plots the ion mobilities observed for the different cation isomers as a function of cluster size. This figure illustrates the cluster size ranges in which each kind of isomer is observed.

For the anions, these same families of structures were also observed, although there were differences in the relative isomer abundances and size distributions.[227,239] Figure 28 displays the ion mobilities as a function of cluster size for the anions. One of the differences between the ion mobility studies of the

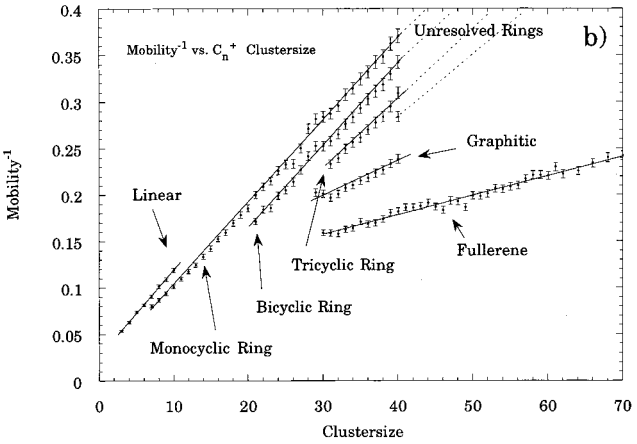

Figure 27. A plot of K_0^{-1} (where K_0 is the ion mobility through the He drift cell) vs cluster size for carbon cluster cations, measured using gas-phase ion chromatography. There is a near linear relationship between K_0^{-1} and the cluster size within each family of structural isomers. (Reprinted with permission from ref 227. Copyright 1995 Elsevier Science B.V.)

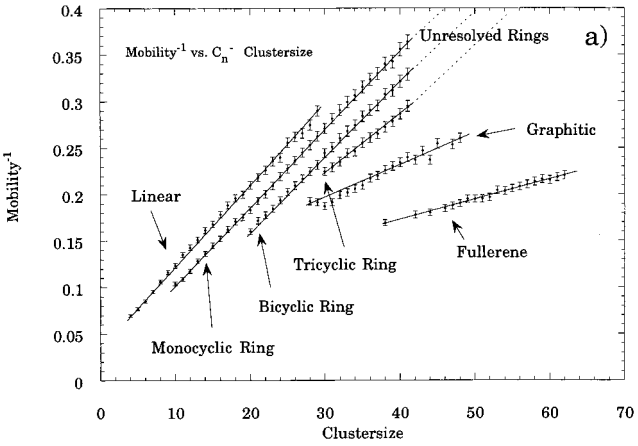

Figure 28. A plot of K_0^{-1} (where K_0 is the ion mobility through the He drift cell) vs cluster size for carbon cluster anions, measured using gas-phase ion chromatography. (Reprinted with permission from ref 227. Copyright 1995 Elsevier Science B.V.)

anions and those of the cations was in the size distribution of the linear chains. Linear isomers were found to coexist with monocyclic rings for C_{10}^- all the way up to C_{30}^-, while the monocyclic ring isomers were not present for clusters smaller than C_{10}^-. Annealing studies showed that cyclic isomers were clearly favored for C_{16}^- and larger anions and became the dominant structure by C_{20}^-. The annealing results for C_{10}^-−C_{15}^- were somewhat inconclusive, as discussed previously for C_{10}^-. Another surprising result of the anion studies was the low prominence of fullerene structures. Small fullerene peaks began to appear at C_{36}^-, but the fraction of these structures in the isomer distributions remained very low for all clusters. Even for C_{60}^-, the distribution was dominated by planar rings, with the fullerene accounting for less than 20% of the isomers. Of course this is entirely dependent upon the conditions under which the clusters were formed and may or may not reflect a reduced stability for the fullerene anions, relative to the ring isomers.

2. Ion–Molecule Reactivity Studies

Prior to the development of gas-phase ion chromatography, the most direct experimental data on the structures of cluster ions came from chemical reactivity studies. As already discussed, reactivity studies provided the first evidence for the existence of cyclic isomers of C_7^+, C_8^+, and C_9^+.[257,258] Parent and Anderson recently reviewed this area of research on metal and semimetal clusters, including carbon clusters.[259] Fourier transform ion cyclotron resonance (FT-ICR) spectrometry or guided ion beam techniques are typically used to react a mass selected carbon cluster with a reactant gas. From the measured reaction cross sections, it is possible to differentiate between, for example, reactive open-shell clusters ions such as linear chains, and less reactive cyclic species. These studies of course provide much useful information about the ion−molecule chemistry of carbon cluster ions. In recent years, carbon cluster cation structural and reactive properties have been investigated by reactions with such species as H_2,[294−296] O_2,[297] N_2O,[289−298] benzene,[299] naphthalene,[300] nitriles,[301,302] chloropropenes,[303] and polyaromatic hydrocarbons.[304] Pozniak and Dunbar recently showed that C_{10}^+ to C_{24}^+ ions whose cyclic isomers satisfied the conditions for aromaticity were less reactive than the other ions in this size range.[302]

In some of these studies, information about the neutral structures was obtained by seeding the reactant in the carrier gas of a laser vaporization−supersonic expansion source.[294−296] Neutral species formed in the expansion were then ionized and observed using time-of-flight mass spectrometry. Long polyacetylenic chains (HC_nH, $n \leq 40$) were thought to be present with H_2 as the reactant gas, leading to the conjecture that neutral carbon chains of this size may be forming. Lagow et al.[34] introduced CF_3 and CN radicals into a fullerene synthesis chamber and found evidence for the formation of stable polyacetylenic carbon chains up to 300 atoms in length, stabilized by free radical end-capping groups. Furthermore, these authors found that in the presence of these free radical capping groups, fullerene synthesis was suppressed in favor of long carbon chains. Therefore, they speculated that long carbon chains are the main precursors to fullerene formation and that these chain species may be responsible for the peaks attributed to polycyclic rings in the ion mobility experiments. An alternative explanation might be that the capping groups actually suppress the formation of polycyclic ring structures, which, in turn, prevents the onset of fullerene formation. This latter explanation is more consistent with the body of evidence compiled by Bowers, Jarrold, McKelvany, and their co-workers, discussed above.[287,288,291,292]

3. Photoelectron Spectroscopy

Yang et al. measured photolectron (PE) spectra of carbon cluster anions as large as C_{84}^-.[77,78] The most significant result of this study was the observation of an abrupt change in the electron affinity at C_{10}^-, which was taken as evidence for a linear to cyclic transition. More recent measurements by Handschuh et al. supported this observation.[273] These authors measured PE spectra of C_5^- to C_{70}^- clusters produced by laser vaporization of graphite, followed by annealing of the clusters in a He discharge. This, according to the authors, ensured that all clusters studied in the PE experiment were present in their most stable structures. Vibrationally resolved PE measurements were consistent with monocyclic rings for even-numbered C_{10}^- to C_{18}^-, bicyclic rings for C_{20}^-, C_{24}^-, and C_{28}^-, and fullerenes for even-numbered clusters larger than C_{30}^-. The results for C_{10}^-, C_{12}^-, and C_{14}^- somewhat conflict with the observations of Bowers and co-workers, who found linear chains to dominate for these clusters upon annealing.[227] These conflicting results further underscore the extreme sensitivity to experimental conditions of the carbon cluster anion isomer distribution.

4. Electronic and Infrared Absorption Spectroscopy

As has already been discussed, Maier and coworkers recently developed a technique whereby mass-selected carbon cluster anions are deposited from the gas phase into a low temperature (4 K) Ne matrix.[207,213,214] Electronic absorption spectra can then be recorded for the anion and, after UV irradiation of the matrix, the corresponding neutral cluster. Several $^2\Pi-X^2\Pi$-type bands for linear C_{11}^- and even-numbered linear C_{12}^-−C_{20}^- have been observed.[207,213,214] In addition, two infrared absorption transitions at 2012.6 and 1819.3 cm^{-1} were observed for mass-selected C_{12}^- that correlated in intensity with the electronic band and disappeared upon UV irradiation.[228] Therefore, these transitions were assigned as antisymmetric stretch vibrations of linear C_{12}^-.

XV. Conclusion

In their 1989 review article, Weltner and Van Zee stated that "the present knowledge of C_n molecules and their ions is almost a monotonically decreasing function of n".[1] This is probably still the case, although the width of the decay has increased significantly in recent years. C_3 is now extremely well-characterized in its ground and several excited electronic states,[39,40] and steps have now been taken to characterize this cluster in the interstellar medium.[5,6] Very precise structural information now exists for the ground electronic states of linear C_4−C_7, C_9, and C_{13} from gas-phase infrared laser spectroscopy experiments.[35−38,236] Similar information for the cyclic isomers in this size range would be of great value. Accurate vibrational energies for all of the linear clusters in the C_2−C_9 size range, as well as a few vibrational frequencies for linear C_{10}−C_{13} now exist from high-resolution laser spectroscopy measurements,[36] as well as from infrared absorption of carbon clusters in cryogenic matrices,[113,228] photoelectron spectroscopy,[41,42] and ab initio quantum chemistry.[58,62] More accurate ab initio techniques have been applied to the cyclic isomers of these clusters, providing more reliable guidance to experimentalists trying to detect and characterize these species.[58,71−73,271] Electronic absorption[46] and mul-

tiphoton photodetachment spectroscopy[47−49] are providing new information about the excited electronic states of linear carbon clusters and their anions as large as C_{20}. Measurements of these transitions in the gas-phase by direct absorption spectroscopy may be the next step toward further characterizing these systems. Finally, the gas-phase ion chromatography experiments have revealed a wealth of insight into the rich variety of structural isomers that are present for clusters larger than C_{20}, including rings, cages, and sheets that were never imagined prior to a few years ago.[51−53]

Clearly, carbon cluster research has been richly rewarding during the years that have passed since the publication of Weltner and Van Zee's monumental review article, due to the unique properties that have been uncovered for these novel species. A very recent advance in fullerene chemistry has reinforced the need for continued investigation of small carbon clusters such as those described in this review. Piskoti et al. have succeeded in synthesizing C_{36},[305] making this the first fullerene smaller than C_{60} to be obtained in bulk quantities by the carbon arc discharge method of Krätschmer et al.[18] Despite the great progress that has been made in the study of small carbon clusters, we are still very far away from a detailed understanding of the growth mechanisms that lead from small, gas-phase carbon chains and rings to highly ordered solids such as this and other fullerenes, as well as nanoscale carbon materials like "buckytubes," in a carbon arc. With the continued characterization of carbon clusters by high-resolution spectroscopy, we hope to eventually be able to monitor in situ the individual species involved in the carbon arc synthesis, and thereby contribute to a more detailed understanding of the kinetics involved. Such an endeavor would almost certainly require new experimental techniques, since currently existing methods would not have the sensitivity to carry out such measurements. A new direct absorption spectroscopy technique that holds great promise for future developments in the study of small carbon clusters is cavity ringdown laser absorption spectroscopy (CRLAS).[306−309] CRLAS is more sensitive than conventional direct absorption spectroscopy techniques and is broadly tunable from the mid-IR to the UV. Two very recent studies underscore the potential of CRLAS in the study of small carbon clusters. Provencal et al. greatly expanded the number of observed rovibrational transitions in the ν_5 band of C_5 using infrared CRLAS,[309] and Maier and coworkers have observed rotationally resolved electronic absorption spectra of C_6H radicals produced in a pulsed discharge source using CRLAS at visible wavelengths.[310] Further applications of CRLAS to the study of small carbon clusters, as well as the development of new experimental and theoretical methods in the years to come, will clearly be needed to solve the challenging problems that still remain in carbon cluster research.

XVI. Acknowledgments

Carbon cluster research carried out in the Saykally laboratory has been generously supported by the National Aeronautics and Space Administration through their Astrophysics, Exobiology, and Infrared Astronomy Programs. A.V.O. thanks the NASA Graduate Student Researchers Program for support from 1992 to 1995. We thank our co-workers, Jim Heath, Andy Cooksy, Martin Gruebele, Roger Sheeks, Charlie Schmuttenmaer, Erica Kuo, Hyun-Jin Hwang, Keiichi Tanaka, Thomas Giesen, Ray Fellers, Bob Provencal, and Frank Keutsch for their major contributions to this effort over the years. We also thank Peter Bernath, Mike Bowers, John Maier, Nasser Moazzen-Ahmadi, Dan Neumark, Fritz Schaefer, and Martin Vala for providing us with figures to be reprinted herein.

XVII. References

(1) Weltner, W., Jr.; Van Zee, R. J. *Chem. Rev.* **1989**, *89*, 1713.
(2) Hinkle, K. H.; Keady, J. J.; Bernath, P. F. *Science* **1988**, *241*, 1319.
(3) Bernath, P. F.; Hinkle, K. H.; Keady, J. J. *Science* **1989**, *244*, 562.
(4) Douglas, A. E. *Astrophys. J.* **1951**, *114*, 466.
(5) Van Orden, A.; Cruzan, J. D.; Provencal, R. A.; Giesen, T. F.; Saykally, R. J.; Boreiko, R. T.; Betz, A. L. In *Proceedings of the Airborne Astronomy Symposium on the Galactic Ecosystem*; Haas, M. R., Davidson, J. A., Erickson, E. F., Eds.; ASP Conference Series; The Astronomical Society of the Pacific: San Francisco, 1995; Vol. 73, pp 67−70.
(6) Haffner, L. M.; Meyer, D. M. *Astrophys. J.* **1995**, *433*, 450.
(7) Woon, D. E.; Herbst, E. *Astrophys. J.* **1996**, *465*, 795−799.
(8) Bettens, R. P. A.; Herbst, E. *Astrophys. J.* **1996**, *468*, 686−693.
(9) Bettens, R. P. A.; Herbst, E. *Astrophys. J.* **1997**, *478*, 585−593.
(10) Fulara, J.; Lessen, D.; Freivogel, P.; Maier, J. P. *Nature* **1993**, *366*, 439−441.
(11) Freivogel, P.; Fulara, J.; Maier, J. P. *Astrophys. J.* **1994**, *431*, L151-L154.
(12) Zhang, Q. L.; O'Brien, S. C.; Heath, J. R.; Liu, Y.; Curl, R. F.; Kroto, H. W.; Smalley, R. E. *J. Phys. Chem.* **1986**, *90*, 525.
(13) Gerhardt, P.; Loffler, S.; Homann, K. H. *Chem. Phys. Lett.* **1987**, *137*, 306−310.
(14) Kroto, H. W.; McKay, K. *Nature* **1988**, *331*, 328−331.
(15) Allendorf, M. D. *J. Electrochem. Soc.* **1993**, *140*, 747.
(16) Koinuma, H.; Horiuchi, T.; Inomata, K.; Ha, H.-K.; Nakajina, K.; Chaudhary, K. A. *Pure Appl. Chem.* **1996**, *68*, 1151−1154.
(17) Kroto, H. W.; Heath, J. R.; O'Brien, S. C.; Curl, R. F.; Smalley, R. E. *Nature* **1985**, *318*, 162.
(18) Krätschmer, W.; Lamb, L. D.; Fostiropoulos, K.; Huffman, D. R. *Nature* **1990**, *347*, 354.
(19) Iijima, S. *Nature* **1991**, *354*, 56.
(20) Iijima, S.; Achihashi, T.; Ando, Y. *Nature* **1992**, *356*, 776.
(21) Ajayan, P. M.; Iijima, S. *Nature* **1992**, *358*, 23.
(22) Ebbesen, T. W.; Ajayan, P. M. *Nature* **1992**, *358*, 220.
(23) Kroto, H. W.; Allaf, A. W.; Balm, S. P. *Chem. Rev.* **1991**, *91*, 1213.
(24) Schwartz, H. *Angew. Chem.* **1992**, *31*, 293.
(25) Kroto, H. W.; Walton, D. R. M. *The Fullerenes: New Horizons for the Chemistry, Physics, and Astrophysics of Carbon*; Cambridge University Press: New York, 1993.
(26) Kroto, H. W.; Fischer, J. E.; Cox, D. E. *The Fullerenes*, 1st ed.; Pergamon: New York, 1993.
(27) Dresselhaus, M. S.; Dresselhaus, G.; Eklund, P. C. *Science of Fullerenes and Carbon Nanotubes*; Academic Press: San Diego, 1996.
(28) Kroto, H. W.; Walton, D. R. M. *Philos. Trans. R. Soc. London A* **1993**, *343*, 103−112.
(29) Bell, M. B.; Feldman, P. A.; Travers, M. J.; McCarthy, M. C.; Gottlieb, C. A.; Thaddeus, P. *Astrophys. J.* **1997**, *483*, L61-L64.
(30) McCarthy, M. C.; Travers, M. J.; Kovács, A.; Gottlieb, C. A.; Thaddeus, P. *Astrophys. J. Suppl.* **1997**, *113*, 105−120.
(31) Rohlfing, E. A.; Cox, D. M.; Kaldor, A. *J. Chem. Phys.* **1984**, *81*, 3322.
(32) Heath, J. R.; Zhang, Q.; O'Brien, S. C.; Kurl, R. F.; Kroto, H. W.; Smalley, R. E. *J. Am. Chem. Soc.* **1987**, *109*, 359.
(33) Kroto, H. W.; Heath, J. R.; O'Brien, S. C.; Curl, R. F.; Smalley, R. E. *Astrophys. J.* **1987**, *314*, 352.
(34) Lagow, R. J.; Kampa, J. J.; Wei, H.-C.; Battle, S. L.; Genge, J. W.; Laude, D. A.; Harper, C. J.; Bau, R.; Stevens, R. C.; Haw, J. F.; Munsen, E. *Science* **1995**, *267*, 362.
(35) Heath, J. R.; Saykally, R. J. In *On Clusters and Clustering*; P. J. Reynolds, Ed.; Elsevier Science: New York, 1993; pp 7−21.
(36) Giesen, T. F.; Van Orden, A.; Hwang, H. J.; Fellers, R. S.; Provencal, R. A.; Saykally, R. J. *Science* **1994**, *265*, 756.
(37) Moazzen-Ahmadi, N.; Thong, J. J. *Chem. Phys. Lett.* **1995**, *233*, 471.

(38) Van Orden, A.; Provencal, R. A.; Keutsch, F. N.; Saykally, R. J. *J. Chem. Phys.* **1996**, *105*, 6111−6116.
(39) Northrup, F. J.; Sears, T. J.; Rohlfing, E. A. *J. Mol. Spectrosc.* **1991**, *145*, 74.
(40) Mladenovic, M.; Schmatz, S.; Botschwina, P. *J. Chem. Phys.* **1994**, *101*, 5891.
(41) Arnold, D. W.; Bradforth, S. E.; Kitsopoulos, T. N.; Neumark, D. M. *J. Chem. Phys.* **1991**, *95*, 8753.
(42) Xu, C.; Burton, G. R.; Taylor, T. R.; Neumark, D. M. *J. Chem. Phys.* **1997**, *107*, 3428−3436.
(43) Presilla-Marquez, J. D.; Sheehy, J. A.; Mills, J. D.; Carrick, P. G.; Larson, C. W. *Chem. Phys. Lett.* **1997**, *274*, 439−444.
(44) Wang, S. L.; Rittby, C. M. L.; Graham, W. R. M. *J. Chem. Phys.* **1997**, *107*, 6032.
(45) Wang, S. L.; Rittby, C. M. L.; Graham, W. R. M. *J. Chem. Phys.* **1997**, *107*, 7025.
(46) Maier, J. P. *Chem. Soc. Rev.* **1997**, *26*, 21−28.
(47) Ohara, M.; Shiromaru, H.; Achiba, Y.; Aoki, K.; Hashimoto, K.; Ikuta, S. *J. Chem. Phys.* **1995**, *103*, 10393.
(48) Zhao, Y.; de Beer, E.; Xu, C.; Taylor, T.; Neumark, D. M. *J. Chem. Phys.* **1996**, *105*, 4905−4919.
(49) Ohara, M.; Shiromaru, H.; Achiba, Y. *J. Chem. Phys.* **1997**, *106*, 9992−9995.
(50) Tulej, M.; Kirkwood, D. A.; Maccaferri, G.; Dopfer, O.; Maier, J. P. *Chem. Phys.* **1998**, *228*, 293−299.
(51) Bowers, M. T.; Kemper, P. R.; von Helden, G.; van Koppen, P. A. M. *Science* **1993**, *260*, 1446.
(52) Bowers, M. T. *Acc. Chem. Res.* **1994**, *27*, 324.
(53) Shelimov, K. B.; Clemmer, D. E.; Hunter, J. M.; Jarrold, M. F. In *The Chemical Physics of Fullerenes 10 (and 5) Years Later*; Andreoni, W., Ed.; NATO ASI Conference Series E, No. 316; Kluwer Academic Publishers: Dordrecht, 1996; pp 71−87.
(54) Ramanathan, R.; Zimmerman, J. A.; Eyler, J. R. *J. Chem. Phys.* **1993**, *98*, 7838.
(55) Sowa-Resat, M. B.; Hintz, P. A.; Anderson, S. L. *J. Phys. Chem.* **1995**, *99*, 10736.
(56) Scuseria, G. E. *Science* **1996**, *271*, 942.
(57) Schmatz, S.; Botschwina, P. *Int. J. Mass Spectrom. Ion Processes* **1995**, *149/150*, 621.
(58) Martin, J. M. L.; Taylor, P. R. *J. Phys. Chem.* **1996**, *100*, 6047.
(59) Raghavachari, K.; Strout, D. L.; Odom, G. K.; Scuseria, G. E.; Pople, J. A.; Johnson, B. G.; Gill, P. M. W. *Chem. Phys. Lett.* **1993**, *214*, 357.
(60) Hutter, J.; Lüthi, H. P.; Diederich, F. *J. Am. Chem. Soc.* **1994**, *116*, 750.
(61) Raghavachari, K.; Zhang, B.; Pople, J. A.; Johnson, B. G.; Gill, P. M. W. *Chem. Phys. Lett.* **1994**, *220*, 385.
(62) Martin, J. M. L.; El-Yazal, J.; François, J. P. *Chem. Phys. Lett.* **1995**, *242*, 570.
(63) Martin, J. M. L.; El-Yazal, J.; François, J. P. *Chem. Phys. Lett.* **1996**, *248*, 345.
(64) Martin, J. M. L. *Chem. Phys. Lett.* **1996**, *255*, 1−6.
(65) Jones, R. O.; Seifert, G. *Phys. Rev. Lett.* **1997**, *79*, 443−446.
(66) Pitzer, K. S.; Clementi, E. *J. Am. Chem. Soc.* **1959**, *81*, 4477.
(67) Raghavachari, K.; Binkley, J. S. *J. Chem. Phys.* **1987**, *87*, 2191.
(68) Liang, C.; Schaefer, H. F., III. *J. Chem. Phys.* **1990**, *93*, 8844.
(69) Parasuk, V.; Almlöf, J. *J. Chem. Phys.* **1989**, *91*, 1137.
(70) Parasuk, V.; Almlöf, J. *J. Chem. Phys.* **1991**, *94*, 8172.
(71) Watts, J. D.; Gauss, J.; Stanton, J. F.; Bartlett, R. J. *J. Chem. Phys.* **1992**, *97*, 8372.
(72) Hutter, J.; Lüthi, P. *J. Chem. Phys.* **1994**, *101*, 2213.
(73) Pless, V.; Suter, H. U.; Engels, B. *J. Chem. Phys.* **1994**, *101*, 4042.
(74) Botschwina, P. *J. Chem. Phys.* **1994**, *101*, 853.
(75) Schmatz, S.; Botschwina, P. *Chem. Phys. Lett.* **1995**, *235*, 5.
(76) Schmatz, S.; Botschwina, P. *Chem. Phys. Lett.* **1995**, *245*, 136.
(77) Yang, S. H.; Pettiette, C. L.; Conceicao, J.; Cheshnovsky, O.; Smalley, R. E. *Chem. Phys. Lett.* **1987**, *139*, 233.
(78) Yang, S.; Taylor, K. J.; Craycraft, M. J.; Conceicao, J.; Pettiette, C. L.; Cheshnovsky, O.; Smalley, R. E. *Chem. Phys. Lett.* **1988**, *144*, 431−436.
(79) Bach, S. B. H.; Eyler, J. R. *J. Chem. Phys.* **1989**, *92*, 358.
(80) Radi, P. P.; Rincon, M. E.; Hsu, M. T.; Brodbelt-Lustig, J.; Kemper, P.; Bowers, M. T. *J. Phys. Chem.* **1989**, *93*, 6187.
(81) Sowa, M. B.; Hintz, P. A.; Anderson, S. L. *J. Chem. Phys.* **1991**, *95*, 4719.
(82) Bouyer, R.; Roussel, F.; Monchicourt, P.; Perdix, M.; Pradel, P. *J. Chem. Phys.* **1994**, *100*, 8912−8919.
(83) Botschwina, P.; Seeger, S.; Mladenovic, M.; Schulz, B.; Horn, M.; Schmatz, S.; Flugge, J.; Oswald, R. *Int. Rev. Phys. Chem.* **1995**, *14*, 169−204.
(84) Adamowicz, L. *J. Chem. Phys.* **1990**, *94*, 1241.
(85) Adamowicz, L. *J. Chem. Phys.* **1990**, *93*, 6685.
(86) Ortiz, J. V. *Chem. Phys. Lett.* **1993**, *216*, 319.
(87) Ortiz, J. V.; Zakrzewski, V. G. *J. Chem. Phys.* **1994**, *100*, 6614.
(88) Ohno, M.; Zakrzewski, V. G.; Ortiz, J. V.; von Niessen, W. *J. Chem. Phys.* **1997**, *106*, 3258−3269.
(89) Northrup, F. J.; Sears, T. J. *J. Opt. Soc. Am. B* **1990**, *7*, 1924.
(90) Fan, Q.; Pfeiffer, G. V. *Chem. Phys. Lett.* **1989**, *162*, 472−478.
(91) Gaumet, J. J.; Wakisaka, A.; Shimizu, Y.; Tamori, Y. *J. Chem. Soc., Faraday Trans.* **1993**, *89*, 1667−1670.
(92) McElvany, S. W. *Int. J. Mass Spectrom. Ion Processes* **1990**, *102*, 81.
(93) Jiao, C. Q.; Phelps, D. K.; Lee, S.; Huang, Y.; Freiser, B. S. *Rapid Commun. Mass Spectrom.* **1993**, *7*, 404−408.
(94) Kaizu, K.; Kohno, M.; Suzuki, S.; Shiromaru, H.; Moriwaki, T.; Achiba, Y. *J. Chem. Phys.* **1997**, *106*, 9954−9956.
(95) Otis, C. E. *Appl. Phys. B* **1989**, *49*, 455.
(96) Creasy, W. R.; Brenna, J. T. *J. Chem. Phys.* **1990**, *92*, 2269.
(97) Campbell, E. E. B.; Ulmer, G.; Hasselberger, B.; Busmann, H.-G.; Hertel, I. V. *J. Chem. Phys.* **1990**, *93*, 6900.
(98) Balfour, W. J.; Cao, J.; Prasad, C. V. V.; Qian, C. X. W. *J. Chem. Phys.* **1994**, *101*, 10343.
(99) Moazzen-Ahmadi, N.; McKellar, A. R. W.; Amano, T. *Chem. Phys. Lett.* **1989**, *157*, 1−4.
(100) Kawaguchi, K.; Matsumura, K.; Kanamori, H.; Hirota, E. *J. Chem. Phys.* **1989**, *91*, 1953.
(101) Rohlfing, E. A.; Goldsmith, J. E. M. *J. Opt. Soc. Am. B* **1990**, *7*, 1915.
(102) Smith, A. M.; Agreiter, J.; Härtle, M.; Engel, C.; Bondybey, V. E. *Chem. Phys.* **1994**, *189*, 315−334.
(103) Ehbrecht, M.; Faerber, M.; Rohmund, F.; Smirnov, V. V.; Stelmokh, O.; Huisken, F. *Chem. Phys. Lett.* **1993**, *214*, 34.
(104) Calabrese, D.; Covington, A. M.; Thompson, J. S. *J. Chem. Phys.* **1996**, *105*, 2936−2937.
(105) Rubin, Y.; Diederich, F. *J. Am. Chem. Soc.* **1989**, *111*, 6870.
(106) Diederich, F.; Rubin, Y.; Knobler, C. B.; Whetten, R. L.; Schriver, K. E.; Houk, K. N.; Li, Y. *Science* **1989**, *245*, 1088.
(107) Rubin, Y.; Knobler, C. B.; Diederich, F. *J. Am. Chem. Soc.* **1990**, *112*, 4966.
(108) Rubin, Y.; Knobler, C. B.; Diederich, F. *J. Am. Chem. Soc.* **1990**, *112*, 1607.
(109) Rubin, Y.; Kahr, M.; Knobler, C. B.; Diederich, F.; Wilkins, C. L. *J. Am. Chem. Soc.* **1991**, *113*, 495.
(110) Tobe, Y.; Matsumoto, H.; Naemura, K.; Achiba, Y.; Wakabayashi, T. *Angew. Chem., Int. Ed. Engl.* **1996**, *35*, 1800−1802.
(111) Krätschmer, W. In *The Chemical Physics of Fullerenes 10 (and 5) Years Later*; Andreoni, W., Ed.; ASI Conference Series E, No. 316; Kluwer Academic Publishers: Dordrecht, 1996; pp 27−35.
(112) Miki, M.; Wakabayashi, T.; Momose, T.; Shida, T. *J. Phys. Chem.* **1996**, *100*, 12135−12137.
(113) Szczepanski, J.; Ekern, S.; Chapo, C.; Vala, M. *Chem. Phys.* **1996**, *211*, 359−366.
(114) Gingerich, K. A. *Chem. Phys. Lett.* **1992**, *196*, 245.
(115) Gingerich, K. A.; Finkbeiner, H. C.; Schmud, R. W., Jr. *Chem. Phys. Lett.* **1993**, *207*, 23.
(116) Gingerich, K. A.; Finkbeiner, H. C.; Schmude, R. W., Jr. *J. Am. Chem. Soc.* **1994**, *116*, 3884.
(117) Martin, J. M. L.; François, J. P.; Gijbels, R. *J. Chem. Phys.* **1991**, *95*, 9420.
(118) Martin, J. M. L.; Taylor, P. R. *J. Chem. Phys.* **1995**, *102*, 8270.
(119) Slanina, Z. *Thermochim. Acta* **1988**, *127*, 237.
(120) Slanina, Z. *Chem. Phys. Lett.* **1990**, *173*, 164.
(121) Rohlfing, E. A. In *Advances in Metal and Semiconductor Clusters*: *Spectroscopy and Structure*; Duncan, M. A., Ed.; JAI Press: Greenwich, CT, 1995; Vol. 3, pp 85−111.
(122) Douay, M.; Nietmann, R.; Bernath, P. F. *J. Mol. Spectrosc.* **1988**, *131*, 261.
(123) Goodwin, P. M.; Cool, T. A. *J. Chem. Phys.* **1989**, *90*, 1296.
(124) Gong, M.; Bao, Y.; Urdahl, R. S.; Jackson, W. M. *Chem. Phys. Lett.* **1993**, *217*, 210.
(125) Huber, K. P.; Herzberg, G. *Molecular Spectra and Molecular Structure IV. Constants of Diatomic Molecules*; Van Nostrand Reinhold: New York, 1979.
(126) Martin, M. *J. Photochem. Photobiol. A* **1992**, *66*, 263.
(127) Watts, J. D.; Bartlett, R. J. *J. Chem. Phys.* **1992**, *96*, 6073.
(128) Pradhan, A. D.; Partridge, H.; C. W., J. B. *J. Chem. Phys.* **1994**, *101*, 3857.
(129) Prasad, C. V. V.; Bernath, P. F. *Astrophys. J.* **1994**, *426*, 812.
(130) Thareja, R. K.; Abhilasha *J. Chem. Phys.* **1994**, *100*, 4019.
(131) Caubet, P.; Dorthe, G. *Chem. Phys. Lett.* **1994**, *218*, 529.
(132) Lambert, D. L.; Sheffer, Y.; Federman, S. R. *Astrophys. J.* **1995**, *438*, 740.
(133) Erman, P.; Iwamae, A. *Astrophys. J.* **1995**, *450*, L31.
(134) Lask, G. M.; Agreiter, J.; Schlachta, R.; Bondybey, V. E. *Chem. Phys. Lett.* **1993**, *205*, 31.
(135) Blunt, V. M.; Lin, H.; Sorkhabi, O.; Jackson, W. M. *J. Mol. Spectrosc.* **1995**, *174*, 274.
(136) Rehfuss, B. D.; Liu, D.-J.; Dinelli, B. M.; Jagod, M.-F.; Ho, W. C.; Crofton, M. W.; Oka, T. *J. Chem. Phys.* **1988**, *89*, 129.
(137) de Beer, E.; Zhao, Y.; Yourshaw, I.; Neumark, D. M. *Chem. Phys. Lett.* **1995**, *244*, 400.
(138) Maier, J. P.; Rösslein, M. J. *J. Chem. Phys.* **1988**, *88*, 4614.
(139) Celii, F. G.; Maier, J. P. *Chem. Phys. Lett.* **1990**, *166*, 517.
(140) Carré, M.; Alikacem, A.; Larzillière, M. *Phys. Rev. A* **1989**, *40*, 3450.
(141) Boudjarane, K.; Carré, M.; Larzillière, M. *Chem. Phys. Lett.* **1995**, *243*, 571.

(142) Zackrisson, M.; Royen, P. *J. Mol. Spectrosc.* **1993**, *161*, 1.
(143) Bruna, P. J.; Wright, J. S. *J. Phys. Chem.* **1991**, *96*, 1630.
(144) Hogreve, H. *Chem. Phys.* **1996**, *202*, 63.
(145) Huggins, W. *Proc. R. Soc. London* **1882**, *33*, 1.
(146) Herzberg, G. *Astrophys. J.* **1942**, *96*, 314.
(147) Gausset, L.; Herzberg, G.; Lagerqvist, A.; Rosen, B. *Astrophys. J.* **1965**, *142*, 45.
(148) Weltner, W., Jr.; McLeod, D., Jr. *J. Chem. Phys.* **1964**, *40*, 1305−1316.
(149) Weltner, W., Jr.; McLeod, D., Jr. *J. Chem. Phys.* **1966**, *45*, 3096.
(150) Merer, A. J. *Can. J. Phys.* **1967**, *45*, 4103.
(151) Bondybey, V. E.; English, J. H. *J. Chem. Phys.* **1978**, *68*, 4641.
(152) Jungen, C.; Merer, A. J. *Mol. Phys.* **1980**, *40*, 95.
(153) Matsumura, K.; Kanamori, H.; Kawaguchi, K.; Hirota, E. *J. Chem. Phys.* **1988**, *89*, 3491.
(154) Schmuttenmaer, C. A.; Cohen, R. C.; Pugliano, N.; Heath, J. R.; Cooksy, A. L.; Busarow, K. L.; Saykally, R. J. *Science* **1990**, *249*, 897.
(155) Kraemer, W. P.; Bunker, P. R.; Yoshimine, M. *J. Mol. Spectrosc.* **1984**, *107*, 191.
(156) Jensen, P.; Rohlfing, C. M.; Almlöf, J. *J. Chem. Phys.* **1992**, *97*, 3399.
(157) Szczepanski, J.; Vala, M. *J. Chem. Phys.* **1993**, *99*, 7371.
(158) Jensen, P. *Collect. Czech. Chem. Commun.* **1989**, *54*, 1209.
(159) Almlöf, J.; Jensen, P.; Northrup, F. J.; Rohlfing, C. M.; Rohlfing, E. A.; Sears, T. J. *J. Chem. Phys.* **1994**, *101*, 5413.
(160) Szczepanski, J.; Vala, M. *J. Chem. Phys.* **1994**, *101*, 5414.
(161) Cheung, H. M.; Graham, W. R. M. *J. Chem. Phys.* **1989**, *91*, 6664.
(162) Jiang, Q.; Graham, W. R. M. *J. Chem. Phys.* **1991**, *95*, 3129.
(163) Moazzen-Ahmadi, N.; McKellar, A. R. W. *J. Chem. Phys.* **1993**, *98*, 7757.
(164) Jørgensen, U. G.; Almlöf, J.; Siegbahn, P. E. M. *Astrophys. J.* **1989**, *343*, 554.
(165) Baker, J.; Bramble, S. K.; Hamilton, P. A. *Chem. Phys. Lett.* **1993**, *213*, 297.
(166) Izuha, M.; Yamanouchi, K. *Chem. Phys. Lett.* **1995**, *242*, 435.
(167) Forney, D.; Freivogel, P.; Grutter, M.; Maier, J. P. *J. Chem. Phys.* **1995**, *104*, 4954−4960.
(168) Chang, K. W.; Graham, W. R. M. *J. Chem. Phys.* **1982**, *77*, 4300−4303.
(169) Sasada, H.; Amano, T.; Jarman, C.; Bernath, P. F. *J. Chem. Phys.* **1991**, *94*, 2401.
(170) Smith, A. M.; Agreiter, J.; Engel, C.; Bondybey, V. E. *Chem. Phys. Lett.* **1993**, *207*, 531.
(171) Hwang, C. H.; Klassen, S. A.; Moazzen-Ahmadi, N.; Tokaryk, D. W. *Chem. Phys. Lett.* **1996**, *250*, 273.
(172) Tokaryk, D. W.; Civis, S. *J. Chem. Phys.* **1995**, *103*, 3928.
(173) Lemire, G. W.; Fu, Z.; Hamrick, Y. M.; Taylor, S.; Morse, M. D. *J. Phys. Chem.* **1989**, *93*, 2313.
(174) Raghavachari, K. *Chem. Phys. Lett.* **1990**, *171*, 249.
(175) Adamowicz, L. *Chem. Phys. Lett.* **1991**, *182*, 45.
(176) Watts, J. D.; Bartlett, R. J. *J. Chem. Phys.* **1992**, *97*, 3445.
(177) Szczepanski, J.; Ekern, S.; Vala, M. *J. Phys. Chem. A* **1997**, *101*, 1841−1847.
(178) Szczepanski, J.; Wehlburg, C.; Vala, M. *J. Phys. Chem. A* **1997**, *101*, 7039−7042.
(179) Faibis, A.; Kanter, E. P.; Tack, L. M.; Bakke, E.; Zabransky, B. J. *J. Chem. Phys.* **1987**, *91*, 6445.
(180) Vager, Z.; Kanter, E. P. *J. Phys. Chem.* **1989**, *93*, 7745.
(181) Grev, R. S.; Alberts, I. L.; Schaefer, H. F., III. *J. Phys. Chem.* **1990**, *94*, 3379.
(182) Martin, J. M. L.; François, J. P.; Gijbels, R. *J. Chem. Phys.* **1990**, *93*, 5037.
(183) Taylor, P. R.; Martin, J. M. L.; François, J. P.; Gijbels, R. *J. Phys. Chem.* **1991**, *95*, 6530.
(184) Scuseria, G. E. *Chem. Phys. Lett.* **1991**, *176*, 27.
(185) Hogreve, H. *J. Chem. Phys.* **1994**, *102*, 3281.
(186) Liang, C.; Schaefer, H. F., III. *Chem. Phys. Lett.* **1990**, *169*, 150.
(187) Andreoni, W.; Scharf, D. *Chem. Phys. Lett.* **1990**, *173*, 449.
(188) Lammertsma, K.; Güner, O. F.; Sudhakar, P. V. *J. Chem. Phys.* **1991**, *94*, 8105.
(189) Nygren, M. A.; Pettersson, L. G. M. *Chem. Phys. Lett.* **1992**, *191*, 473.
(190) Martin, J. M. L.; François, J. P.; Gijbels, R. *J. Chem. Phys.* **1991**, *94*, 3753.
(191) Martin, J. M. L.; Schwenke, D. W.; Lee, T. J.; Taylor, P. R. *J. Chem. Phys.* **1996**, *104*, 4657.
(192) Algrananti, M.; Feldman, H.; Kella, D.; Malkin, E.; Miklazky, E.; Naaman, R.; Vager, Z.; Zajfman, J. *J. Chem. Phys.* **1989**, *90*, 4617.
(193) Kella, D.; Zajfman, D.; Heber, O.; Majer, D.; Feldman, H.; Vager, Z.; Naaman, R. *Z. Phys. D* **1993**, *26*, 340.
(194) Graham, W. R. M.; Dismuke, K. I.; Weltner, W., Jr. *Astrophys. J.* **1976**, *204*, 301.
(195) Shen, L. N.; Withey, P. A.; Graham, W. R. M. *J. Chem. Phys.* **1991**, *94*, 2395.
(196) Szczepanski, J.; Vala, M.; Shen, L. N.; Withey, P. A.; Graham, W. R. M. *J. Phys. Chem. A* **1997**, *101*, 8788−8792.
(197) Thompson, K. R.; DeKock, R. L.; Weltner, W., Jr. *J. Am. Chem. Soc.* **1971**, *93*, 4688.
(198) Bernholdt, D. E.; Magers, D. H.; Bartlett, R. J. *J. Chem. Phys.* **1988**, *89*, 3612.
(199) Vala, M.; Chandrasekhar, T. M.; Szczepanski, J.; Van Zee, R.; Weltner, W., Jr. *J. Chem. Phys.* **1989**, *90*, 595.
(200) Shen, L. N.; Graham, W. R. M. *J. Chem. Phys.* **1989**, *91*, 5115.
(201) Withey, P. A.; Shen, L. N.; Graham, W. R. M. *J. Chem. Phys.* **1991**, *95*, 820.
(202) Heath, J. R.; Saykally, R. J. *J. Chem. Phys.* **1991**, *94*, 3271.
(203) Moazzen-Ahmadi, N.; Thong, J. J.; McKellar, A. R. W. *J. Chem. Phys.* **1994**, *100*, 4033.
(204) Kurtz, J.; Huffman, D. R. *J. Chem. Phys.* **1990**, *92*, 30.
(205) Szczepanski, J.; Vala, M. *J. Phys. Chem.* **1990**, *95*, 2792.
(206) Forney, D.; Fulara, J.; Freivogel, P.; Jakobi, M.; Lessen, D.; Maier, J. P. *J. Chem. Phys.* **1995**, *103*, 48.
(207) Freivogel, P.; Fulara, J.; Jakobi, M.; Forney, D.; Maier, J. P. *J. Chem. Phys.* **1995**, *103*, 54.
(208) Freivogel, P.; Grutter, M.; Forney, D.; Maier, J. P. *Chem. Phys. Lett.* **1996**, *249*, 191.
(209) Watts, J. D.; Cernusak, I.; Bartlett, R. J. *Chem. Phys. Lett.* **1991**, *178*, 259.
(210) Adamowicz, L. *Chem. Phys.* **1991**, *156*, 387.
(211) Schäfer, M.; Grutter, M.; Fulara, J.; Forney, D.; Frievogel, P.; Maier, J. P. *Chem. Phys. Lett.* **1996**, *260*, 406−408.
(212) Freivogel, P.; Grutter, M.; Forney, D.; Maier, J. P. *J. Chem. Phys.* **1997**, *107*, 22−27.
(213) Freivogel, P.; Grutter, M.; Forney, D.; Maier, J. P. *J. Chem. Phys.* **1997**, *107*, 4468−4472.
(214) Forney, D.; Grutter, M.; Freivogel, P.; Maier, J. P. *J. Phys. Chem. A* **1997**, *101*, 5292−5295.
(215) Zhao, Y.; de Beer, E.; Neumark, D. M. *J. Chem. Phys.* **1996**, *105*, 2575−2582.
(216) Raghavachari, K. *Z. Phys. D* **1989**, *12*, 61.
(217) Adamowicz, L.; Kurtz, J. *Chem. Phys. Lett.* **1989**, *162*, 342.
(218) Kurtz, J.; Adamowicz, L. *Astrophys. J.* **1991**, *370*, 784.
(219) Botschwina, P.; Sebald, P. *Chem. Phys. Lett.* **1989**, *160*, 485.
(220) Heath, J. R.; Cooksy, A. L.; Gruebele, M. H. W.; Schmuttenmaer, C. A.; Saykally, R. J. *Science* **1989**, *244*, 564.
(221) Kranze, R. H.; Graham, W. R. M. *J. Chem. Phys.* **1992**, *96*, 2517.
(222) Moazzen-Ahmadi, N.; McKellar, A. R. W.; Amano, T. *J. Chem. Phys.* **1989**, *91*, 2140.
(223) Moazzen-Ahmadi, N.; Flatt, S. D.; McKellar, A. R. W. *Chem. Phys. Lett.* **1991**, *186*, 291.
(224) Kitsopoulos, T. N.; Chick, C. J.; Zhao, Y.; Neumark, D. M. *J. Chem. Phys.* **1991**, *95*, 5479.
(225) Kolbuszewski, M. *J. Chem. Phys.* **1994**, *102*, 3679.
(226) Adamowicz, L. *Chem. Phys. Lett.* **1991**, *180*, 466.
(227) Gotts, N. G.; von Helden, G.; Bowers, M. T. *Int. J. Mass Spectrom. Ion Processes* **1995**, *149/150*, 217.
(228) Freivogel, P.; Grutter, M.; Forney, D.; Maier, J. P. *Chem. Phys.* **1997**, *216*, 401−406.
(229) Raghavachari, K.; Whiteside, R. A.; Pople, J. A. *J. Chem. Phys.* **1986**, *85*, 6623.
(230) Zajfman, D.; Feldman, H.; Heber, O.; Kella, D.; Majer, D.; Vager, Z.; Naaman, R. *Science* **1992**, *258*, 1129.
(231) Zajfman, D.; Kella, D.; Heber, O.; Majer, D.; Feldman, H.; Vager, Z.; Naaman, R. *Z. Phys. D* **1993**, *26*, 343.
(232) Van Zee, R. J.; Ferrante, R. F.; Zeringue, K. J.; Weltner, W., Jr. *J. Chem. Phys.* **1987**, *86*, 5212.
(233) Van Zee, R. J.; Ferrante, R. F.; Zeringue, K. J.; Weltner, W., Jr. *J. Chem. Phys.* **1988**, *88*, 3465.
(234) Vala, M.; Chandrasekhar, T. M.; Szczepanski, J.; Pellow, R. *High Temp. Sci.* **1990**, *27*, 19.
(235) Kranze, R. H.; Graham, W. R. M. *J. Chem. Phys.* **1993**, *98*, 71.
(236) Hwang, H. J.; Van Orden, A.; Tanaka, K.; Kuo, E. W.; Heath, J. R.; Saykally, R. J. *Mol. Phys.* **1993**, *79*, 769.
(237) Arnold, C. C.; Zhao, Y.; Kitsopoulos, T. N.; Neumark, D. M. *J. Chem. Phys.* **1992**, *97*, 6121.
(238) Graham, W. R. M.; Dismuke, K. I.; Weltner, W., Jr. *Astrophys. J.* **1976**, *204*, 301.
(239) von Helden, G.; Kemper, P. R.; Gotts, N. G.; Bowers, M. T. *Science* **1993**, *259*, 1300.
(240) Szczepanski, J.; Auerbach, E.; Vala, M. *J. Phys. Chem. A* **1997**, *101*, 9296−9301.
(241) von Helden, G.; Gotts, N. G.; Palke, W. E.; Bowers, M. T. *Int. J. Mass Spectrom. Ion Processes* **1993**, *138*, 33.
(242) von Helden, G.; Hsu, M.-T.; Bowers, M. T. *J. Chem. Phys.* **1991**, *95*, 3835.
(243) von Helden, G.; Hsu, M.-T.; Gotts, N.; Bowers, M. T. *J. Phys. Chem.* **1993**, *97*, 8182.
(244) Martin, J. M. L.; François, J. P.; Gijbels, R. *J. Chem. Phys.* **1990**, *93*, 8850.
(245) von Helden, G.; Palke, W. E.; Bowers, M. T. *Chem. Phys. Lett.* **1993**, *212*, 247.
(246) Slanina, Z.; Kurtz, J.; Adamowicz, L. *Chem. Phys. Lett.* **1992**, *196*, 208.
(247) Martin, J. M. L.; El-Yazal, J.; François, J.-P. *Chem. Phys. Lett.* **1996**, *252*, 9.

(248) Kranze, R. H.; Rittby, C. M. L.; Graham, W. R. M. *J. Chem. Phys.* **1996**, *105*, 5313−5320.
(249) Heath, J. R.; Sheeks, R. A.; Cooksy, A. L.; Saykally, R. J. *Science* **1990**, *249*, 895.
(250) Heath, J. R.; Saykally, R. J. *J. Chem. Phys.* **1991**, *94*, 1724.
(251) Heath, J. R.; Van Orden, A.; Kuo, E.; Saykally, R. J. *Chem. Phys. Lett.* **1991**, *182*, 17.
(252) Schauer, S. N.; Williams, P.; Compton, R. N. *Phys. Rev. Lett.* **1990**, *65*, 625.
(253) Gnaser, H.; Oechsner, H. *Nucl. Instr. Methods* **1993**, *B82*, 518.
(254) Adamowicz, L. *J. Chem. Phys.* **1991**, *95*, 8669.
(255) Sommerfeld, T.; Scheller, M. K.; Cederbaum, L. S. *Chem. Phys. Lett.* **1993**, *209*, 216−222.
(256) Dolgounitcheva, O.; Zakrzewski, V. G.; Ortiz, J. V. *J. Chem. Phys.* **1998**, *109*, 87−93.
(257) McElvany, S. W. *J. Chem. Phys.* **1988**, *89*, 2063−2075.
(258) Parent, D. C.; McElvany, S. W. *J. Am. Chem. Soc.* **1989**, *111*, 2393−2401.
(259) Parent, D. C.; Anderson, S. L. *Chem. Rev.* **1992**, *92*, 1541.
(260) von Helden, G.; Gotts, N. G.; Bowers, M. T. *Chem. Phys. Lett.* **1993**, *212*, 241−246.
(261) Slanina, Z.; Kurtz, J.; Adamowicz, L. *Mol. Phys.* **1992**, *76*, 387.
(262) Slanina, Z.; Lee, S.-L.; François, J.-P.; Kurtz, J.; Adamowicz, L. *Chem. Phys. Lett.* **1994**, *223*, 397.
(263) Forney, D.; Grutter, M.; Freivogel, P.; Maier, J. P. In *Proceedings of the 10th International Symposium on Atomic, Molecular, Cluster, Ion, and Surface Physics*; Maier, J. P., Quack, M., Eds.; VDF: Zürich, 1996; pp 106−107.
(264) Martin, J. M. L.; Taylor, P. R. *Chem. Phys. Lett.* **1995**, *240*, 521.
(265) Kranze, R. H.; Withey, P. A.; Rittby, C. M. L.; Graham, W. R. M. *J. Chem. Phys.* **1995**, *103*, 6841.
(266) Slanina, Z.; Lee, S.-L.; François, J.-P.; Kurtz, J.; Adamowicz, L. *Mol. Phys.* **1994**, *81*, 1489.
(267) Wu, Z. J.; Meng, Q. B.; Zhang, S. Y. *Chem. Phys. Lett.* **1997**, *267*, 271−275.
(268) Heath, J. R.; Saykally, R. J. *J. Chem. Phys.* **1990**, *93*, 8392.
(269) Van Orden, A.; Hwang, H. J.; Kuo, E. W.; Saykally, R. J. *J. Chem. Phys.* **1993**, *98*, 6678.
(270) Wakabayashi, T.; Momose, T.; Shida, T.; Shiromaru, H.; Ohara, M.; Achiba, Y. *J. Chem. Phys.* **1997**, *107*, 1152−1155.
(271) Watts, J. D.; Bartlett, R. J. *Chem. Phys. Lett.* **1992**, *190*, 19.
(272) Achiba, Y.; Kittaka, C.; Moriwaki, T.; Shiromaru, H. *Z. Phys. D* **1991**, *19*, 427.
(273) Handschuh, H.; Ganteför, G.; Kessler, B.; Bechthold, P. S.; Eberhardt, W. *Phys. Rev. Lett.* **1995**, *74*, 1095−1098.
(274) Martin, J. M. L.; François, J. P.; Gijbels, R.; Almlöf, J. *Chem. Phys. Lett.* **1991**, *187*, 367.
(275) Bleil, R.; Tao, F.-M.; Kais, S. *Chem. Phys. Lett.* **1994**, *229*, 491.
(276) Feyereisen, M.; Gutowski, M.; Simons, J. *J. Chem. Phys.* **1992**, *96*, 2926.
(277) von Helden, G.; Hsu, M. T.; Gotts, N. G.; Kemper, P. R.; Bowers, M. T. *Chem. Phys. Lett.* **1993**, *204*, 15.
(278) Brabec, C. J.; Anderson, E. B.; Davidson, B. N.; Kajihara, S. A.; Zhang, Q.-M.; Bernholc, J.; Tománek, D. *Phys. Rev. B* **1992**, *46*, 7326.
(279) Parasuk, V.; Almlöf, J. *Chem. Phys. Lett.* **1991**, *184*, 187.
(280) Grossman, J. C.; Mitas, L.; Raghavachari, K. *Phys. Rev. Lett.* **1995**, *75*, 3870.
(281) Taylor, P. R.; Bylaska, E.; Weare, J. H.; Kawai, R. *Chem. Phys. Lett.* **1995**, *235*, 558.
(282) Bakowies, D.; Thiel, W. *J. Am. Chem. Soc.* **1991**, *113*, 3704.
(283) Smalley, R. E. *Acc. Chem. Res.* **1992**, *25*, 98.
(284) Bates, K. R.; Scuseria, G. E. *J. Phys. Chem. A* **1997**, *101*, 3038−3041.
(285) von Helden, G.; Porter, E.; Gotts, N. G.; Bowers, M. T. *J. Phys. Chem.* **1995**, *99*, 7707.
(286) von Helden, G.; Gotts, N. G.; Bowers, M. T. *J. Am. Chem. Soc.* **1993**, *115*, 4363.
(287) von Helden, G.; Gotts, N. G.; Bowers, M. T. *Nature* **1993**, *363*, 60.
(288) Hunter, J.; Fye, J.; Jarrold, M. F. *Science* **1993**, *260*, 784.
(289) Hunter, J. M.; Fye, J. L.; Jarrold, M. F. *J. Chem. Phys.* **1993**, *99*, 1785.
(290) Hunter, J.; Fye, J.; Jarrold, M. F. *J. Phys. Chem.* **1993**, *97*, 3460.
(291) Hunter, J. M.; Fye, J. L.; Roskamp, E. J.; Jarrold, M. F. *J. Phys. Chem.* **1994**, *98*, 1810.
(292) McElvany, S. W.; Ross, M. W.; Goroff, N. S.; Diederich, F. *Science* **1993**, *259*, 1594.
(293) Shelimov, K.; Hunter, J. M.; Jarrold, M. F. *Int. J. Mass Spectrom. Ion Processes* **1994**, *138*, 17.
(294) Rohlfing, E. A. *J. Chem. Phys.* **1990**, *93*, 7851.
(295) Hallet, R. P.; McKay, K. G.; Balm, S. P.; Allaf, A. W.; Kroto, H. W.; Stace, A. J. *Z. Phys. D* **1995**, *34*, 65.
(296) Doverstal, M.; Lindgren, B.; Sassenberg, U.; Yu, H. *Z. Phys. D* **1991**, *19*, 447.
(297) Sowa, M. B.; Anderson, S. L. *J. Chem. Phys.* **1992**, *97*, 8164.
(298) Sowa-Resat, M.; Smolanoff, J. N.; Goldman, I. B.; Anderson, S. L. *J. Chem. Phys.* **1994**, *100*, 8784.
(299) Pozniak, B.; Dunbar, R. C. *J. Am. Chem. Soc.* **1994**, *116*, 4113.
(300) Zimmerman, J. A.; Creasy, W. R. *J. Chem. Phys.* **1992**, *96*, 1942.
(301) Sun, J.; Grützmacher, H.-F.; Lifshitz, C. *J. Phys. Chem.* **1994**, *98*, 4536.
(302) Pozniak, B. P.; Dunbar, R. C. *J. Am. Chem. Soc.* **1997**, *119*, 7343−7349.
(303) Sun, J.; Grützmacher, H.-F.; Lifshitz, C. *Int. J. Mass Spectrom. Ion Processes* **1994**, *138*, 49.
(304) Zimmerman, J. A.; Creasy, W. R. *J. Chem. Phys.* **1991**, *95*, 3267.
(305) Piskoti, C.; Yarger, J.; Zettl, A. *Nature* **1998**, *393*, 771.
(306) Scherer, J. J.; Paul, J. B.; O'Keefe, A.; Saykally, R. J. *Chem. Rev.* **1997**, *97*, 25.
(307) Paul, J. B.; Saykally, R. J. *Anal. Chem.* **1997**, *69*, A287.
(308) Paul, J. B.; Scherer, J. J.; O'Keefe, A.; Saykally, R. J. In *Laser Focus World*; March, 1997; Vol. 33, No. 3; pp 71-80.
(309) Provencal, R. A.; Paul, J. B.; Michael, E.; Saykally, R. J. *Photonics Spectra* **1998**, *32* (6), 159.
(310) Linnartz, H.; Motylewski, T.; Maier, J. P. In *Proceedings of the 53rd International Symposium on Molecular Spectroscopy*; Columbus, OH, June 15−19, 1998.

CR970086N